Universität Potsdam, Institut für Biochemie und Biologie
Arbeitsgruppe Molekularbiologie, Prof. Dr. Bernd Müller-Röber

Molecular and physiological characterisation of selected DOF transcription factors in the model plant *Arabidopsis thaliana*

Dissertation
zur Erlangung des akademischen Grades
“doctor rerum naturalium”
(Dr. rer. nat.)

in der Wissenschaftsdisziplin
„Molekulare Pflanzenbiologie“

eingereicht
an der
Mathematisch-Naturwissenschaftlichen Fakultät
der
Universität Potsdam

von
Jonas Krebs

Potsdam
November 2009

Published online at the
Institutional Repository of the University of Potsdam:
URL http://opus.kobv.de/ubp/volltexte/2010/4183/
URN urn:nbn:de:kobv:517-opus-41831
http://nbn-resolving.org/urn:nbn:de:kobv:517-opus-41831

Erklärung

Hiermit erkläre ich, dass ich die vorliegende Arbeit selbständig und unter Verwendung keiner anderen als den von mir angegebenen Quellen und Hilfsmitteln verfasst habe. Ferner erkläre ich, dass ich bisher weder an der Universität Potsdam noch anderweitig versucht habe, eine Dissertation einzureichen oder mich einer Doktorprüfung zu unterziehen.

Jonas Krebs Potsdam, 04.11.2009

Acknowledgements

Firstly, I would like to thank Prof. Dr. Bernd Mueller-Roeber for giving me the possibility to work on the exciting projects, his wise guidance and nevertheless enough scientific freedom to realize my own ideas. I would like to express my deep gratitude to Dr. Slobodan Ruzicic for the great supervision, encouragement, dedication, friendship and patience during all time of this work. I would also like to thank Dr. Miroslaw Kwasniewski for the excellent discussions, the nice atmosphere in the office and friendship. I am grateful to Prof. Dr. Eberhard Schäfer, Prof. Dr. Christian Hardtke and Dr. Carsten Müssig for agreeing to examine this thesis. I would like to acknowledge Dr. Karin Koehl and her Green Team, special Linda Bartetzko, of the Max-Planck-Institute of Molecular Plant Physiology for performing the plant transformations and for taking care of the plants in the greenhouse. I am also grateful for the excellent technical support provided by the Institute, in particular to Dr. Eugenia Maximova for assistance in microscopy and Josef Bergstein for the expert photography. I am indebted to the German Research Foundation (DFG) to financially supporting my PhD. I thank all my colleagues from AG Mueller-Roeber for the nice atmosphere and friendship. A special thank to Dr. Barbara Koehler and Dr. Fernando Arana for the fun we had in the lab and beside. I would like to thank also my family for their unconditional support and encourage. My thanks also for all others who have helped me and were not mentioned here.

Table of contents

Abbreviations

aa	amino acid(s)
ABC transporter	ATP-binding cassette transporter
ACC	1-aminocyclopropane-1-carboxylic acid
AD	activation domain
amiRNA	artificial micro RNA
AP2/EREBP	apetala2/ethylene response element binding protein
APC	anaphase-promoting complex
ARE	auxin response element
ARF	auxin response factor
bHLH	basic helix loop helix
bp	base pair(s)
cDNA	complementary DNA
ChIP	chromatin immuno preciptitation
COI	cortex endodermis initial
BD	binding domain
d	day(s)
DAG	days after germination
DNA	deoxyribonucleic acid
DOF	DNA binding with one finger
DPE	downstream promoter element
E. coli	*Escherichia coli*
ERF	ethylene response factor
FACS	fluorescent activated cell sorting
FC	fold change
GFP	green fluorescent protein
GUS	β-glucuronidase
h	hour(s)
HAT	histone acetyl transferase
IAA	indole-3-acetic acid
INR	initiator element
ISWI	imitation switch
kb	kilobase pairs
KO	knock-out
LB	left border
mRNA	messenger RNA
miRNA	micro RNA
NAC	NAM, ATAF, and CUC
NLS	nuclear localization signal
nt	nucleotide(s)
ORF	open reading frame
OX	overexpression
PCR	polymerase chain reaction
PGP	p-glycoprotein
Pol I	RNA polymerase I
Pol II	RNA polymerase II
Pol III	RNA polymerase III
QC	quiescent centre
qRT-PCR	quantitative real-time PCR
RB	right border
RE	response element
RNA	ribonucleic acid
rRNA	ribosomal RNA
TBP	TATA-binding protein
T-DNA	transfer DNA
TF	transcription factor
TIGR	The Institute for Genomic Research
tRNA	transfer RNA
Trp	tryptophan
UTR	untranslated region
YOH	yeast one hybrid
YTH	yeast two hybrid

1. Summary

About 2,000 of the more than 27,000 genes of the genetic model plant *Arabidopsis thaliana* encode for transcription factors (TFs), proteins that bind DNA in the promoter region of their target genes and thus act as transcriptional activators and repressors. Since TFs play essential roles in nearly all biological processes, they are of great scientific and biotechnological interest.

This thesis concentrated on the functional characterisation of four selected members of the *Arabidopsis* DOF-family, namely DOF1.2, DOF3.1, DOF3.5 and DOF5.2, which were selected because of their specific expression pattern in the root tip, a region that comprises the stem cell niche and cells for the perception of environmental stimuli. DOF1.2, DOF3.1 and DOF3.5 are previously uncharacterized members of the *Arabidopsis* DOF-family, while DOF5.2 has been shown to be involved in the phototrophic flowering response. However, its role in root development has not been described so far.

To identify biological processes regulated by the four DOF proteins in detail, molecular and physiological characterization of transgenic plants with modified levels of *DOF1.2*, *DOF3.1*, *DOF3.5* and *DOF5.2* expression (constitutive and inducible over-expression, artificial microRNA) was performed. Additionally expression patterns of the TFs and their target genes were analyzed using promoter-GUS lines and publicly available microarray data. Finally putative protein-protein interaction partners and upstream regulating TFs were identified using the yeast two-hybrid and one-hybrid system. This combinatorial approach revealed distinct biological functions of DOF1.2, DOF3.1, DOF3.5 and DOF5.2 in the context of root development. *DOF1.2* and *DOF3.5* are specifically and exclusively expressed in the root cap, including the central root cap (columella) and the lateral root cap, organs which are essential to direct oriented root growth. It could be demonstrated that both genes work in the plant hormone auxin signaling pathway and have an impact on distal cell differentiation. Altered levels of gene expression lead to changes in auxin distribution, abnormal cell division patterns and altered root growth orientation. *DOF3.1* and *DOF5.2* share a specific expression pattern in the organizing centre of the root stem cell niche, called the quiescent centre. Both genes redundantly control cell differentiation in the root´s proximal meristem and unravel a novel transcriptional regulation pathway for genes enriched in the QC cells.

Furthermore this work revealed a novel bipartite nuclear localisation signal being present in the protein sequence of the DOF TF family from all sequenced plant species.

Summing up, this work provides an important input into our knowledge about the role of DOF TFs during root development. Future work will concentrate on revealing the exact regulatory networks of DOF1.2, DOF3.1, DOF3.5 and DOF5.2 and their possible biotechnological applications.

2. General Introduction

2.1 Root morphology

2.1.1 The root structure

The plant root system mediates the uptake of nutrients and water from the soil and provides anchorage. During evolution root architecture adapted to these purposes leading to the formation of a streamlined main axis, which is capable of penetrating the soil and the formation of lateral roots and root hairs to maximize the absorption.

Although it is not possible to clearly separate their boarders, the root can be subdivided vertically into four developmental zones: I) the root cap that defends the apical meristem from mechanic injuries; II) the meristematic zone that is located directly behind the root cap and harbours the initial cells for the distinct cell types; III) the elongation zone, which is the site of rapid cell extension and IV) the differentiation zone, where cells achieve their final properties (Fig.1a). Differentiation occurs already in earlier stages but cells do not finalise the differentiation process until they achieve the differentiation zone. In the model plant *Arabidopsis thaliana* these four developmental zones stretch across a length of 1mm (Dolan et al., 1993) in other species that region is more extended.

Horizontally the root consists of concentric cylinders of epidermis, cortex, endodermis and pericycle surrounding the bilateral symmetric organized vascular tissue that, in turn, is made of phloem, xylem and procambium. Due to the roots radial symmetry and the lack of cell movement that is limited by the presence of a cell wall, clonally related cells form cell files that originate from one stem cell of the meristem (Fig.1b).

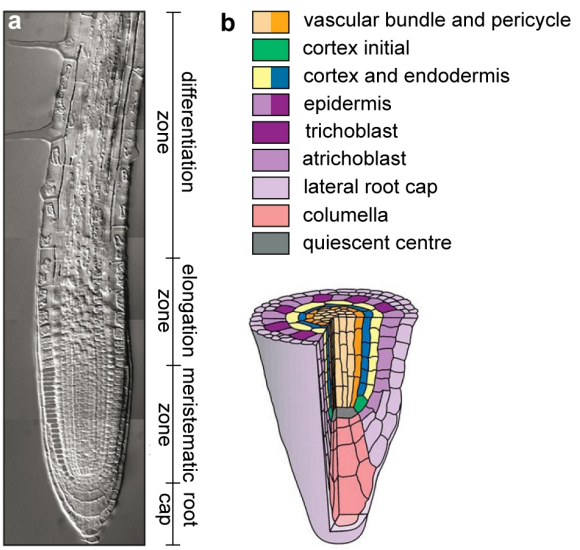

Figure 1. Morphological organization of the *A. thaliana* root.

a: Vertical subdivision into differentiation zone, elongation zone, meristematic zone and root cap. All four zones stretch a region of 1mm. Modified from (Grieneisen et al., 2007). **b:** Radial organization. All cell files of the distinct root tissues arise from a small set of stem cells, which are located at the root tip and surround the mitotically inactive quiescent centre (grey). Cortex (yellow) and endodermis (blue) share one common initial cell (green), which divides periclinally to produce two cell files. Also the epidermis (which can be subdivided at later stages of development into root hair cells (trichoblasts; pink) and non root hair cells (atrichoblasts; dark violet)) and the lateral root cap (bright violet) share one common initial. The columella (magenta) and vascular bundle/pericycle (orange) have their own set of stem cells. Adapted from (Benfey and Scheres, 2000).

2.1.2 The root apical meristem and its embryonic origin

Meristems are defined as populations of dividing cells. But not all cells in the meristematic zone divide with the same frequency. Usually the centrally located cells divide, if at all, much less frequent than the surrounding cells. For that reason these mitotically inactive cells are called the quiescent centre (QC) of the root meristem.

In *Arabidopsis thaliana* the QC consists of four to seven cells (Fig.1b, grey), which are surrounded by a ring of four different types of more frequently dividing initials/stem cells: initials for the cortex/endodermis, the epidermis/lateral root cap, the columella and the vascular tissue/pericycle. All types of initials undergo asymmetric divisions and produce one daughter cell to renew itself and one daughter cell that will differentiate. The cortex/endodermis initials (Fig.1b, green) first divide anticlinally (orthogonal to the growth axis). Subsequently the daughter cells undergo a periclinal (parallel to the growth axis) division resulting in two cell files of the cortex (Fig.1b, yellow) and endodermis (Fig.1b, blue) tissue. The primary *Arabidopsis thaliana* root consists initially of only one single cell layer of each: endodermis and cortex. However, at later developmental stages (more than two weeks after germination) the endodermis undergo further asymmetric cell divisions (Baum, 2002). The columella (basal part of root cap) initials are located directly on the basal side of the QC cells and divide solely anticlinally leading to single cell files. They are surrounded by a ring of initials that give rise to the epidermis and lateral root cap. Anticlinal divisions of these initials produce the epidermal cell file, whereas periclinal and subsequent anticlinal divisions of the same initial give rise to the lateral root cap tissue. The pericycle and vascular tissue originate from their own initials that are located above the QC cells. These initials together with their direct descendants are called the promeristem. All different types of stem cells including the QC are called the stem cell niche.

By definition *Arabidopsis thaliana* possesses a closed root vertex, since distinct root tissues can be traced back to their own initials (v. Guttenberg, 1960). *Nicotiana tabacum* and *Zea mays* are other prominent dicotyledonous and monocotyledonous species, respectively, with a closed root vertex. However in roots of many plant species it is not possible to clearly allocate the different tissues to certain initials. In this case the root possesses an open vertex.

To compare the mitotic activity of the QC cells, initials and surrounding tissue, cell division rates were monitored by incorporation of the nucleotide analogue bromo deoxyuridine (BrdU) into replicating DNA (Fujie, 1993). Within a 24h period the DNA precursor was incorporated in 7% of the QC cells, while in the surrounding cell tier of the initials incorporation could be observed in 28% of cells. Two cell distances from the QC, 84% of cells incorporated the BrdU, indicating that cell division rates increase progressively up the root and reach a maximum that depends mainly on root age and growth conditions (Beemster and Baskin, 1998). In 6 day-old seedlings the cell division peak is found at a distance of around 600µm from the QC, while in older plants the peak is located further up at around 1000µm (Scheres, 2002).

By the use of clonal analysis it is possible to trace back cell fates to their embryonic origin. In the case of roots this approach was performed by transformation of plants with a construct carrying an Ac or Dc transposon inserted in the *E. coli* β-glucuronidase (*uid*A) gene. Cells are marked by the excision and the associated restoration of the enzyme's activity. The identity of the QC and the columella was already set up in the globular stage of embryogenesis, and can be traced back to the lens-shaped upper hypophyseal derivate cell (Scheres, 1994). The hypophysis itself derives from the zygote's basal daughter cell after the first division and is the only contribution of the basal cell to the later embryo.

Although it is possible to trace back all different root domains to certain regions in the heart stage embryo resulting in a "cell fate map", individual cells are able to take on either root or hypocotyl fates until the last embryonic cell division, suggesting that the major factor determing a cell´s fate is not its clonal origin but its positional information within the tissue (Scheres, 1994).

This hypothesis was confirmed by the results obtained from laser ablation studies of single root cells. If the cell fate information is determined irreversibly already in the initial cell, its ablation should result in the complete elimination of the differentiated cell file. However, after the ablation of the cortex/endodermis initial cell that normally give rise to the cortex and endodermis cell files, adjacent pericycle cells started to divide periclinally to regenerate cortex and endodermis files. Pericycle cells that entered the cortex position changed there fate and received cortex/endodermis initial identity. Similarly upon ablation of the QC, cells of the promeristem re-specify and receive columella initial and QC identity (Scheres, 2002).

Taken together these data indicate that the determination of a plants cell fate occurs relatively flexible and is reversible if signals that determine position change.

2.1.3 The quiescent centre

The QC is considered to be the organizing centre of the stem cell niche. Through direct cell-cell contacts it keeps the surrounding stem cells undifferentiated, which was elegantly demonstrated by laser ablation experiments (van den Berg et al., 1997). Upon ablation of single QC cell only direct contacting initials lost their stem cell status and started to divide and differentiate, a process which was the most evident in the columella initials where starch granuli started to accumulate, an attribute of only differentiated columella cells. Thus, the size and the placement of the stem cell population are controlled by short-ranging signals emerging from the QC cells. However, the nature of these signals and the exact mechanism is still unknown.

On the basis of present information, two independent signalling pathways are essential for the establishment and maintenance of the QC. The plant hormone auxin and its downstream acting PLETHORA transcription factors play an important role regarding longitudinal information; the SCARECROW/SHORT ROOT pathway defines positional information along the radial axis (Scheres, 2002).

2.1.4 The root cap

The root cap is the terminal tissue of roots of almost all plants. It has a simple structure and is composed of the columella as the central part and the lateral root cap in the outer portion. Both tissues originate from different stem cells. The columella daughter cells are organized in three layers (S1-S3) and undergo rapid elongation and differentiation, producing starch granuli (statolithes) whose gravitational sedimentation triggers root gravity perception. During their passage to the outside of the cap, cells change from statocytes into secretory cells which produce mucilage, and then finally differentiate into border cells which detach from the cap (Barlow, 1975). Beside the gravity perception that was ascribed to the root cap already by Haberland in 1914 (reviewed in (Barlow, 1975)), within the past two decades the functions of the root cap have been shown to be considerably more diverse and to include directed root growth (tropism) in response to the perception and processing of many environmental stimuli like light (phototropism), obstacles (thigmotropism), gradients of temperature (thermotropism), humidity (hydrotropism) or ions and other chemicals (chemotropism); (Hasenstein and Evans, 1988); (Ishikawa and Evans, 1990); (Okada and Shimura, 1990); (Fortin and Poff, 1991); (Takahashi, 1997); (Eapen et al., 2003).

Molecular-genetic analysis of *Arabidopsis* mutants showing impaired gravitropism have led to the identification of auxin influx and efflux carriers as well as other potential signal transduction molecules, supporting the hypothesis that auxin transport plays an important role in the root gravitropic response. Therefore, not only columella cells but also lateral root cap and epidermal tissue are strongly involved in the gravity response (Friml et al., 2002), (Muller et al., 1998), (Swarup et al., 2001), (Swarup et al., 2005).

2.1.5 Lateral roots

In contrast to axillary shoot buds that are composed of undifferentiated cells and give rise to vegetative meristems, lateral roots are formed from non-meristematic tissue. In angiosperms lateral roots derive from pericycle cells adjacent to xylem poles at some distance from the primary root apical meristem in the differentiation zone (Esau, 1965). At initial stages of lateral root development cell division pattern fundamentally differ from primary roots and include dedifferentiation and subsequent proliferation of induced mature pericycle cells whereas cell divisions at later stages are very similar to those of the primary root. Auxin, a plant specific hormone, was shown to act at the earliest stages of lateral root primordia initiation and to promote the activation of previously quiescent pericyle cells to divide (Himanen et al., 2002). The process of lateral root development was subdivided into 8 stages (stage I to VIII), of which each possesses specific anatomical characteristics and cell division pattern (Malamy and Benfey, 1997). The appearance of anticlinal pericycle cell divisions is the first visible evidence for lateral root formation resulting in 8-10 “short” cells (in comparison to pericycle cells on the opposite of the stele). The full emergence of the lateral root from the parent root displays the last stage. By the use of tissue- and cell type-specific β-glucuronidase marker lines it was also

possible to trace back the distinct root layer´s origin to defined stages of lateral root formation. The epidermis´ identity is for instance set up already in stage II, whereas the root cap is defined at stage VI. Since at later stages of lateral root development the cellular organization of the meristem, including cell type specific initials, resembles that of the primary root, the question arises at which stage the meristem is established. Due to the lack of initial-specific marker lines, which could enable easily monitoring of arising meristem identity, (Laskowski et al., 1995) identified an important stage in lateral root development at which an excised lateral root primordia was able to continue to develop in hormone free media and therefore starts to get autonomous. This switch does occur between stage II and V.

2.2 Plant hormones affecting root development

2.2.1 General characterization

Plant hormones (phytohormones) are important biotic factors that are involved in virtually every developmental process. The role of the seven major hormones, including abscisic acid, gibberellin, auxin, ethylene, cytokinin, brassinosteroid, and jasmonate, has been extensively studied.

By the use of genetic screens numerous genes have been identified to be involved in hormone signal transduction. However, although these screens were originally designed to identify specific components involved in early hormone signalling, mutations in these genes often alter the sensitivity to more than one hormone at the whole-plant level. Furthermore, a variety of hormone response genes were identified through screens, which were originally designed to identify regulators of sugar metabolism. Collectively, these facts indicate that the linear representation of the hormone signalling pathways controlling a specific aspect of plant growth and development is not sufficient, and that hormones interact with each other and with a variety of developmental and metabolic signals (Gazzarrini and McCourt, 2003).

2.2.2 Auxin: biosynthesis, transport and signalling

The phytohormone auxin, with indole-3-acetic acid (IAA) as its naturally most abundant form, plays a role in nearly every aspect of plant growth and development including embryogenesis (Liu et al., 1993), leaf vascular patterning (Mattsson et al., 2003) and root gravitropism (Swarup et al., 2005). Numerous experiments also revealed a tight correlation between auxin and primary and lateral root development. Increased levels of auxins, either by exogenous application or by augmented synthesis inhibit primary root elongation and stimulate lateral root formation (Boerjan et al., 1995; Celenza et al., 1995). Additionally, mutants with decreased endogenous auxin levels display severe defects in lateral root formation (Fukaki et al., 2002). Auxin is initially synthesized in young leaf and flower tissue and the shoot apex and then transported to different target tissues where it triggers signalling cascades (Benjamins and Scheres, 2008). Up to now the exact cellular sites of auxin biosynthesis are not known but by the use of auxin labelling and quantification studies and the physiological characterization of

putative biosynthetical genes two auxin biosynthesis pathways were proposed. The tryptophan (Trp) dependant pathway involves cytochrome P450 as a catalysator (Mikkelsen et al., 2000); the existence of a Trp independent pathway was mainly proven by labelling experiments and involves indolic Trp-precursors (Ouyang et al., 2000).

The rapidness of the auxin signalling cascade that leads to the upregulation of auxin responsive genes within minutes can be explained by its molecular mode of functioning. The TRANSPORT INHIBITOR RESPONSE 1 (TIR1) protein which is part of the SCF^{TIR1} (for SKP1, Cullin, and F-Box protein) complex, was shown to be the auxin receptor and mediates, upon auxin binding, the ubiquitination and degradation of AUX/IAA proteins. AUX/IAAs functionally interact with auxin response factors (ARFs) and thereby inhibit their binding to auxin response elements (ARE), with the consensus sequence TGTCTC in promoter regions of target genes. Upon ubiquitination and degradation of the AUX/IAAs, the ARFs are released and can activate their target genes (Dharmasiri and Estelle, 2002; Hagen and Guilfoyle, 2002).

One unique feature of the auxin transport is its bidirectionality. From the shoot apex auxin is transported acropetaly (towards the root tip) through the vascular tissue; the outer root tissue mediates the basipetal transport upwards to the base. Additionally auxin transport displays polarity, resulting in a strictly regulated distribution and a concentration maximum in the QC and columella initials in the root tip (Fig.2e) (Feraru and Friml, 2008).

By the use of the auxin reporter DR5, that consists of a tandem copy of the auxin response element TGTCTC fused to a reporter gene and marks cells with a peak in free auxin, it could be shown that unequal auxin accumulation is already detetectable in early embryogenesis after the first division of the zygote, where auxin is directed to the apical cell (Fig.2a). At later stages the auxin peak coincides with the cells that give rise to the QC (Fig.2b-d) (Friml et al., 2003).

In its protonated form the weak acid auxin is able to enter the cell passively by diffusion. Due to the higher pH of the cytosol auxin is subsequently deprotonated and trapped in the cell. Therefore auxin needs to be transported actively out of the cell through plasmamembrane localized efflux carrier proteins (Rubery, 1974). Molecular genetic studies revealed that this efflux is mediated by the PIN FORMED (PIN) protein family, which consist in *Arabidopsis thaliana* of eight members that possess specific but overlapping expression pattern in the root meristem (Blilou et al., 2005; Paponov et al., 2005). An important aspect is that the specific asymmetric membrane localization of the PIN proteins coincides with the direction of the auxin transport and that these changes in PIN expression and localization during development allow remodelling of the auxin “superhighway”. Additionally it was demonstrated that auxin distribution appears to be altered in *pin* mutants (Sabatini et al., 1999; Blilou et al., 2005).
Beside the PIN proteins, the MULTIDRUG RESISTANCE (MDR)-p-glycoprotein (PGP) family of membrane proteins was shown to mediate auxin efflux (Noh et al., 2001) and recent data

revealed the colocalization and specific interaction of PIN and PGP protein families (Blakeslee et al., 2007). Additionally more recent data give evidence for the contribution of the asymmetrically localized auxin influx carrier AUX1 to polar auxin transport (Swarup et al., 2001).

Although auxin is biological active only in it its free, unbound form, approximately 99% of the total auxin pool in plants is conjugated to amino acids and sugars (Park et al., 2001; Pollmann et al., 2002). Thus, the regulation of hormone homeostasis is additionally severely dependent on the hydrolysis of auxin conjugates.

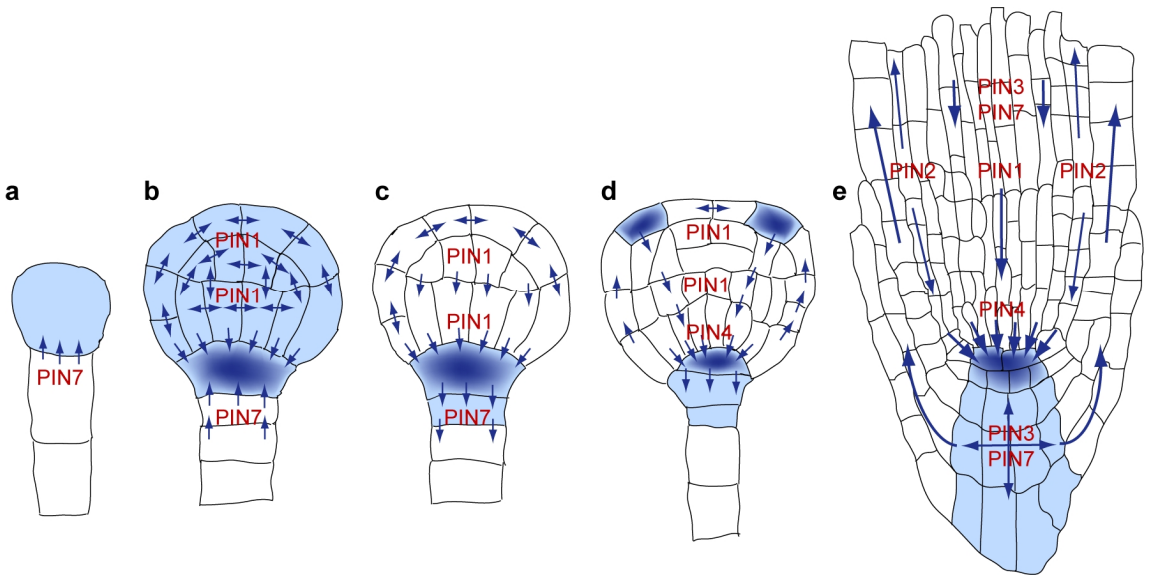

Figure 2. Establishment of the apical-basal polarity and polar localization of PIN proteins in the *Arabidopsis* embryo and the primary root tip.

At early stages of embryogenesis, PIN7 localizes to the apical sides of suspensor cells, mediating auxin flow into the proembryo (**a**), where PIN1 is localized first in a nonpolar manner (**b**). At the middle globular stage, PIN1 basal polarity in provascular cells is established, followed by PIN7 relocation to the basal side of suspensor cells. These PIN polarity rearrangements result in redirection of the auxin flow to the basal part of the embryo, where auxin accumulation contributes to root meristem specification (**c**). At later stages, PIN4 expression in the central root meristem aids the establishment of local auxin accumulation in the centre of developing root meristems. Furthermore, PIN1 relocates at the apical surface of the proembryo to establish two symmetrically positioned auxin accumulation foci, marking sites of future embryonic leaves (**d**). In the primary root tip PIN1 is localized at the basal (root apex-facing) side of the root vasculature; PIN2 at the basal side of the cortical cells and at the apical (shoot apex-facing) side of the epidermal and root cap cells; PIN3 in an apolar manner in the columella cells of the root; PIN4 at the basal side of cells in the central root meristem and with less pronounced polarity in the cells of the quiescent centre; and PIN7 at the basal side of the stele cells and apolar in the columella cells (**e**). Modified from (Feraru and Friml, 2008).

2.2.3 Ethylene

The gaseous hormone ethylene is involved, as a key regulator, in many aspects of higher plant development, best known for its role in fruit ripening (Chaves, 2006). Dark-grown seedlings that were exposed to ethylene exhibit characteristic phenotypic growth responses collectively termed the “triple response” (Knight, 1910): 1) A shortened and thickened hypocotyl, 2) an inhibition of root elongation and 3) an exaggerated apical hook (Guzman and Ecker, 1990). In

roots the effects of ethylene and its precursor 1-aminocyclopropane-1-carboxylic acid (ACC) have been studied more extensively and described to cause three growth responses: The induction of ectopic root hairs (Tanimoto et al., 1995), an increase in the width of the root (Smalle et al., 1997) and a rapid but reversible downregulation of cell elongation (Le et al., 2001).

It could be revealed that low concentrations of exogenously applied ACC promote, whereas higher doses strongly inhibit the initiation of lateral root primordia. However, high concentrations of ACC stimulate the emergence of existing lateral root primordial (Ivanchenko et al., 2008).

Recent data revealed that ethylene is also involved in the modulation of cell divisions in the QC during postembryonic root development (Ortega-Martinez et al., 2007).

In contrast to the simple structure of the auxin response pathway, the signalling cascade of the gaseous hormone ethylene is more complex. In *Arabidopsis thaliana* ethylene is sensed by a family of five receptors that function as negative regulators of the pathway. Binding of the hormone turns off the receptors, leading to the inactivation of CTR1, a Raf-like kinase that directly interacts with the receptors and, in turn, negatively regulates the activity of EIN2, a protein with unknown chemical activity. Derepression of EIN2 upon ethylene perception results in the activation of EIN3 and EIN3-like transcription factors which initiate a transcriptional cascade of hundreds of genes. EIN3 binds to promoters *of ETHYLENE RESPONSE FACTOR* (*ERF*) genes that regulate the expression of many downstream genes (Stepanova and Alonso, 2005).

Ethylene mutants that have been isolated using a screen with an altered triple response can be subdivided into two classes: 1) mutants that display a constitutive triple response phenotype even in the absence of ethylene and 2) mutants that possess ethylene insensitivity.

A constitutive ethylene response can result from both, either an ethylene over-production (*eto* mutants) (Guzman and Ecker, 1990) or mutations in the signal transduction pathway as has been found with the *ctr1* mutant (Kieber et al., 1993). Examples of ethylene-insensitive mutants are *etr1-1*, that possesses a mutation in an ethylene receptor (Bleecker et al., 1988) or *ein2*, with a mutated element of the signal transduction pathway (Alonso et al., 1999).

2.2.4 Ethylene/auxin interaction

Since numerous hormones affect overlapping processes, the physiological consequences of a hormone action can not be observed separately but in a combinatory manner. These hormone interactions can occur at the level of biosynthesis, of signalling or *via* a common action (Teal, 2008). The crosstalk between ethylene and auxin has been extensively studied in several aspects of development. In the root apex ethylene positively regulates auxin biosynthesis which

was demonstrated by measuring IAA and auxin-responsive reporter gene activity after ethylene induction (Swarup et al., 2007). Furthermore WEAK ETHYLENE INSENSITIVE2/ANTHRANILATE SYNTHASE1 (WEI2/ASA1) and WEI7/ASB1 genes that encode subunits of a rate-limiting enzyme of Trp biosynthesis, anthranilate synthase, are up-regulated by ethylene and WEI2/WEI7 mutants display altered endogenous auxin levels (Stepanova et al., 2005). The inhibitory effect of ethylene on root cell elongation is dependant on the basipetal transport of auxin to the elongation zone *via* the lateral root cap where ethylene activates local auxin responses. Beside the auxin biosynthesis ethylene also affects the auxin transport machinery (Swarup et al., 2007).

When auxin and ACC are applied simultaneously, the capacity of auxin to stimulate lateral root formation is not blocked by ACC in root tissue that was formed prior to the application of ACC. In opposite, auxin is not able to rescue the inhibitory effect of ethylene on primordia initiation in root tissue that formed after the exposure to ACC. Furthermore, in mutants that block auxin response (*slr1*, *arf7* and *arf19*) the initiation of lateral roots is insensitive to the stimulating effect of low concentrated ACC (Ivanchenko et al., 2008).

2.2.5 Cytokinins and their interaction with auxin

Similar to auxins, cytokinins have been implicated in nearly all aspects of plant growth and development including cell division, shoot initiation and leaf senescence (Mok and Mok, 2001). In their naturally occurring forms cytokinins are adenine derivates often with isoprenoid side chains, like the most abundant cytokinin in *Arabidopsis*, trans-zeatin. The root tip was shown to be the major location of cytokinin biosynthesis. Since cytokinins are also found in the xylem sap, it has been suggested that this class of hormones is transported from the root tip to the aerial parts of the plant and that purine transporters are involved in this transport (Gillissen et al., 2000).

The cytokinin signalling pathway is similar to the bacterial two-component phosphotransfer response systems and involves histidine kinases, histidine phosphotransfer proteins and downstream two classes of response regulators (ARRs), of which one class act as transcription factors (Mok and Mok, 2001).

The interaction of cytokinin and auxin is another example for the diverse effects of hormones in combinatory signalling pathways. Already in 1957 it has been demonstrated that the ration of cytokinin to auxin determines the type of organs that will regenerate from undifferentiated callus tissue *in vitro*: while a high cytokinin to auxin ratio usually promotes the production of many shoots and few roots, an opposite ratio induces the formation of more roots and less shoots. Equal concentrations result in the in the proliferation of undifferentiated tissue (Skoog and Miller, 1957).

By the use of a synthetic cytokinin reporter construct (TCS) it could be demonstrated that cytokinins are active already during early embryogenesis and auxin antagonizes cytokinin signalling which plays an important role in the specification of the root stem-cell niche (Muller and Sheen, 2008).

2.3 Genetic analysis of root development

Forward and reverse genetic approaches revealed genes that play an important role in the establishment and development of the root tissue. Beside transcription factors that are discussed in detail separately (see bellow), several cell cycle, hormone transport and biosynthetic related genes were identified (overview in (Scheres, 2002)). In the last decade much effort has been done to link gene functions to common regulating pathways.

HOBBIT

The *HOBBIT* (*HBT*) gene, which encodes a homolog of the CDC27 subunit of the anaphase-promoting complex APC, is required for the correct orientation of embryonic cell divisions in the embryonic root primordium and for the maintenance of cell division and cell differentiation in the QC, columella root cap and lateral root cap cells at postgerminative stages (Willemsen et al., 1998). Cell type specific marker lines revealed that HBT is rather involved in progression of cell differentiation than in pattern formation and that its transcription is cell cycle regulated (Blilou et al., 2002).

CULLIN3

CULLIN3 (CUL3) belongs to a class of Cullin-RING ubiquitin ligases (CRL3s) that control the degradation of important regulatory proteins in all eukaryotes. Modulating the emission of ethylene the Arabidopsis *CUL3* gene is involved in the regulation of primary root growth. Decreased levels of *CUL3* transcript result in the reduction of root meristem size and cell number. Furthermore *CUL3* plays a role in distal root patterning, by a mechanism that is independent of ethylene (Thomann et al., 2009).

MERISTEM-DEFECTIVE

Mutations in the *MERISTEME-DEFECTIVE* (*MDF*) gene, which encodes a putative RS domain containing protein, result in a loss of stem cell and meristematic activity in the root and shoot. Decreased levels of *PIN2*, *PIN4* and *PLT*, *SCR* and *SHR* in the *mdf* mutant and an associated defective auxin maximum in the root tip indicate that MDF acts in the auxin signalling pathway upstream of *PIN* and *PLT* gene expression (Casson et al., 2009).

PIN family

The *PIN* genes are thought to encode components of the auxin efflux machinery, mediating polar auxin transport and possess specific but overlapping expression patterns in the root meristem. In contrast to the strong phenotypic effects of auxin transport inhibitors and the *gnom*

mutant, which display impaired PIN1 vesicle transport (Steinmann et al., 1999), all single *pin* mutants described so far display different but only weak phenotypes in primary roots resulting, for instance, in agravitropic root growth in the *pin2* (Muller et al., 1998) and *pin3* (Friml et al., 2002) mutant or altered distal cell patterning like it was observed in the *pin4* mutant (Friml et al., 2002). The simultaneous investigation of five *PIN* genes revealed that PINs collectively control auxin distribution to regulate cell division and cell expansion in the primary root and the joint action of these genes plays a crucial role in pattern formation by focusing the auxin maximum (Blilou et al., 2005).

2.4 Cell type specific gene expression

Beside investigations on the level of single genes, several approaches were performed to get insight into relative expression levels of multiple genes among different cell types simultaneously. By use of root cell type specific GFP marker lines assisted with fluorescent activated cell sorting (FACS) and microarray analysis the relative expression of more than 22,000 genes in *Arabidopsis* was mapped to 15 different zones of the root (Birnbaum et al., 2003).

To identify genes that are enriched in the QC in comparison to the surrounding tissue a similar experiment was performed using a QC-specific GFP marker line (Nawy et al., 2005). Among 290 genes that were found in total to be transcriptionally enriched in the QC, several genes have already been described to be expressed in the stem cell niche. *Vice versa*, by promoter reporter gene fusions new genes could be confirmed to be expressed in the QC.

Furthermore an extended variant of the root expression map has been used to identify cell-type–specific stress responses to high salinity and iron deprivation (Dinneny et al., 2008).

2.5 Transcription factors

Transcription factors (TFs) are defined as proteins that are capable of binding directly to *cis*- or response elements (REs) in the promoters of target genes in a sequence specific manner resulting in their transcriptional activation or repression by interacting with the basal transcription initiation complex (Fig.3). Most known TFs can be grouped into families by their DNA binding domain (Riechmann et al., 2000). Increasing genomic sequence information of various monocots and dicots species gave insight into structural and functional similarities and differences of transcription factors on a genome-wide scale. The *Arabidopsis thaliana* genome was initially estimated to contain 1533 TF open reading frames (ORFs) (Riechmann et al., 2000). More recent approximations suggested a TF gene number of 2304, which account 7,5% of the estimated total number of genes (Pérez-Rodríguez, 2009). These differences in the amount of genes result from the used bioinformatic search stringency and different definitions of unclassified TFs.

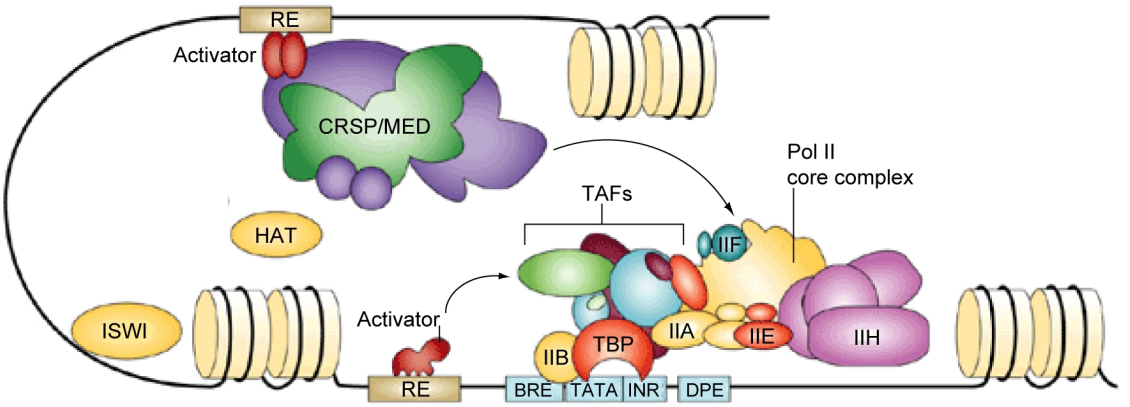

Figure 3. Schematic representation of the eukaryotic transcription initiation complex.

The promoter-recognition and DNA-melting activities are divided among the general transcription factors, which include TFIIA, TFIIB, TFIID, TFIIE, TFIIF and TFIIH (not all polypeptides are shown). TFIIA, TFIIB, and TFIID recognize the promoter-proximal DNA elements including the TATA box, the BRE (TFIIB recognition element), the initiator (INR) element and the downstream promoter element (DPE). TFIIF binds to Polymerase (Pol)II and helps to recruit the enzyme to the promoter region. TFIIE binds TFIIH and helps recruit it to the promoter region. TFIIH melts the DNA allowing PolII access to the template strand. In addition, TFIIH can phosphorylate the carboxy-terminal domain of PolII to help it escape the promoter. ISWI (imitation switch) and histone acetyl transferases (HATs) work to remodel and modify chromatin structure and can be present in numerous multisubunit complexes. CRSP/MED complexes are thought to mediate signals between enhancer-bound factors and the transcriptional machinery. RE, response element; TAF, TATA-binding protein (TBP)-associating factor. Modified from (Taatjes, 2004).

The *Arabidopsis thaliana* TF genes have been classified into 60 families. Additional 22 gene families encode for other transcriptional regulators (Pérez-Rodríguez, 2009). Six TF families include more than 100 members, which are the APETALA2/ETHYLENE RESPONSE ELEMENT BINDING PROTEIN (AP2/EREBP) family (146 members, splicing variants excluded), the basic helix-loop-helix (bHLH) family (136 members), the C2H2 Zn-finger family (101 members), the MADS family (103 members), the MYB family (145 members) and the NAC family (101 members) (Pérez-Rodríguez, 2009).

Many transcription factor families are plant-specific. These include large families like the AP2/EREBP and NAC TFs and numerous smaller ones like the trihelix DNA binding proteins, the auxin response factors (ARFs) or TFs of the GRAS family (Riechmann et al., 2000; Pérez-Rodríguez, 2009).

Beside the transcriptional regulation by TFs themselves, the cleavage of TF transcripts by endogenous microRNAs (miRNAs) seems to play an important role in their regulation. In *Arabidopsis thaliana* among 49 predicted targets of 14 miRNAs, 34 were identified to be TFs (Qu and Zhu, 2006). The transcripts of auxin response factors ARF10, ARF16 and ARF17, for example, are targeted by miRNA160 and their negative regulation plays a critical role in seed germination and post germination stages (Liu et al., 2007) and miRNA166-mediated cleavage of

the homeobox TF *AtHB15* mRNA is a key step in the regulation of vascular development (Kim et al., 2005).

2.5.1 DOF domain TF family

DOF (DNA-binding with one finger) proteins are plant-specific transcription factors with a DNA-binding domain forming a single Cys2/Cys2 Zn^{2+}-finger of 52 amino acid residues that recognizes *cis*-regulatory elements containing the common core 5´-A/TAAG-3´ (Yanagisawa and Schmidt, 1999). The highly conserved DOF domain is located as a single copy generally in the N-terminal region of the protein, whereas the C-terminal part of the protein that contains the transactivation domain is characterized by very divergent amino acid sequences (Yanagisawa, 2002).

While a single *DOF* gene was identified by bioinformatics searches in the *Chlamydomonas reinhardtii* genome (Moreno-Risueno et al., 2007), the genomes of higher plants contains a number of *DOF* genes. For example, 37 putative genes encoding DOF domain proteins were identified in the Arabidopsis genome (Yanagisawa, 2002) and a similar number (30 genes) were found in the genome of rice (Lijavetzky et al., 2003).

DOF TFs have been proposed to regulate plant specific vital processes such as light-responses (Yanagisawa and Sheen, 1998; Papi et al., 2002), phytochrome signalling (Park et al., 2003), responses to plant hormones including auxin (Kisu et al., 1998) and gibberellin (Mena et al., 2002), seed germination (Gualberti et al., 2002), tissue-specific expression in endosperms (Vicente-Carbajosa et al., 1998), leaves (Yanagisawa and Sheen, 1998) or guard cells (Plesch et al., 2001). Yet only a few members of the DOF family have been functionally characterized.

2.5.2 Transcription factors involved in root development

Many of the genes that have been identified to be involved in root development encode for TFs that in turn can interact with other transcriptional activators and repressors, resulting in cascades of genes that lead to elementary morphological, physiological or metabolic developmental programs. In the last decade extensive progress was achieved in the definition of these complex functional transcription factor networks.

Due to the increasing evidence that sequences other than upstream non-coding can contribute to modulating gene expression, the regulation of 61 cell-type enriched root TFs has been investigated by comparing the signals of GFP reporter constructs driven by each TF's upstream non-coding sequence fused to the reporter gene alone or together with the TF's coding sequence. It was found that the upstream non-coding sequence was sufficient to recapitulate the mRNA expression pattern for 80% of the TFs. Interestingly 25% of *Arabidopsis* root TFs undergo posttranscriptional regulation *via* microRNA-mediated mRNA degradation or *via* intercellular protein movement, suggesting that modulation of transcription factor protein expression pattern after transcription is relatively frequent (Lee et al., 2006).

MONOPTEROS (MP)/BODENLOS (BDL)

The primary root meristem is established through stereotyped cell divisions in early stages of embryogenesis. Mutations in either the *MP* or *BDL* genes, which belong to the family of auxin response factor (*ARF5*) and *AUX/IAA* (*IAA19*) genes, respectively, result in abnormal cell divisions of the apical daughter cell of the zygote and affect the orientation of the proembryo. In both mutants, the apical daughter cell divides horizontally to form four instead of two tiers of embryonic cells leading to the formation of a double octant proembryo (Berleth, 1993; Hamann et al., 1999). By consequence, the hypophysis fails to undergo asymmetric cell divisions that would give rise to the precursors of the QC and columella cells. While strong alleles do not develop a primary root at all, less severe alleles result in strongly reduced root systems (Berleth, 1993). The *mp*/*bdl* double mutant shows identical phenotypes that are observed in the single mutants, suggesting that both genes act in the same developmental pathway (Hamann et al., 1999). Indeed, *MP* and *BDL* are expressed in the same tissue. First signs of expression are evident after the asymmetric division of the hypophysis, where both *BDL* and *MP* mRNAs are observed in its smaller lens-shaped daughter cell that gives rise to the QC of the root meristem. Thus, there was a coordinated basal shift in the expression domains of both genes at the globular stage. At later stages in embryogenesis, *MP* but not *BDL* is expressed in the central root cap (Fig.4a and 4b), which displays the only conspicuous difference between the two gene expression patterns. Furthermore it could be shown that both proteins physically interact (Hamann et al., 2002). Beside the strong interaction between the MP and BDL pathways it was demonstrated that MP and its homolog *NON-PHOTOTROPIC HYPOCOTYL4* (*NPH4, ARF7*) possess overlapping and non-redundant functions and are both capable of controlling axis formation in the embryo and auxin-dependent cell expansion (Hardtke et al., 2004). Recent data revealed the involvement of an additional protein interaction partner, TOPLESS (TP), a transcriptional co-repressor, which directly binds to BDL and is required for its repressive activity (Szemenyei et al., 2008) and *DORNROESCHEN* (*DRN*), which encodes a member of the AP2-type transcription factor family, and is a direct target of MP (Cole et al., 2009).

SCARECROW (SCR)/SHORT ROOT (SHR)

The GRAS family transcription factors SCR and SHR have been identified in screens for mutants, that disrupt patterning of the ground tissue and vascular cylinder (Scheres, 1995). In both mutants instead of cortex and endodermis a single mutant layer is found between the procambium and the epidermis. The use of tissue specific markers revealed that the mutant layer is specified differently in both mutants. While in *scr* markers for both, the endodermis and cortex are present in the single mutant layer, in *shr* only markers for the cortex are found, indicating that SCR is required for the correct periclinal division of the cortex/endodermis initial cell but is not involved in the cell specification, whereas SHR is required for both, the initial cell division as well as the specification of the endodermis (Di Laurenzio et al., 1996).

Ectopic expression of *SHR* driven by the 35S promoter leads to supernumerary cell layers with altered cell fates (Helariutta et al., 2000). However, when *SHR* is expressed under control of the

SCR promoter a very specific increase in ground tissue layers was detected (Nakajima et al., 2001). In strongly expressing lines, these additional ground tissue cells express endodermal markers, confirming the tight correlation between the presence of SHR protein and endodermal cell fate.

SHR is transcribed exclusively in the vascular tissue (Fig.4f), but its protein moves on cell layer outwards to the endodermis including the cortex/endodermis initials and the QC cells (Fig.4g), where it directly activates *SCR* expression. *SCR*, in turn, is expressed solely in the endodermal cell file, the cortex/endodermis initials and the QC cells (Fig.4h) and its protein forms a heterodimer with SHR, which is required for SHR to bind to the *SCR* promoter. This feedback loop is suggested to facilitate the rapid up-regulation of *SCR* expression and sequester the SHR protein in the nucleus of endodermal cells, which anticipates the movement to further cell layers (Levesque et al., 2006; Cui et al., 2007). Addtionally, both *scr* and *shr*, lack an appropriately specified QC and fail to maintain columella initials (Sabatini et al., 2003).

WOX5

WUSCHEL (WUS) is a well characterized homeobox TF, which is expressed in the organizing centre of the shoot apical meristem and keeps stem cells undifferentiated and induces expression of the gene encoding for the signal peptide CLAVATA3 (CLV3), which in turn restricts the size of the *WUS* expression domain (Mayer et al., 1998). With the purpose to identify similar signalling pathways in the root, the WUSCHEL-RELATED HOMEOBOX (WOX) family was screened for functions in the root meristem (Haecker, 2003). *WOX5* was found to be expressed in the QC (Fig.4e) and its embryonic precursor cells. *wox5* null mutants display terminal differentiation in distal stem cells and, redundantly with *SCR* and *SHR,* also provoke differentiation of the proximal meristem, since *wox5/scr* and *wox5/shr* double mutants show more severe phenotypes than the single mutant lines. In opposite, ectopic expression of *WOX5* blocks the differentiation of distal stem cell descendents that normally differentiate. Importantly, both *WOX5* and *WUS* are interchangeable to maintain the stem cells status in either the shoot or root apical meristem (Sarkar et al., 2007).

In *bdl* or *mp* mutants *WOX5* expression is rarely detected, consistent with the finding that *BDL*/*MP*-mediated auxin signalling is required for the embryonic initiation of the QC. Furthermore, *WOX5* expression is reduced or undetectable in *shr* and *scr* mutants, whereas *SCR* is correctly expressed in *wox5* null mutant roots. These data indicate that *WOX5* expression depends on the induction by MP-mediated auxin signalling and on SHR/SCR activity. By contrast, the PLETHORA TFs PLT1 and PLT2 play only a minor role in promoting *WOX5* expression in the QC (Sarkar et al., 2007).

PLETHORA (PLT) transcription factors

The AP2/EREBP transcription factors PLT1 and PLT2 were identified in a screen of GUS enhancer trap lines for GUS staining of the distal region of the root meristem. *PLT1*/*PLT2* mRNA is detectable in the QC, the surrounding stem cells and the uppermost cell tier of differentiated columella cells (Fig.4k and 4l, respectively). While mutations in single *PLT* genes cause only subtle defects in distal cell division pattern and root cell elongation, *PLT1*/*PLT2* double mutants display severe root phenotypes with an extremely reduced root size and a decrease in the number of meristematic cells, whereas the number of columella cells is increased and include differentiated cells at the position of columella initials. Taken together with the lack of QC marker gene expression the data indicate that PLT1 and PLT2 are redundantly required for correct QC establishment and stem cell maintenance. Furthermore it was demonstrated that *PLT1* and *PLT2* are still active in the *scr* and *shr* mutant background and conversely, that *SCR* and *SHR* are active in the *plt1plt2* double mutant, indicating that both pathways provide independent inputs in the root stem cell niche specification. *MP* and *NPH4* work upstream of the *PLT* genes since in *mp/nph4* double mutants *PLT* transcripts are rarely detectable. Ectopic expression of *PLT* genes lead to the ectopic formation of the root stem cell niche and transformations into root or hypocotyl identity (Aida et al., 2004) More recent data revealed two further plethora TFs, AINTEGUMENTA-LIKE6 (AIL6/PLT3) and BABY BOOM (BBM). *PLT3* messenger RNA accumulates in the root stem cell niche with the strongest signal in the columella stem cell layer (Fig.4m). *BBM* transcript accumulates in the quiescent centre and columella stem cells (Fig.4n). The activities of all four PLT homologues (PLT1, PLT2, AIL6/PLT3 and BBM) are additive and dosage dependant to maintain the stem cell identity and to determine the size of the transit-amplifying daughter cells. (Galinha et al., 2007).

JACKDAW (JKD) AND MAGPIE (MGP)

The C2H2 zinc finger transcription factors JKD and MGP were identified in screens of GUS promoter trap lines for mutants harbouring an expression pattern similar to *SCR* and defects in the asymmetric cell divisions of the ground tissue. *JKD* transcript is detectable in the QC, the cortex/endodermis stem cells, and to a lesser extent in mature cortex and endodermis cells (Fig.4c), whereas *MGP* mRNA accumulates in ground tissue and stele cells but is absent from the QC (Fig.4d). *jkd* mutants display a slight reduction in root length compared with wild-type, furthermore the root meristem cell number is reduced in comparison to that of wild-type. Columella cells adjacent to the QC contain starch granules, indicating the absence of columella stem cells in the *jkd* mutant. In contrast *mgp* RNAi lines reveal no phenotype on their own. Additionally the *jkd* mutant roots display ectopic periclinal divisions in the cortex resulting in ground tissue with three layers which, in turn, possess more cell numbers as are found in the wild-type endodermis and cortex.

During embryogenesis *JKD* expression is not affected in *scr* and *shr* mutants. However at postgerminative stages QC and ground tissue stem cell expression of *JKD* is strongly reduced

in the *shr* but not in the *scr* mutant. In contrast, *MGP* mRNA is hardly detectable at any developmental stages in the *shr* background and strongly reduced in the *scr* mutant. In *plt1plt2* double mutants, neither *JKD* nor *MGP* transcript accumulation was affected (Welch et al., 2007).

SOMBRERO (SMB)/FEZ

The NAC-domain transcription factors SMB and FEZ were identified by screening mutagenized columella/lateral root cap marker lines for expression changes. *SMB* and *FEZ* transcripts accumulate in embryonic domains that give rise to the columella and lateral root cap and their descendants (Fig.4i and 4j, respectively). FEZ promotes periclinal cell divisions of the lateral root cap/epidermis stem cells leading to the formation of lateral root cap as *fez* mutants possess highly reduced periclinal division rates, whereas anticlinal divisions that form the epidermis are not effected. SMB, in turn, represses *FEZ* acitivity and inhibits stem cell-like divisions in the root cap daughter cells. *smb* mutants possess an extra layer of small stem cell-like cells below indicating its role in daughter cell fate. Through the positive regulation of its repressor SMB, FEZ generates a feedback loop for controlled switches in cell division plane. Interestingly, the initiation of *FEZ* and *SMB* transcription does not require any known root patterning protein like SHR, SCR, PLT1, -2 or -3, WOX5 or RETINOBLASTOMA RELATED (RBR) protein (Willemsen et al., 2008).

ARF10/ARF16

The redundantly working auxin response factors *ARF10/ARF16* were shown to be expressed in the root with a high maximum in the central root cap (Fig.4o), an expression pattern that strongly coincides with the expression of the DR5 auxin reporter gene (Liu et al., 2007). Together with *ARF17* which is expressed in a less specific manner in the root, *ARF10* and *ARF16* activity is negatively regulated by miRNA160, which, in turn, is expressed in the vascular bundle of primary and lateral roots, but not in root cap cells. Ectopic expression of miRNA160 leads to similar phenotypes as observed in *the arf10/arf16* double knock-out mutant and results in agravitropism, reduced primary root length and an increased number of lateral roots. Root cap cells are irregular in shape and lacking starch granules, in accordance with the absence of the gravitropic response. Expression of miRNA-cleavage resistant forms of *ARF10* and *ARF16* leads to pleiotropic phenotypes like serrated leaves, curled stems and a reduced lateral root number. In the *mp* mutant background *ARF16* transcript is not detectable, confirming the upstream regulating role of auxin signalling (Wang et al., 2005).

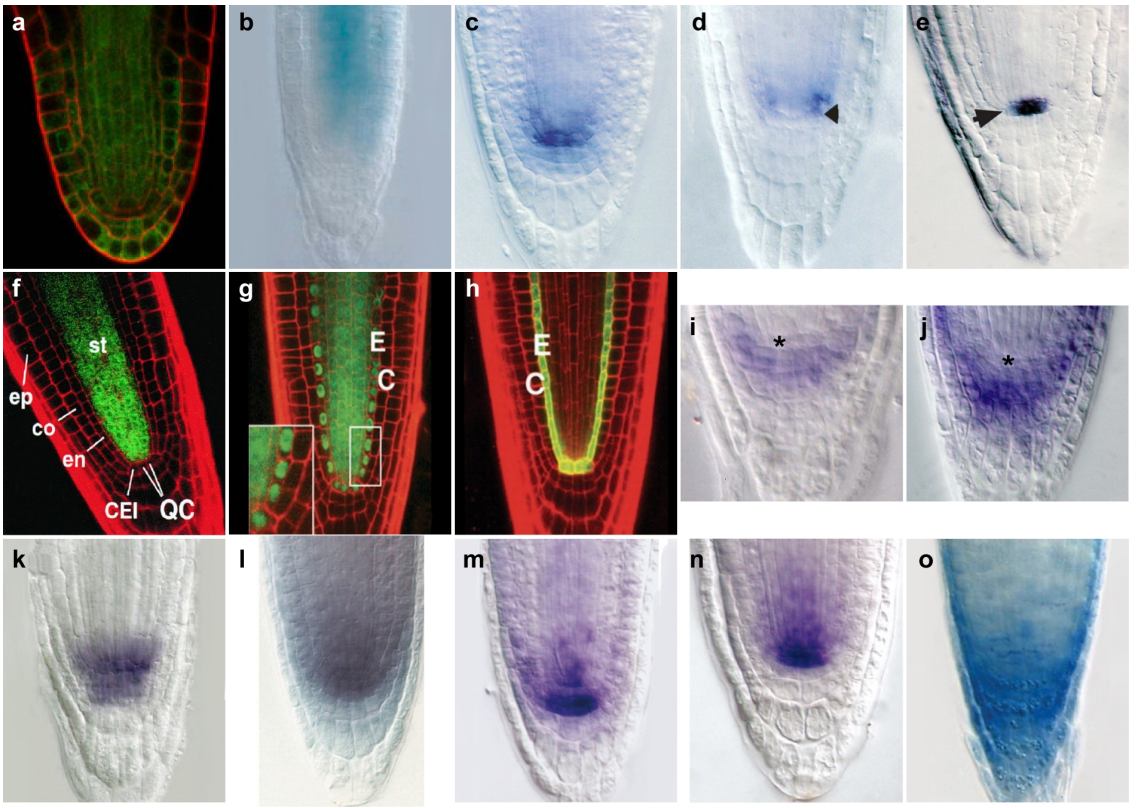

Figure 4. Expression pattern of TF and transcriptional activator genes involved in root development.

a *pMP::GFP* in the lateral root (Vidaurre et al., 2007). **b** *pBDL::GUS* in the primary root (Dharmasiri et al., 2005). **c** Whole-mount *in situ* hybridization with a *JKD* probe in 3-dpg wild-type Col-0 seedling (Welch et al., 2007). **d** *MGP* expression in 3-dag wild-type seedling. Arrowhead marks cortex/endodermis stem cell (Welch et al., 2007). e *WOX5* mRNA expression in the quiescent centre (marked by arrowhead) (Sarkar et al., 2007). **f** *pSHR:::GFP* in 6-day-old wild-type seedling. ep, epidermis; co, cortex; en, endodermis; CEI, cortex/endodermal initial; QC, quiescent center; and st, stele (Helariutta et al., 2000). **g** SHR-GFP localization (*pSHR::SHR-GFP*) in 6-day-old wild-type seedling. The inset is an enlarged image of the framed area. **h** *pSCR::GFP* in 6-day-old wild-type seedling. C, cortex; E, endodermis (Cui et al., 2007). **i** Whole-mount *in situ* hybridization with a *FEZ* probe. **j** *SMB* mRNA. Asterisks indicate position of QC (Willemsen et al., 2008). **k** Whole-mount *in situ* hybridization with *PLT1* probe in wild-type WS. **l** Whole-mount *in situ* hybridization with *PLT2* probe in wild-type WS (Aida et al., 2004). **m** *In situ* hybridization with *PLT3*-specific probe in roots of 3-dag-old wild-type plants. **n** Whole-mount *in situ* hybridization with *BBM* in roots of 3-dag-old wild-type plants (Galinha et al., 2007). **o** *pARF16::GUS* in the primary root tip (Wang et al., 2005).

2.6 Aim of the thesis

Our research group has a major focus on the functional characterisation of transcription factors, particularly on *Arabidopsis thaliana* DOF proteins. In previous studies it was shown that *DOF3.1* possesses a specific expression pattern in the quiescent centre and a strong root phenotype in RNAi plants, which, however, was absent in *dof3.1* T-DNA insertion lines. The aim in this project was to identify further *DOF* genes expressed in the QC which share redundancy with *DOF3.1* and to evolve the physiological role of DOF TFs in the stem cell niche. Additionally, previous work in the group revealed an *Arabidopsis* diacyl-glycerol-kinase gene (*AtDGK7*) with specific expression in the columella and lateral root cap cells. Since *dgk7* T-DNA insertion lines were shown to possess reduced number of lateral roots, in this work by the use of promoter deletion studies upstream regulating factors should be identified and characterized in detail to unravel transcriptional activating pathways in the root cap. Finally preliminary data indicated that DOF proteins possess a novel type of bipartite NLS, which should be further analysed by GFP fusion proteins combined with the transient protoplast transformation system.

3. *Arabidopsis* DOF1.2 and DOF3.5 zinc finger proteins integrate auxin status and developmental plasticity of the root cap

1. Jonas Krebs[1]
2. Slobodan Ruzicic[2]
3. Bernd Mueller-Roeber[1]

[1] *Department of Molecular Biology, Institute for Biochemistry and Biology, University of Potsdam, Karl-Liebknecht-Str. 25 Haus 20, D-14476, Golm, Germany*

[2]*Cooperative Research Group, Max-Planck Institute for Molecular Plant Physiology, Am Muehlenberg 1, D-14476, Golm, Germany*

Manuscript in preparation

Authors´ contributions

The experimental work was entirely performed by Jonas Krebs. The research was designed and planned by Jonas Krebs and Slobodan Ruzicic. Bernd Mueller-Roeber supervised the group as a whole.

3.1 Abstract

Mechanisms that control cellular patterning and the cytological structure of root cap cells, as a central organ in the process of orientated root growth and sensing of the environment, are poorly understood. In *Arabidopsis*, the gradient of auxin distribution, precisely defined by *PIN* genes, is required for the specification of the lateral root cap (LRC) and columella (COL) cells building a gravity sensing centre. Moreover, auxin influences the process of border cell formation and their detachment in the surrounding, a process of extreme importance in protecting the root against abiotic and biotic stress. Here we show that the root cap specific genes *DOF1.2* and *DOF3.5*, two novel members of a plant-specific zinc finger family, operate in an auxin-regulated loop including two members of the ARF family, *ARF10* and *ARF16*. Auxin transport inhibitors initiate within minutes expression of *DOF1.2*. Furthermore, *DOF1.2* affects expression of *PIN2* and *PIN4* genes in the root cap boundaries. The tissue-specific expression and defects in the roots of *dof1.2* mutants suggest that *DOF1.2* has a central role in the differentiation of columella cells affecting both, the establishment of gravity-sensing properties and the process of border cell release. In addition, DOF1.2 represents a cross point in the integration of hydrotropic stimuli from the surrounding and the endogenous gravitropic program.

3.2 Introduction

Growth and morphogenesis of the plant root result from an integrated action of endogenous developmental programs and an adaptation to environmental stimuli. The radial pattern of the *Arabidopsis* root relies on a precise program of cell division and differentiation taking its origin in the stem cell niche located in the root apex. Only a few dozen of basal derivatives of the stem cell niche build the root cap, principally by periclinal divisions in the epidermis/LRC stem cells that generate the LRC and anticlinal divisions in the COL cells that generate the columella (Dolan et al., 1993; Willemsen et al., 2008). Functionally the root cap evolves also a dual role. On one hand by the differentiation and deposition of starch grains in columella cells the gravity sensing center is being defined (Sack, 1997). On the other hand, by poorly understood mechanisms the most outer cell layers of LRC and COL are being detached from the root cap and released in the external environment (Driouich et al., 2007). Recent data emphasise a possible involvement of these border cells (BC) in the protection of the root system against abiotic and biotic stresses (Hawes et al., 2000; Pan et al., 2004).

The identity of the root cap is largely defined by the action of the phytohormons auxin and ethylene (Ponce et al., 2005). The orientation of cell division in root cap cells can be influenced by the accumulation of auxin upon treatment with auxin efflux inhibitors (Sabatini et al., 1999). But, auxin defines also the differentiation of root cap cells, promoting the starch grains formation and thus potentiates the gravitropic response (Sabatini et al., 1999; Ponce et al., 2005). In addition, auxin and auxin transport inhibitors significantly increase the sloughing process (del Campillo et al., 2004; Driouich et al., 2007). The distribution of auxin in the root primordial is

regulated by temporary and spatially programmed collective action of PIN auxin efflux facilitator proteins (Blilou et al., 2005). In the range of the root cap the auxin gradient could be contributed by action of PIN2, located apically in the membrane of LRC cells (Muller et al., 1998), PIN3 and PIN7, distributed uniformly in the membranes of second and third tiers of COL cells (Friml et al., 2002; Blilou et al., 2005) and presumably by plasma membrane located PIN4, detected around the quiescent center (QC) and cells surrounding it (Friml et al., 2002). *pin3*, *pin4* and *pin7* single mutants exhibit only subtle defects in the division of the QC and COL cells (Friml et al., 2002). Different mutant combinations of *PIN1*, *PIN3*, and *PIN7* genes with *pin2* give rise to phenotypical changes identical to those observed after genetic ablation of root cap cells (Tsugeki and Fedoroff, 1999). In addition, such plants displayed a high accumulation of the auxin reporter *DR5::GUS* in provascular cells. This indicated the mediator role of COL cells in the lateral auxin redistribution (Blilou et al., 2005). The redistribution of auxin by *PIN2* from the root tip upward in the epidermal cells contributes massively to the gravity response of plant root, explaining the agravitropic phenotype observed in *pin2* mutants (Muller et al., 1998; Wisniewska et al., 2006). The expression status of *PIN* genes seems not only to affect the gravity response function of the root cap but also its sloughing properties: *AtPIN4* antisense and *pin4* plants displayed up to eight additional non-detached layers of the root cap (Friml et al., 2002).

The regulation of expression of auxin response genes represents a cascade mechanism including auxin dependent ubiquitination and degradation of proteins from the Aux/IAA family, which are able to dimerize with members of the auxin response factor (ARF) family, and thereby repress their function. ARFs are transcriptional activators or repressors that regulate the expression of auxin response genes by specific binding to the TGTCTC auxin response element (AuxRE) in the promoter regions of these genes (Guilfoyle and Hagen, 2007). At least two ARFs display a root cap specific expression, namely *ARF10* and *ARF16*, whose mode of expressional regulation implicates micro RNA miR160 (Wang et al., 2005).

Despite considerable efforts, up to date no regulatory factor was identified, which integrates components involved in the establishment of the auxin gradient, the processes of morphological differentiation of the root cap and the functional sensing of gravity (and other tropism). Here, we identify the *DOF1.*2 and *DOF3.*5 genes, encoding members of the plant-specific DOF transcription factor family, specifically expressed in the root cap. We show that the expression of both genes temporarily coincides with the development of the gravitropic response in the primordial root and narrow the region responsible for the cell-specific expression of *DOF1.2* gene. We find that the expression of *DOF3.5* and one further root cap specific gene, *AtDGK7*, is regulated by DOF1.2. Our study reveals that the expression of *DOF1.2* and *DOF3.5* is dependent on the auxin gradient in the root apex and, through a loop mechanism, is regulated by ARF10 and ARF16. We demonstrate that DOF1.2 is required for the proper patterning of columella cells, their differentiation and hence the gravitropic response of the root. Since *DOF1.2* suppressing lines lack a hydrotropic response we have strong indication that DOF1.2

represents a cross point in the hydrotropic and gravitropic response pathways. Moreover, we observe the effects of DOF1.2 on expression of the *PIN2* and *PIN4* genes as well as changes in the distribution of an auxin reporter indicating the existence of an auxin dependent loop mechanism in the root cap region. These data provide unambiguous evidence that DOF1.2 works as a key regulator of signal transduction pathways and a central integrator of most important stimuli and developmental processes in the root cap.

3.3 Material and Methods

3.3.1 Plant materials and growth conditions

Arabidopsis thaliana seeds were surface-sterilized using sodium hypochlorite solution (10%) and sown on nutrient agar medium (1x Murashige and Skoog and 1% sucrose, pH 5,8). The vertically orientated plates were stored for two days under vernalization conditions (16 hours light, 22°C and 8 hours dark, 4°C) and subsequently transfered to long day growth conditions (16 hours light, 22°C and 8 hours dark, 18°C).

The Q0680 GFP marker line and T-DNA insertion lines *dof1.2-1* (GABI_921E09), *dof1.2-2* (SAIL_99_C09) and *dof1.2-3* (SALK_053911) were obtained from the Nottingham *Arabidopsis* Stock Center (NASC) and the insertion site were tried to be confirmed by PCR-based genotyping.
In the case of *dof1.2-1* PCR was performed using the gene specific primer pairs 5' CCCGGGAAAATGGTTTGTCAGGAAAA 3' (forward) and 5' TCTAGATCAAATCCCGAACCTGGTAA 3' (reverse) and the GABI T-DNA primer o8409 5´ ATATTGACCATCATACTCATTGC 3´.
To confirm the T-DNA insertion in *dof1.2-2* and *dof1.2-3* PCR reaction was performed using the gene specific primer pairs 5' CTCGAGATGTTGCCGTACATTGGACA 3' and 5' TCTAGATCAAATCCCGAACCTGGTAA 3' (reverse) and the T-DNA primers LB3 (5´ TAGCATCTGAATTTCATAACCAATCTCGATACAC 3´) and LBa1 (5´ TGGTTCACGTAGTGGGCCATCG 3´) respectively.

The T-DNA insertion sites could be confirmed only in the case of *dof1.2-1* and *dof1.2-2* (Supplementary Fig.1) and lines were propagated to homozygosity.

The *arf10/arf16* double knock-out as well as the *p35S*::*miRNA160C* line was kindly provided by Professor Xiao-Ya Chen, Shanghai, China.

3.3.2 Vector construction and transformation

All PCR products were amplified using *Pfu* polymerase and after A-tailing first cloned into the pCR2.1 cloning vector (Invitrogen, Karlsruhe, Germany). For subsequent cloning into binary

vectors, pCR2.1 vector was digested as described in the following. The used restriction enzyme sites are part of the listed primer sequences and monitored with bold letters.

Plasmids for *DOF1.2* promoter-GUS fusions were generated by cloning of 600bp to 100bp of the upstream intergenic region (with respect to ATG) using the forward primers 5' **CCCGGG**CGATAAGCAAACCCGAAACA 3' (604bp), 5' **CCCGGG**GACATCTCTCATTTTTCTAA 3' (508bp), 5' **CCCGGG**AAAATGGTTTGTCAGGAAAA 3' (393bp), 5' **CCCGGG**CCAATTGTTTACCAAAACTT 3' (302bp), 5' **CCCGGG**GCCCACGTTTACTTCGAAAC 3' (198bp), 5' **CCCGGG**CACACCCGTATATATAGAGT 3' (106bp) and the reverese primer 5' **GTCGAC**AATCCCGAACCTGGTAAGAT 3' into pGPTV-HYG vector that was previously digested with HindIII, blunted and subsequently digested with SalI. In the case of *DOF3.5* a 1,5kb fragment of the upstream intergenic region was cloned into pGPTV-KAN vector using the forward primer 5' **GTCGAC**GCAGAAAGGAGTTAAAGTGC 3' and the reverse primer 5' **TCTAGA**ATCTCTCTCGCTCTTCTTTA 3'.
The construct for artificial microRNA mediated downregulation of *DOF1.2* was generated by using the primers I (5' GATCAACGAGGACAAGCCGGAGCTCTCTCTTTTGTATTCC 3'), II (5' GAGCTCCGGCTTGTCCTCGTTGATCAAAGAGAATCAATGA 3') III, (5' GAGCCCCGGCTTGTCGTCGTTGTTCACAGGTCGTGATATG 3') and IV (5' GAACAACGACGACAAGCCGGGGCTCTACATATATATTCCT 3') following the protocol of the Web MicroRNA Design tool (http://wmd.weigelworld.org/cgi-bin/mirnatools.pl). To express the obtained gene specific amiRNA fragment under control of the endogenous *DOF1.2* promoter, the *DOF1.2* 604bp promoter fragment specified above was cloned into the pBI-JFH1 vector that was digested with HindIII blunted and subsequently digested with SalI. The amiRNA fragment was digested with SalI and XbaI and cloned into the modified pBI-JFH1 vector that was likewise digested with SalI and XbaI.

For overexpression of *DOF1.2* its coding sequence was amplified using the primer pairs 5' **CTCGAG**ATGTTGCCGTACATTGGACA 3' (forward) and 5' **TCTAGA**TCAAATCCCGAACCTGGTAA 3' (reverse) and for constitutive overexpression cloned into pJFH1 vector that was previously digested with XhoI and XbaI, For the purpose of inducible overexpression the obtained fragment was cloned into pER8 vector (kindly provided by Nam-Hai Chua, Rockefeller University, New York) that was previously digested with XhoI and SpeI.

The DR5rev::GFP plasmid was kindly provided by Gerd Jürgens (Universität Tübingen, Germany).

All plasmids were transformed for cloning procedures into *E. coli* DH5α competent cells, for plant transformation into the *Agrobacterium tumefaciens* strain GV3101.

Plant transformation was performed by the floral dip method (Clough and Bent, 1998) and the *Arabidopsis thaliana* Col-0 ecotype. All primary transformants were selected on nutrient agar medium supplemented with either 50mg l^{-1} kanamycin, 20mg l^{-1} hygromycin or and propagated to T2 generation.

One selected DR5rev::GFP transformant and the Q0680 marker line were crossed with the *DOF1.2* overexpression lines #1 and #2 and the *DOF1.2* amiRNA lines #9 and #13.

3.3.3 Gene expression analysis

RNA was extracted from whole seedlings using the RNeasy Kit (QIAGEN). Genomic DNA was digested on the columns using the RNase free DNase set (QIAGEN). cDNA was prepared from 3µg of total RNA with Superscript III reverse transcriptase (Invitrogen, Karlsruhe, Germany) and quantified with the ABI 7300 realtime PCR machine with the SYBR green master mix (ABI). PCR was performed in 96 well reaction plates (ABI) using the standard absolute quantification protocol. Realtime PCR primer pairs were designed using the Primer Express software tool (ABI). Expression levels were normalized to ubiquitin 10 (UBQ10) expression levels. All realtime PCR experiments were done in three technical replicates and statistical relevance was estimated using the *t*-test. All realtime PCR primer sequences are listed in supplementary data. The primer efficiency was calculated using LinRegPCR (Ramakers et al., 2003).

3.3.4 Auxin (-inhibitor) effects

Seeds were grown on nutrient agar plates and transfered 6DAG into liquid control medium (1x Murashige and Skooge, 1% sucrose, pH 5,8) or medium supplemented with 1µM IAA, 10µM TIBA or 10µM NPA. After 15min, 30min, 2h, 3h and 6h 20 seedlings were transfered to liquid nitrogene and RNA was extracted followed by cDNA synthesis and realtime PCR measurements.

3.3.5 Inducible expression analysis

Seeds were grown on nutrient agar plates and transfered 6DAG into liquid control medium or medium supplemented with 20µM β-estradiol. After 3h and 6h 20 seedlings were transfered to liquid nitrogen and RNA was extracted as described.

For early phenotypic analysis seeds were germinated and grown on nutrient agar medium as control and medium supplemented with 20µM β-estradiol.

To study the short term effects of induction seeds were grown vertically on nutrient agar plates for 11days and β-estradiol (20µM) or MOCK was pipetted directly on the roots.

3.3.6 Preparation of water stress medium plates

The experimental system was slightly modified from (Eapen et al., 2003). Seeds were grown vertically on square plates containing normal MS medium. Four days after germination the

medium was cut horizontally 30mm below the root tip using a sterile razorblade, the lower part of the medium was removed and replaced by MS medium supplemented with 2,5% glycerol and 0,5% alginic acid. After solidification plates were placed vertically.

3.3.7 Microscopy

Starch granules in the columella root cap were visualised with 1% Lugol solution (Merck). Seedlings were stained for 3 min, rinsed with water, cleared with chloral hydrate solution and photographed with Nomarski optics on NIKON eclipse E600 microscope and a NIKON DXM1000 camera.

β-Glucuronidase activity was visualised by staining for 0.5 to 24 hours at 37°C in 0.5 mg/ml X-gluc (DUCHEFA), 0.02% Triton X-100, 0.5 mM $K_4Fe(CN)_6$ H_2O, 0.5 mM $K_3Fe(CN)_6$, and 50 mM sodium phosphate buffer, pH 7.2.
For staining of embryos, siliques of soil-grown plants were harvested and slit open with forceps under binocular to collect ovules which were transferred to staining buffer. Stained seedlings and ovules were cleared with chloral hydrate prior to Nomarski optic microscopy.

For laser scanning confocal microscopy seedlings were mounted in 10µM propidium iodide solution and analysed using the Helium/Neon laser of a Leica SP2 microscope. GFP and propidium iodide were excited using a single wavelength excitation at 488 nm. Emission was characterized from 500 to 520 nm (GFP) and 600 to 650 (propidium iodide).

3.3.8 Sequences and bioinformatic tools

All *Arabidopsis* gene sequences were derived from TAIR database (www.arabidopsis.org). To obtain the *DOF1.2 Brassica oleracea* promoter sequence, 500nt (with respect to ATG) of the *Arabidopsis thaliana* promoter region were blasted using the *Brassica oleracea* Blast Search tool of the J. Craig Venter Institute (http://blast.jcvi.org/er-blast). The *Brassica* clone BONRG34TF was identified to contain 253nt of the putative orthologue promoter sequence. To identify further upstream promoter sequence of the *Brassica* orthologue the complete BONRG34TF sequence was blasted again and lead to the identification of the clone BOHOW78TF which contain 774nt of the *Brassica* promoter sequence. A similar approach was used to identify the putative orthologue *DOF3.5* promoter sequence: 500nt of the *Arabidopsis thaliana* promoter region were blasted leading to the identification of the contig BOGWM03TF with 500nt *Brassica* promoter sequence. Promoter comparison analysis between *Arabidopsis* and *Brassica* were performed using the FootPrinter webserver (http://genome.cs.mcgill.ca/cgi-bin/FootPrinter3.0/FootPrinterInput2.pl) and 500nt of each promoter sequence.

3.3.9 Realtime PCR primer sequences

Primer name	Primer sequence 5´→ 3´	Primer name	Primer sequence 5´→ 3´
EF1a for	TGAGCACGCTCTTCTTGCTTTCA	PIN3 for	AAGGCGGAAGATCTGACCAAGG
EF1a rev	GGTGGTGGCATCCATCTTGTTACA	PIN3 rev	TGCTGGATGAGCTACAGCTTTG
UBQ10 for	CACACTCCACTTGGTCTTGCGT	PIN4 for	CGGATGCTGAGATAGGAAACGA
UBQ10 rev	TGGTCTTTCCGGTGAGAGTCTTCA	Pin4 rev	TCTCGATGCGTTTGATTTCCTC
DOF1.2 for	GAGATTCAAGAGATCCTGGAATGC	PIN5 for	TGTACGGACAACAGGCTGTTGA
DOF1.2 rev	CATGAAGCTCCCCTGAGAAACTAA	PIN5 rev	CCACACGATGGCTTGAAATACC
DOF3.5 for	CTATAGCCTCACTCAGCCTCGCTA	PIN6 for	ATCATTTCAGATGCAGGTCTTGGG
DOF3.5 rev	CACCTTTGGTCCAATATCTGCG	PIN6 rev	CAGCGCCATAAACAGGCCTAAAC
ARF10 for	TCCAATTCGTTGGCCTAATTCACC	PIN7 for	CGTGTGGCCATTGTTCAAGCTG
ARF10 rev	AAATGGCTGCGGAATCCTAATCTTC	PIN7 rev	CCCTGTACTCAAGATTGCGGGATG
ARF16 for	GGCGGGAGATTCGATTGTCTTC	PIN8 for	ATGGCCATGTTCAGCTTAGGTC
ARF16 rev	CGGGCTTGATCTAATAAGGGGATTG	PIN8 rev	CTGATGCAATACGCAGAAGCAATC
PIN1 for	GGCATGGCTATGTTCAGTCTTGGG	AUX1 for	CAGCTGCGCATCTAACCAAGTG
PIN1 rev	ACGGCAGGTCCAACGACAAATC	AUX1 rev	GATGAGATAAGCAGTCCAGCTTCC
PIN2 for	ATGATCACCGGCAAAGACATGT	DGK7 for	GGACACATTGGCTGCTAAAGGA
PIN2 rev	TAGCAACGTATAGCGGCACCA	DGK7 rev	CCATGATCCGTATCTTTTCTCTGC

3.4 Results and discussion

3.4.1 *AtDGK7* is specifically expressed in the columella and the lateral root cap

AtDGK7 belongs to the family of diacyl-glyerol kinase (*DGK*) genes in *Arabidopsis thaliana* (Gomez-Merino *et al*., 2004), and exhibits a highly specific expression pattern in roots (Fig.5A). The earliest signs of *AtDGK7* promoter activity appear during the first days after germination in the root tip (Arana, Gomez-Merino, Mueller-Roeber, unpublished), and correlate well temporally and spatially with the development of gravitropic sensing. The expression of *pAtDGK7::GUS* was concentrated exclusively in specialized columella cells and the lateral root cap. During development of later roots, the expression was also observed in pericycle cells and the tips of lateral roots. T-DNA insertions in the *AtDGK7* gene resulted in a decreased number of lateral roots in transgenic plants when compared to the wild-type (unpublished data).

3.4.2 DOF transcription factor binding site is necessary for *AtDGK7* expression

To identify *cis*-elements in the *AtDGK7* promoter region that are responsible for the cell-specific expression pattern, promoter deletion constructs were prepared and fused with the β-glucuronidase reporter gene. In a first approach, eight constructs covering the region of 800bp upstream from the translational start, in steps of 100bp, were prepared. The GUS expression that was observed using the -800 to -400bp promoter fragments resembled the expression pattern of the previously described -1500bp promoter region. In contrast, no GUS activity could be detected in the -300 to -100bp constructs, leading to the assumption that the *cis*-element

responsible for the activation of transcription could be located between -400 and -300bp. To further narrow down the *cis*-element, two further constructs coresponding the regions of -368 and -331bp were prepared. GUS expression was only detectable in the -368bp construct (Fig.5A).

Subsequently, publicly available databases were screened to identify known transcription factor binding sites within these 37 nucleotides. Indeed, at position 333-336 a binding site for the plant specific DOF transcription factor family (A/TAAG or CTTT, ref.) could be found (Fig.5A and 5B, highlighted in red).

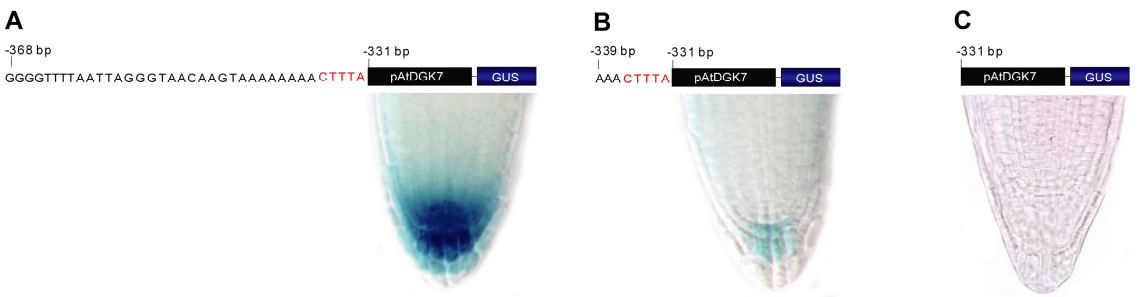

Figure 5. Influence of promoter length of the *AtDGK7* gene on the expression of *GUS* reporter gene.

(**A**) *AtDGK7* promoter of 368bp length drives GUS expression in the central and lateral root cap. (**B**) A truncated promoter fragment of 339bp fundamentally reflect the GUS expression pattern observed in (**A**), but results in weaker intensity. (**C**) No GUS signal was detectable in the case of 331bp promoter length. The promoter region between -339 and -331bp, containing a DOF binding site (highlighted in red), was identified as crucial for the expression of *AtDGK7*.

To confirm the putative relevance of the DOF binding site for the expression of *AtDGK7*, another promoter fragment of 339bp, including the the DOF binding site, was designed (Fig. 5B). Additionally a 400bp promoter fragment with a mutated DOF binding site was generated. The -339bp promoter-GUS fusion (with the DOF binding site) essentially reflected the previously observed expression pattern, but with a somewhat weaker GUS staining (Fig.5B). In contrast, GUS activity could neither be observed in the -331bp nor the mutated -400bp promoter-GUS fusion construct (Fig.5C; data not shown).

3.4.3 *DOF1.2* and *AtDGK7* expression patterns highly overlap *in silico*

As the DOF transcription factor family in Arabidopsis comprehends 36 members (Yanagisawa 2002), two different screenings were performed to identify the transcription factor gene most probably responsible for the control of *AtDGK7* expression. On the one hand, the expression pattern of *AtDGK7* was compared with the expression patterns of all members of the *Arabidopsis thaliana* DOF family existing in the public gene expression data sets like Genevestigator (Zimmermann et al., 2004) and the “Root Expression Map” (Birnbaum et al., 2003), a high resolution expression map of 15 distinct zones of the *Arabidopsis thaliana* root.

On the other hand, a collection of promoter-reporter gene constructs for all members of the *Arabidopsis* DOF transcription factor family that was established in our group was inspected for an overlapping expression pattern.

The expression values of *AtDGK7* itself obtained from the "Root Expression Map" strongly resembled a GUS expression pattern with a maximum of expression in the lateral root cap and the root tip (Fig.6). Among all *DOF* genes present in the databases, only one member, *DOF1.2* (*At1g21340*), showed a highly similar expression pattern to *AtDGK7* (Fig.6).

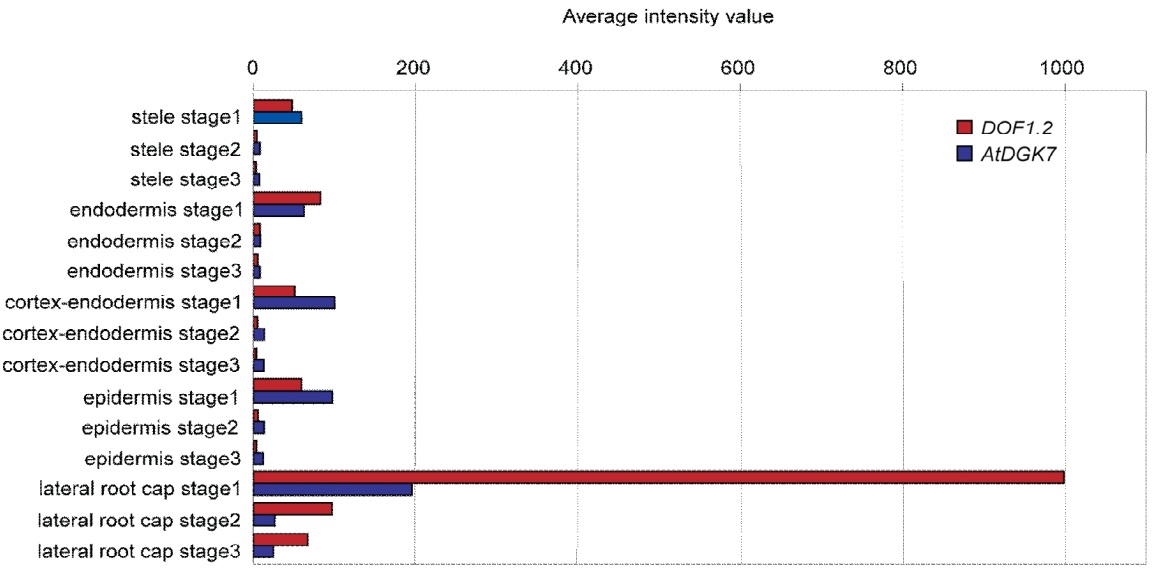

Figure 6. Expression intensity of *DOF1.2* and *AtDGK7* in the root tip according to the "Root Expression Map".

Stage1, stage2 and stage3 correspond to regions of 0-150µm, 150-300µm and 300-450µm, respectively, counted from the root tip in basipetal direction (Birnbaum et al., 2003).

3.4.4 *DOF1.2* and *DOF3.5* are specifically expressed in the columella and lateral root cap

To confirm the root tip specific expression pattern of *DOF1.2*, a promoter fragment of 600bp (comprising the whole intergenic region upstream of the translational start codon) was fused to the β-glucuronidase reporter gene. The *DOF1.2* promoter was activated in the radicle tip of germinating seeds (Fig.7B). GUS activity was also high in the root during the post-germinative stages, very specific in the columella and lateral root cap cells (Fig.7A). During lateral root development GUS expression was detectable after the emergence of the lateral root from the parent root (Fig.7C).

Inspecting our collection of available promoter-reporter gene constructs for Arabidopsis *DOF*-genes, *DOF*3.5 (At3g52440) could be identified as a further *DOF* gene with an expression pattern similar to that of *pAtDGK7::GUS* (Fig.7D-F). As the probe for *DOF3.5* does not exist on conventional Arabidopsis microarrays, no expression data were present for *DOF3.5* in any of

the investigated publicly available databases. Based on our findings we concluded that *DOF1.2* and *DOF3.5* are the most possible regulators of *AtDGK7*.

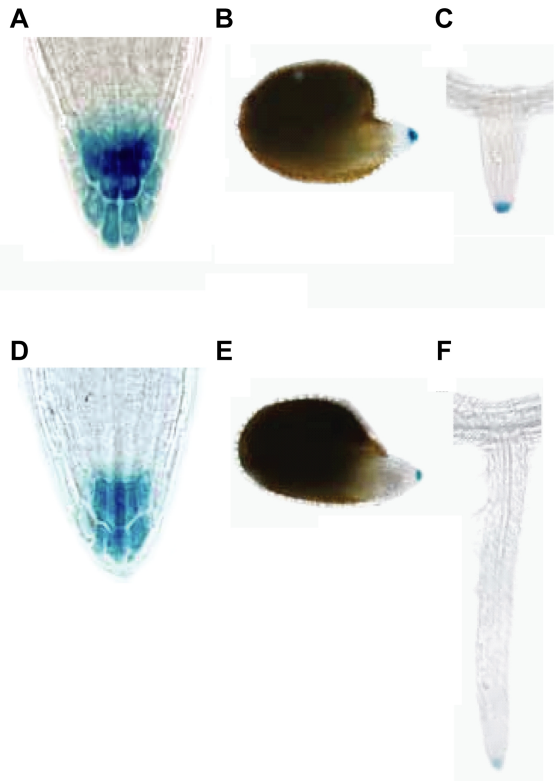

Figure 7. Expression pattern of *pDOF1.2::GUS* and *pDOF3.5::GUS*.

Expression pattern of *pDOF1.2::GUS* (**A-C**) and *pDOF3.5::GUS* (**D-F**) in the primary root tip (**A, D**), germinated seeds (**B, E**) and developing lateral roots (**C, F**).

3.4.5 *DOF1.2* and *DOF3.5* possess distinct but highly conserved promoter regions

Intriguingly, among all DOF proteins, DOF1.2 and DOF3.5 are phylogeneticaly the closest relatives. However, almost no similarity could be identified at the promoter level of these genes. Both genes appear to be evolutionary conserved, possessing their own orthologues in *Brassica oleracea*. Comparing the promoter sequences of *Arabidopsis' DOF1.2* and *DOF*3.*5* with the corresponding sequences in *Brassica* revealed a presence of highly conserved blocks in their structure (Fig.8). This analysis revealed that the conserved region of the *DOF1.2* promoter is located in its very proximal part, up to -280bp upstream of the translational start codon. In the case of *DOF3.5* a highly conserved part of the promoter region is spread over a longer region of several hundred base pairs. Thus, considering the same expression pattern and high similarity at the protein level *DOF1.2* and *DOF3.5* may be functionally redundant, but probably regulated independently at the expression level.

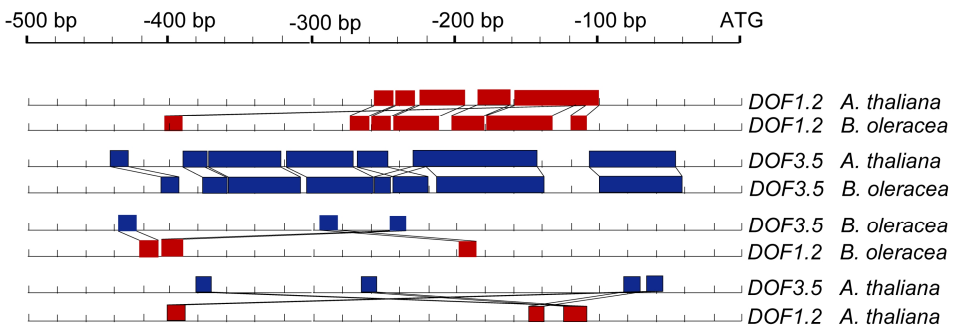

Figure 8. Comparison of the promoter regions of *DOF1.2, DOF3.5* from *Arabidopsis* and the corresponding *Brassica* orthologues.

To identify relevant motives in the *DOF1.2* and *DOF3.5* promoter regions, putative *Brassica* orthologues were identified by BLAST search against coding regions of the available *Brassica oleracea* BAC clone sequences of the J. Craig Venter Institute (http://blast.jcvi.org/er-blast). A phylogentic approach was used to compare 500bp upstream intergenic regions of *DOF1.2* and *DOF3.5* with the corresponding regions of the putative orthologues in *Brassica oleracea* and among each other. Blocks of similarity of at least 12 nucleotides with one mutated base pair at maximum are represented as red (*DOF1.2*) or blue (*DOF3.5*) boxes.

In a further step, the promoter region of *DOF1.2* was dissected using promoter deletion-reporter gene constructs. By this approach, the minimal promoter of *DOF1.2* gene could be narrowed down to a region between -200bp and -100bp upstream of the translational start codon. The -100bp fragment of *DOF1.2* was not able to drive expression of the GUS reporter gene (data not shown). These findings supported well the data obtained from the phylogenetic studies, confirming the importance of the evolutionary conserved promoter region for the regulation of *DOF1.2* expression.

3.4.6 Physiological characterisation of *DOF1.2* by analyses of transgenic lines

To reveal the physiological relevance of the *DOF1.2* gene, the consequences of its constitutive and inducible overexpression (using the β-estradiol inducible system (Zuo et al., 2000)) as well as its suppression were analysed. By screening the collections of insertion mutants from the SALK institute (http://signal.salk.edu/cgi-bin/tdnaexpress) and GABI-Kat (http://www.gabi-kat.de), three independent lines with a T-DNA insertion in the *DOF1.2* gene could be identified (Fig.9).

3.4.7 Identification and confirmation of *DOF1.2* T-DNA insertion lines

The following genotyping of these lines revealed that only the line GABI_921E09A (later assigned as *dof1.2-1*) and SAIL_99_C09 (later assigned as *dof1.2-2*) indeed possess an insertion in the gene (Supplementary Fig.1). In the case of *dof1.2-1* the insertion is located 254bp upstream of the translational start codon (the length of the 5´UTR region is not described for *DOF1.2*), in the case of *dof1.2-2* in the coding sequence, 279 downstream of the startcodon. Both lines were further propagated to homozygosity (data not shown). However, the expression level of *DOF1.2* transcript was found to be 112-fold increased in *dof1.2-1* when compared to wild-type plants (data not shown).

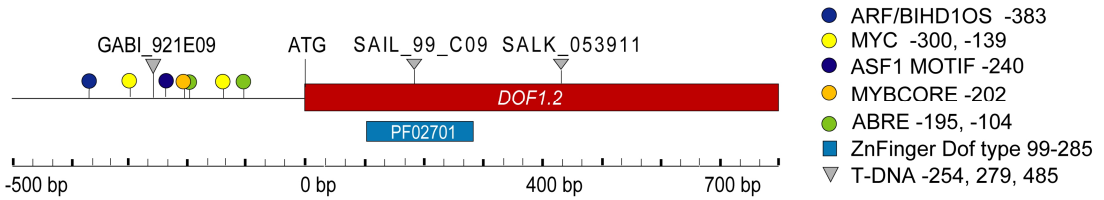

Figure 9. Structure of the *DOF1.2* gene with selected *cis*-elements, available insertions lines and a functional domain.

Predicted gene structure of *DOF1.2* obtained from the TAIR database (http://www.arabidopsis.org). The red box represents the exon, the thin black line depicts the region upstream from the translational start codon. The translation initiation codon is indicated by ATG. The position of the T-DNA insertions in the *DOF1.2* gene is shown above, as the grey triangles. On the left of the figure, upstream of the predicted translation start site (ATG), *cis*-acting elements in the promoter of *DOF1.2* are indicated. *Cis*-acting elements are indicated as follows: yellowish circles, elements related to drought stress; bluish circles, elements related to auxin signals, green circle, ABRE. The blue box below the transcript model represents the position of the C_2C_2 DOF zinc finger motif PF02701 according to the Pfam Database (http://pfam.sanger.ac.uk/).

3.4.8 Confirmation of altered *DOF1.2* expression levels in artifical microRNA and overexpressing lines

The artificial microRNA (amiR) system was used as a further approach to suppress the *DOF1.2* expression. For this purpose a gene specific hairpin construct was expressed under control of the endogenous *DOF1.2* promoter. Suppressed levels of *DOF1.2* transcript could be confirmed in five independent transgenic amiRNA lines (in the following assigned as *amiR-dof1.2-1*), revealing a decrease to 10% of the wild-type gene expression level (Fig.10A). The constitutive overexpression of *DOF1.2 (*assigned as *35S::DOF1.2)* could be confirmed in four independent lines resulting in an up to 256-fold increase of gene expression compared to wild-type (Fig.10B). Also in the case of inducible overexpression (*35Sind::DOF1.2)* strongly increased levels of *DOF1.2* expression could be measured upon the induction by β-estradiol (data not shown).

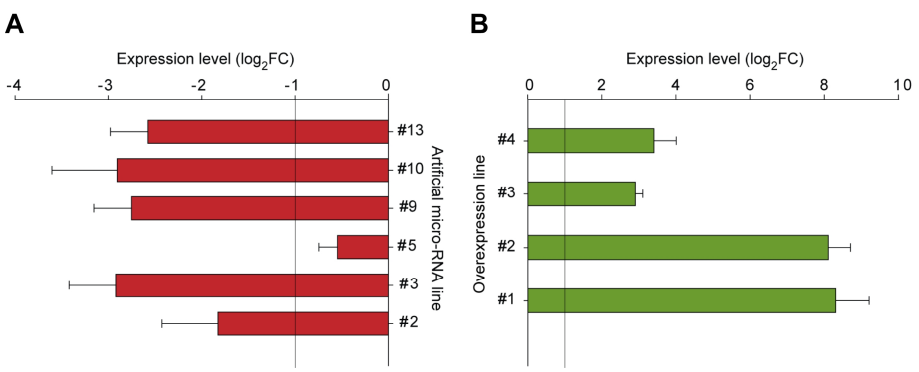

Figure 10. Expression level of *DOF1.2* gene in *amiR-dof1.2-1* (A) and *35S::DOF1.2* (B) transgenic plants.
The *DOF1.2* expression level in the *DOF1.2* transgenic lines was measured by quantitative real-time RT-PCR. All overexpression lines possess an increased expression of *DOF1.2*, varying from 8-to 256-fold change when compared to the wild-type. The amiRNA lines showed a decrease of *DOF1.2* transcript abundance of only 10% of the wild-type level.

3.4.9 Changes in *DOF1.2* expression lead to altered root cap structure

Basically, the root cap has a simple structure, being composed of the columella in the central region and the lateral root cap in the outer portion. The columella initials, located immediately under the quiescent center (QC) cells, generally divide only anticlinally, and their daughter cells undergo rapid elongation and differentiation, producing starch granules that mediate gravity sensing (Sack, 1997). The epidermal/lateral root cap cell initials undergo both anticlinal and periclinal divisions (Dolan *et al*., 1993). Stem cell divisions and daughter cell differentiation are continuous as the root grows indeterminately, with the outermost cells being detached from the root. The root cap contributes to plant adaptations to environments as a primary site for perception of underground signals.

Both transgenic situations, the repression and overexpression of *DOF1.2*, resulted in dramatic changes of the organisation of the root cap. Supression of the *DOF1.2* transcript level resulted in non-uniform changes in the organisation of the root cap, affecting both, columella and lateral root cap, but also sporadically the surrounding cells such as the QC. A reduced number of columella tiers arising from missing periclinal divisions of columella initials could be observed in the majority of the investigated plants. In addition, atypical periclinal divisions in lateral root cap also appeared frequently (Fig.11A). At this developmental stage (4DAG) the overexpressing plants displayed even more dramatic changes. In general, starting from the first columella layer, the columella cells displayed interrupted cell boundaries, resulting in a “fusion” of several cells in one (Fig.11C). The outermost layer of the columella, in wild-type usually evolving protective function by the production of mucilage and cell release, appeared with number of ruptures in the basal cell walls resulting in a characteristic rancid appearance of root tip. Consequently, the root cap appeared somewhat shorter than that of the wild-type (Fig.11B). In contrast to wild-type roots and especially those of *amiR-dof1.2-1* plants, no typical signs of detaching the outermost columella layer were observed in overexpression lines (Fig.11A-C).

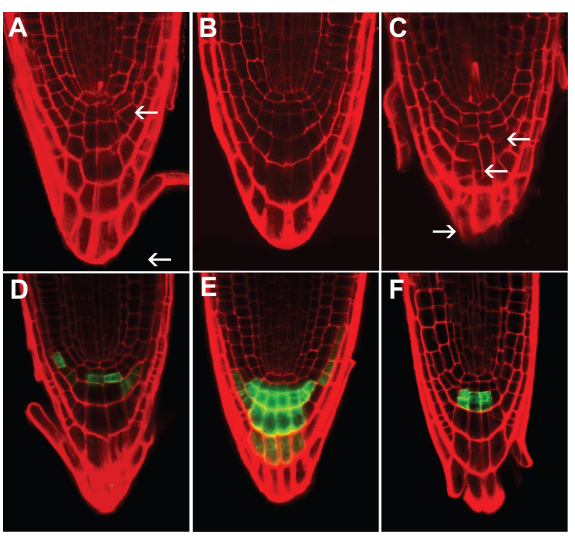

Figure 11. Disruption or overexpression of *DOF1.2* results in defects in patterning and identity of root distal cells.

(**A**) Cellular division pattern in roots of *DOF1.2* amiRNA lines, (**B**) wild-type, and (**C**) *DOF1.2* overexpression lines, 4DAG. White arrowheads indicate aberrantly dividing cells.
(**E**) GFP enhancer trap line Q0680 in *DOF1.2* amiRNA (**D**) and overexpression (**F**) lines, 4DAG.
Cell outlines were stained by propidium iodide (red).

To analyse, whether the consequences of *DOF1.2* overexpression and the attended disruption of boarder cells resulted in a change of columella cell identity, two selected overexpression and amiRNA lines were crossed with the GFP enhancer trap line J0680, which marks columella cells in the tiers S1-S3 as well as cells of the lateral root cap (Fig.11E). In *DOF2.1* overexpression lines GFP signal was almost exclusively restricted to columella cells of tier S1, no signal could be observed in the lateral root cap (Fig.11F). In contrast, in amiRNA lines, cells of the lateral root cap sporadically showed GFP expression. Similarly to the overexpression situation, GFP signal was only detectable in columella cell tier S1, but not in S2 and S3 (Fig.11A).

3.4.10 Altered *DOF1.2* expression affect starch content and boarder cell realease

The columella cells of plants with a suppressed level of *DOF1.2* transcript displayed an irregular pattern of the distribution of starch grains, probably resulting from disturbed cell divisions (Fig.12A, D).

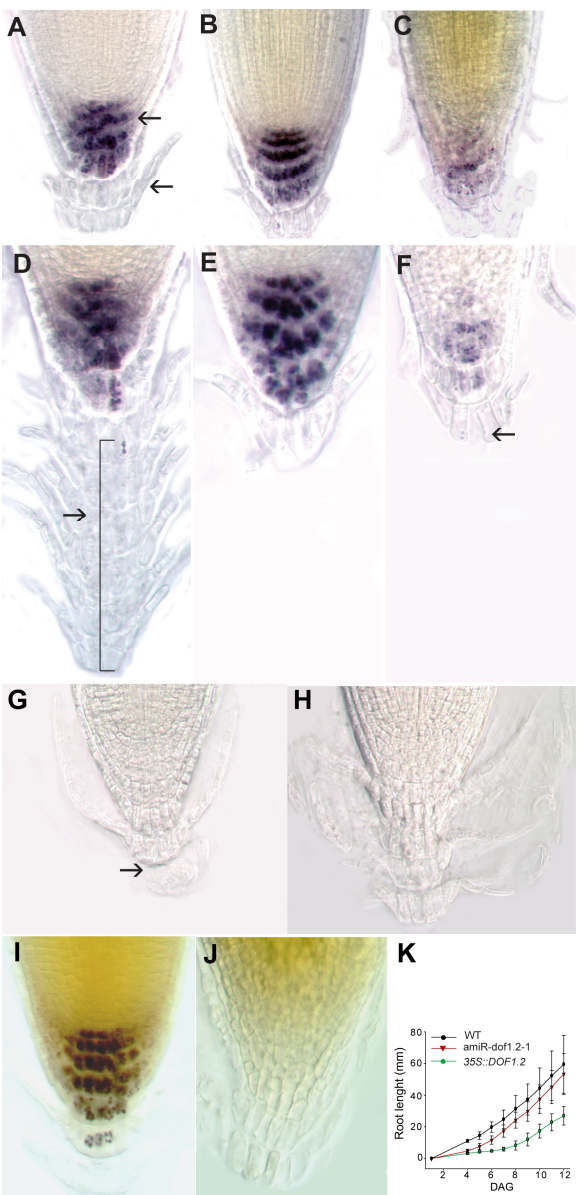

Figure 12. Disruption or overexpression of *DOF1.2* results in defects in differentiation and patterning of root distal cells.

Cellular pattern and starch content in roots of wild-type (**B**) and *DOF1.2* amiRNA (**A**) and overexpression (**C**) lines, 4DAG. Impaired boarder cell release in *DOF1.2* amiRNA (**D**) and overexpression (**F**) lines compared to wild-type (**E**), 14dag.
Impaired boarder cell release in *dof1.2-2* mutant (**H**) compared to wild-type (**G**) in 12dag-old seedlings.
Root tip and starch granules in roots of 12dag old *DOF1.2* inducible overexpression plants, 2 days after application of the inducer β-estradiol (**J**) or DMSO as control (**I**).
(**K**) Root lengths of wild-type and *DOF1.2* transgenic lines.
Arrows indicate altered cell divisions and impaired boarder cell release.

The root cap of plants overexpressing *DOF1.2* exhibited a strong reduction of starch grains (Fig.12C, F), a phenomenon that was much more evident in *35Sind::DOF1.2* inducible overexpression lines, which completely lacked starch granules when grown on medium supplemented with the inducer β-estradiol (Fig.12J) when compared to *35Sind::DOF1.2* plants treated with DMSO as control (Fig.12I).

Furthermore, *DOF1.2* transgenic lines displayed an impaired release of distal boarder cells (Fig.12D-H). Fourteen days after germination the roots of *amiR-dof1.2-1* had multiplied columella layers and up to ten layers of detached lateral root cap cells were observed on the base of root tip (Fig.12D), a phenotype that was absent in wild-tpye (Fig.12E). In these additional layers starch grains could be observed only sporadically (Fig.12D). The increase in the number of boarder cell layers was also seen in the *dof1.2-2* knock-out line (Fig.12H), but not in *dof1.2-1* mutants (data not shown) when compared to wild-type seedlings (Fig.12G). Similar to the observed phenotype in overexpression lines at 4DAG, overexpression lines at 14DAG appeared with ruptures in the boarder cell layer (Fig.12F, arrow).

3.4.11 *DOF1.2* overexpression plants grow agravitropicly and lack gravitropic response

As expected, roots of *35S::DOF1.2* plants and *35Sind::DOF1.2* plants, grown on medium supplemented with the inducer β-estradiol, were agravitropic due to lack of starch granules (Fig.13A). More detailed analyses of root growth orientation in both overexpression lines revealed that roots of *35S::DOF1.2* plants possessed a reduced but partial gravitropic growth and were found to grow downwards and sidewards with same proportions (Fig.13A). In contrast, roots of *35Sind::DOF1.2* plants, grown on medium supplemented with the inducer β-estradiol, completely lacked gravitropic growth and were found to grow upwards out of the medium (Fig.13A). Gravitropic growth of *amiR dof1.2-1* roots was comparable to wild-type (Fig.13A).

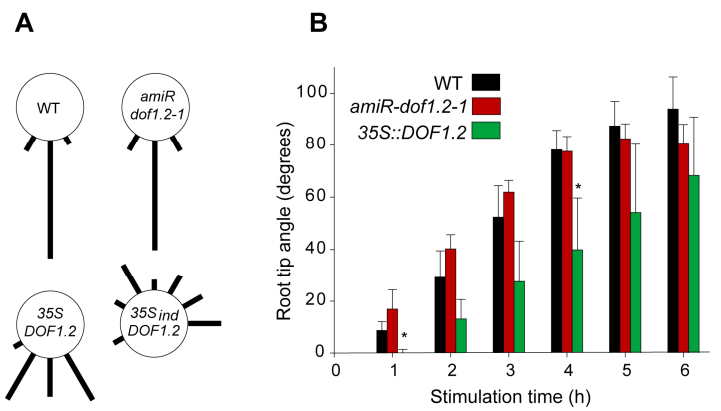

Figure 13. Orientation of root growth and gravitropic response in wild-type and *DOF1.2* transgenic plants.

(**A**) Orientation of root growth in wild-type and *DOF1.2* suppressing and overexpressing lines**.** The orientation of the black bars indicates direction of root growth. Their length correlates with number of seedlings (n=30). (**B**) Gravitropic response of wild-type and *DOF1.2* transgenic plants. Stars indicate significant changes.

To reveal if the reduction of starch granules in roots of *DOF1.2* overexpressing plants also affected the gravitropic response, wild-type, *35S::DOF1.2* and *amiR-dof1.2-1* seedlings were grown four days on a vertically oriented plate. On the fourth day the plate was turned by 90° and bending of the roots was monitored by measuring the degree of the roots´ reorientation every

hour. Roots of *35S::DOF1.2* plants showed a clear delay in the gravitropic response, while no significant changes could be observed in *amiR-dof1.2-1* plants relative to wild-type (Fig.13B).

3.4.12 *DOF1.2* transgenic plants possess altered root structure at later developmental stages

In general, roots of *35S::DOF1.2* plants were shorter and less developed when compared to the wild-type plants (Fig.12K, 14B, 14C). The *amiR-dof1.2-1* plants also developed more slowly then wild-type plants (Fig.12K) and generated a less developed lateral root system (Fig.14A).

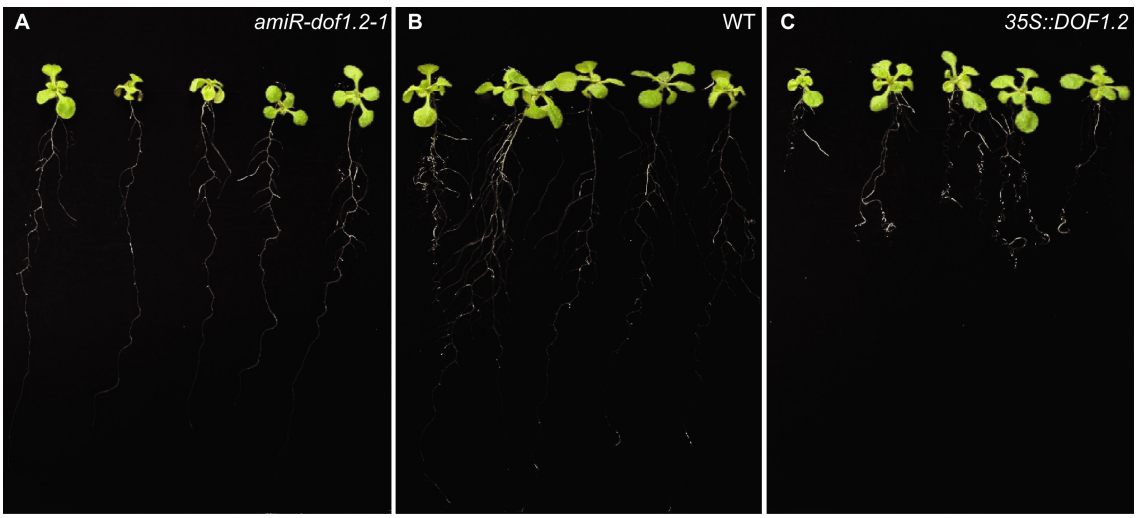

Figure 14. Root morphology of *amiR-dof1.2-1*, wild-type and *35S::DOF1.2* seedlings.

Seedlings were grown on vertical plates for 17dag. Clear differences in root architecture and gravitropic response were observed.

3.4.13 Expression levels of *AtDGK7* and *DOF3.5* in *DOF1.2* transgenic plants

To confirm the regulatory effect of DOF transcription factors on expression of the *AtDGK7* gene, the expression level of *AtDGK7* was measured in *DOF1.2* transgenic lines. A significantly reduced level of *AtDGK7*, but also of *DOF3.5* transcript could be measured in *amiR-dof1.2-1* plants (Table 1). The intensity of suppression correlated strongly with the intensity of *DOF1.2* supression (data not shown). In one of the four available *35S::DOF1.2* insertion lines an increase of *DOF3.5* transcript abundance was observed (Table 1).

Table 1. Expression of *DOF3.5 and AtDGK7* genes in *amiR-dof1.2-1* and *35S::DOF1.2* transgenic lines

	amiR-dof1.2-1				*35S::DOF1.2*			
	LINE #3		LINE #9		LINE #1		LINE #2	
	t-test	log_2FC	t-test	log_2FC	t-test	log_2FC	t-test	log_2FC
DOF3.5	**0.05**	**-2.3**	**0.01**	**-2.0**	0.12	1.0	**0.02**	**1.8**
AtDGK7	**0.00**	**-2.8**	**0.01**	**-2.5**	0.38	-0.4	0.02	-0.1

The log_2FC represent mean of at least 2 replicates. Expression values statistically significant and above/under the threshold of +/-1 are given in bold.

3.4.14 Expression levels of *AtDGK7* and *DOF1.2* in *DOF3.5* transgenic plants

We also asked, whether DOF3.5 is able to affect the *AtDGK7* expression. To this end *amiR-dof3.5-1* plants were generated. Of four positive transformants that were able to grow on selection media no one exhibited significant change in *DOF3.5* transcript level (data not shown). However, in one of identified transgenic lines the expression level of *AtDGK7* and *DOF1.2* was significantly reduced (t-test/log_2FC values for *DOF1.2*: 0.00/-6.1 and for *AtDGK7*: 0.00/-1.5, respectively). However, since no reduced levels of *DOF3.5* expression could be measured, the question remains unanswered at what degree DOF3.5 contributes to the regulation of *AtDGK7*.

3.4.15 Application of auxin and auxin transport inhibitors alter *AtDGK7*, *DOF1.2* and *DOF3.5* gene expression

In roots, the auxin response maximum serves as a positional cue for cell fate determination and distal organization (Sabatini *et al.,* 1999). We asked therefore to what degree auxin influences the expression of *DOF1.2, DOF3.*5 and *AtDGK7* genes. No changes in expression were observed either in *DOF1.2* or in *DOF3.5* during the first six hours upon the application of auxin. Subsequently, the effect of the auxin efflux inhibitors NPA and TIBA was investigated. Hereby, especially in the case of the polar auxin transport inhibitor TIBA, a strong and fast induction of both genes could be observed already 15 minutes upon application of inhibitors (Fig.15). A weak, but continuously increasing expression was observed in case of *AtDGK7* gene upon application of TIBA. Neither auxin nor NPA did significantly affect the expression of *AtDGK7* (Fig.16A).

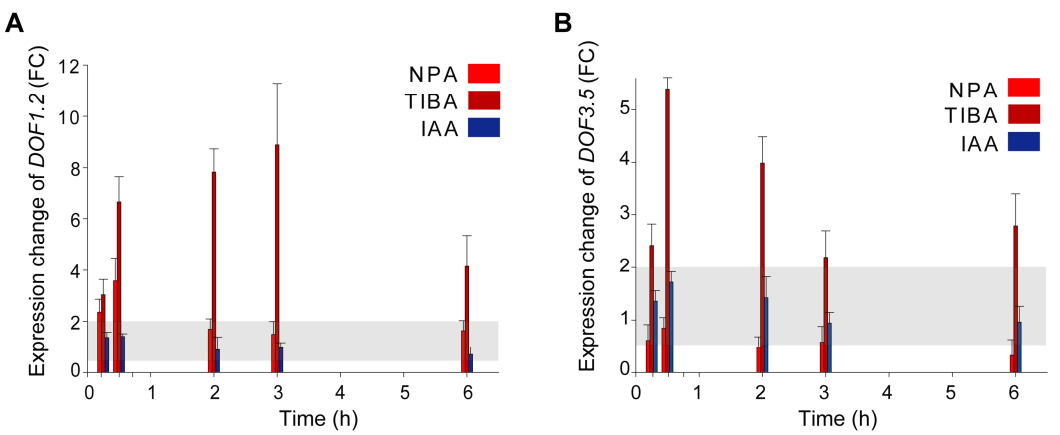

Figure 15. Influence of auxin and auxin transport inhibitor NPA and TIBA on expression of *DOF1.2* and *DOF3.5*.

Expression of *DOF1.2* (**A**) and *DOF3.5* (**B**) was measured by qRT-PCR in pool of plants after application of NPA (10µM), TIBA (10µM) or IAA (1µM). Horizontal grey area indicates region between upper and lower threshold level without change in expression.

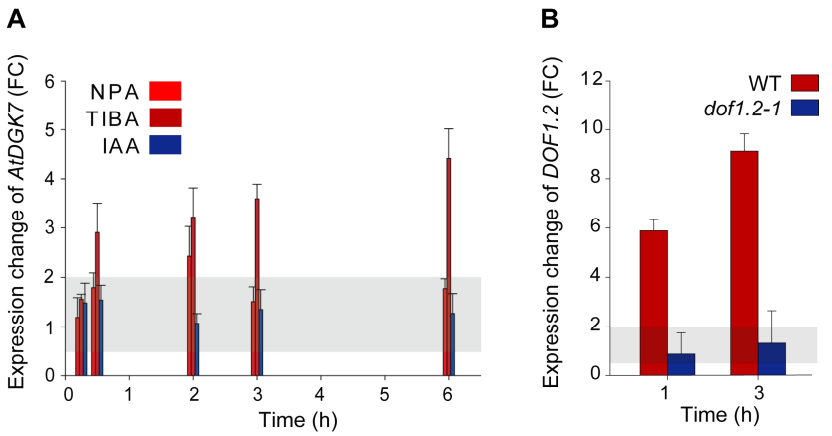

Figure 16. Influence of auxin and auxin transport inhibitor NPA and TIBA on expression of *AtDGK7* and on *DOF1.2* in wt and *dof1.2-1* mutant.

(**A**) AtDGK7 expression was measured by qRT-PCR in pool of plants after application of NPA (10µM), TIBA (10µM) or IAA (1µM). (**B**) DOF1.2 expression was measured by qRT-PCR in pool of plants 1h and 3h after application of TIBA (10µM) in 4DAG-old wild-type and *dof1.2-1* seedlings. Horizontal grey area indicates region between upper and lower threshold level without change in expression.

3.4.16 ARFs as putative negative regulators of *DOF1.2* and *DOF3.5* expression

Interestingly, no effect of TIBA on *DOF1.2* expression could be observed in *dof1.2-1* plants (Fig.16B). Therefore, one could conclude that *cis*-element/s responsible for the implementation of auxin in the regulation of *DOF1.2* expression are located further upstream of -254bp (the position of the T-DNA insertion site in the *dof1.2-1* mutant, Fig.9) from translational start codon. Indeed, the core of an ARF binding sequence is present at position -383bp (Fig.9). Further putative ARF binding sites could be identified in the more distal promoter region. The promoter region of the *DOF3.5* gene even contains a perfect ARF binding site. Summing up, the two findings, that firstly, when compared to wild-type, elevated endogenous levels of *DOF1.2* could be measured in the *dof1.2-1* mutant, in which the core ARF binding sequence is spatially separated from the basic transcription apparatus, and that secondly, the application of the auxin transport inhibitor TIBA resulted in an increase of *DOF1.2* and *DOF3.5* transript abundance in the wild-type but not in the *dof1.2-1* mutant, lead us to the assumption that ARFs could act as mediators in an auxin-regulated suppression of *DOF1.2* and *DOF3.5*.

3.4.17 ARF10 and ARF16 negatively regulate *DOF1.2*, *DOF3.5* and *AtDGK7* expression

The Arabidopsis genome contains 23 *ARF* genes. According to Wang *et al.* (2005) at least two of them display specific expression in the root cap, namely *ARF10* (*At2g28350*), and *ARF16* (*At4g30080*) and control root cap formation. Screening public databases we could identify at least one further *ARF* gene expressed in root cap (*ARF8*). Recent investigations have shown the importance of miR160, which targets *ARF10* and *ARF16*. The overexpression of miR160 led to suppression of root cap specific expression of *ARF10* and *ARF16*. We therefore investigated the expression of the *DOF1.2* and *DOF3.5* genes in plants with a *35S::miR160C* genotype (Table 2).

Table 2. Expression of *DOF1.2, DOF3.5 and AtDGK7* genes in *35S::miR160C* transgenic lines

	REPLICATE 1		REPLICATE 2	
	t-test	log_2FC	t-test	log_2FC
DOF1.2	**0.02**	**2.6**	0.20	1.3
DOF3.5	**0.03**	**1.1**	**0.01**	**1.9**
AtDGK7	**0.00**	**1.8**	0.11	0.8

The log_2FC represent mean of at least 2 replicates. Expression values statistically significant and above/under the threshold of +/-1 are given in bold.

A significant increase of expression was observed in case of the *DOF3.5* gene, whereby in case of *DOF1.2* the changes appeared as non-consistent from experiment to experiment. Intriguingly, no change in expression could be measured either for *DOF1.2* or for *DOF3.5* in *arf10-2/arf16-2* double mutants. This suggests existence of additional *ARF* genes putatively regulating expression of *DOF* genes in the root cap.

3.4.18 Altered *DOF1.2* expression results in changes of auxin distribution

In an additional approach the influence of DOF1.2 on the distribution of auxin and the attended expression of *ARF* genes was investigated. Hereby the expression of *DR5rev::GFP* was monitored in *DOF1.2* transgenics (Fig.17A-C).The *35S::DOF1.2* plants showed a reduction of *DR5rev::GFP* signal in the basal layers of columella cells (Fig.17C). The typical signal concentrated on protophloem strand, observed in wild-type plants, was replaced by a broad expression in provascular tissue (Fig.17B, 17C, arrows). This result strongly indicated the capability of *DOF1.2* to influence the pattern of auxin distribution in the root apical meristem.

3.4.19 *ARF10* and *ARF16* are differentially expressed in *DOF1.2* transgenic plants

Furthermore, the expression of the root cap specific *ARF10* and *ARF16* genes was tested in transgenic *DOF1.2* plant. For both genes a decrease in transcript abundance could be observed in *amiR-dof1.2-1* plants (Fig.17E). This could be at least partially caused by the strong phenotypical changes observed in *amiR-dof1.2-1* plants.

3.4.20 *PIN2* and *PIN4* are differentially expressed in *DOF1.2* transgenic plants

The auxin gradient in roots is precisely regulated by the expression and specific localisation of PIN proteins. The Arabidopsis genome contains eight *PIN* genes. Interestingly, *pin4* plants display the same changes in the root tip anatomy as the *amiR-dof1.2-1* plants (Friml et al., 2002). Therefore we investigated the expression of all *PIN* genes in transgenic *DOF1.2* plants using qRT-PCR. At the 4DAG stage no changes could be observed in expression of any of the *PIN* genes. However, at the 7DAG stage suppression of *DOF1.2* resulted in a decrease of transcript level of several *PIN* genes. Intriguingly, the most consistent changes were observed in case of *PIN2* and *PIN4* (Fig.17D), which are involved in the root gravitropism control (Muller

et al., 1998) and boarder cell release (Friml et al., 2002), respectively. The late response in expression changes of *PIN* genes indicates a rather indirect regulation of *PIN* genes through DOF1.2, which subsequently causes changes in auxin distribution in *DOF1.2* transgenics. The changed auxin status could further lead to the observed changes in expression of the tested *ARF* genes.

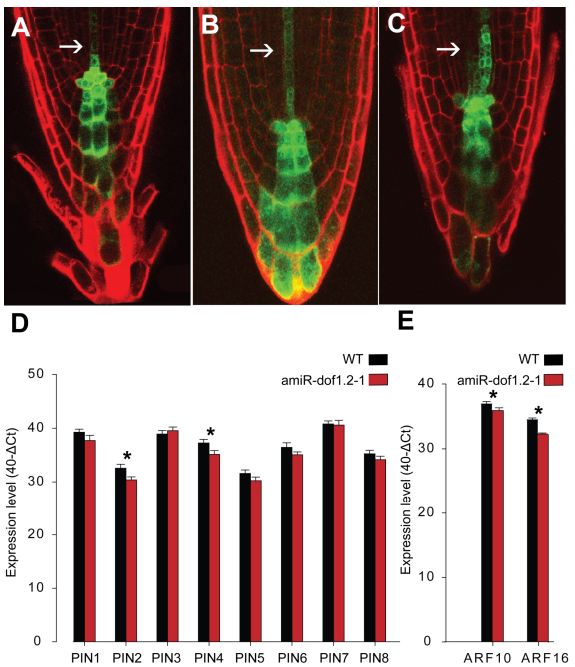

Figure 17. Auxin distribution in wild-type and *DOF1.2* transgenic plants. Expression of *PIN* and *ARF10* and *ARF16* genes in wild-type and *amiR-dof1.2-1* plants 7DAG.

DR5::GFP expression in *amiR-dof1.2-1* (**A**), wild-type (**B**) and *35S::DOF1.2* (**C**) plants. Arrows indicate differences in auxin distribution.
Expression levels of the *Arabidopsis PIN1-8* genes (**D**) and *ARF10* and *ARF16* (**E**) in 7DAG-old wild-type and *amiR-dof1.2-1* plants. The stars indicate significant alterations in gene expression.

3.4.21 DOF1.2 is involved in the hydrotropic response

Analyses of public gene expression databases indicated a negative influence of long-term drought stress on *DOF1.2* expression (data not shown). Strikingly, an overrepresentation of all important *cis*-elements involved in signal transduction during drought stress was observed in the conserved minimal promoter of the *DOF1.2* gene (Fig.9). We therefore postulated role of *DOF1.2* in hydrotropism, a biological process, which stimulates starch degradation and causing agravitropic root growth in response to environmental changes in the water potential (Eapen et al., 2003).

To reveal a putative involvement of DOF1.2 in the hydrotropic response, we used an experimental system that was established to monitor different behaviours in hydrotropic growth (Eapen et al., 2003), consisting of vertically orientated nutrient agar medium plates, which have been horizontally divided. The lower part of the normal medium (NM) was replaced by nutrient agar medium supplemented with 2.5% glycerol and 0.5% alginic acid to reduce the water potential (hence termed water stress medium, WSM). When wild-type and *amiR-dof1.2-1* seedlings were grown on WSM plates, differences in the hydrotropic growth behaviour were obvious. While in wild-type plants retarded root growth was observed starting at 8DAG and plants arrested in growth 12DAG (Fig.18A, 18D), no differences in root growth were found in

amiR-dof1.2-1 plants between the NM and WSM plates (Fig.18A) and 12DAG roots continued growing (Fig.18D). Furthermore, the degradation of starch during the hydrotropic response, which was previously reported (Takahashi et al., 2003), was detected in the wild-type (Fig.18B), but not in *amiR-dof1.2-1* roots (Fig.18C), supporting the role of DOF1.2 in the integration of gravitropic and hydrotropic responses.

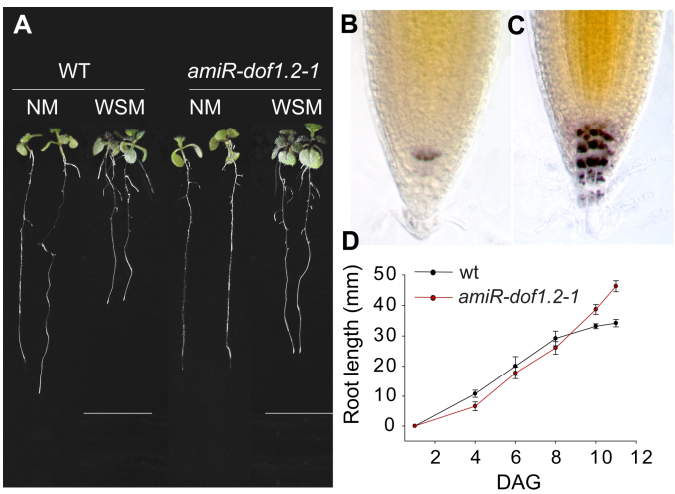

Figure 18. Hydrotropic response of wild-type and *amiR-dof1.2-1* plants.

(**A-D**) wild-type (WT) and *amiR-dof1.2-1* plants were grown on normal nutrient agar medium (NM) and medium supplemented with 2,5% glycerol and 0,5% alginic acid to reduce the water potential (water stress medium, WSM). Wild-type plants on WSM arrested in growth (**A, D**) and degradation of starch in the root tip was obvious (**B**), while *amiR-dof1.2-1* plants on WSM grew comparable to control plates (**A, D**) and starch content in the root tip was not affected (**C**).

3.4.22 Conclusion and proposed model of the DOF1.2 regulatory pathway

Taking together, we propose a model (Fig.19a, b) in which DOF1.2 regulates the expression of *AtDGK7*. The expression of *DOF1.2*, in turn, is regulated by the auxin status, probably by contribution of the auxin efflux facilitators PIN2 and PIN4 and root cap specific *ARF* genes. The ARF10 and ARF16 proteins act most probably as repressors of *DOF1.2*. Prolonged drought stress leads to deepening of roots enabled by synergistic synthesis of starch granules. Until today no regulators integrating hydrotropic and gravitropic responses, which is crucially important for making decisions about the direction of root growth, have been identified. We suggest that *DOF1.2* acts as an integrator of these two signals. In this model *DOF1.2* would be suppressed under conditions of drought stress, where the gravitropic response, principally based on auxin distribution, dominates and favoring the downward directed (gravitropic) growth of the root. In this context, the additional boarder cell layers observed in the *dof1.2-2* and *amiR-dof1.2-1* mutants could exert a protective function (Fig.19d). Once reaching soil with an appropriate water potential, a degradation of starch granules prevents a further root deepening. *DOF1.2* is under these conditions probably higher expressed involving an unknown stimulating hydrotropic signal (Fig.19a, c). Further experiments with *DR5rev::GFP* reporter gene in the *amiR-dof1.2-1* background and analysis of *DOF1.2* expression under short-term water-stress condition will enable better understanding of this fine tuned process of regulated gene expression.

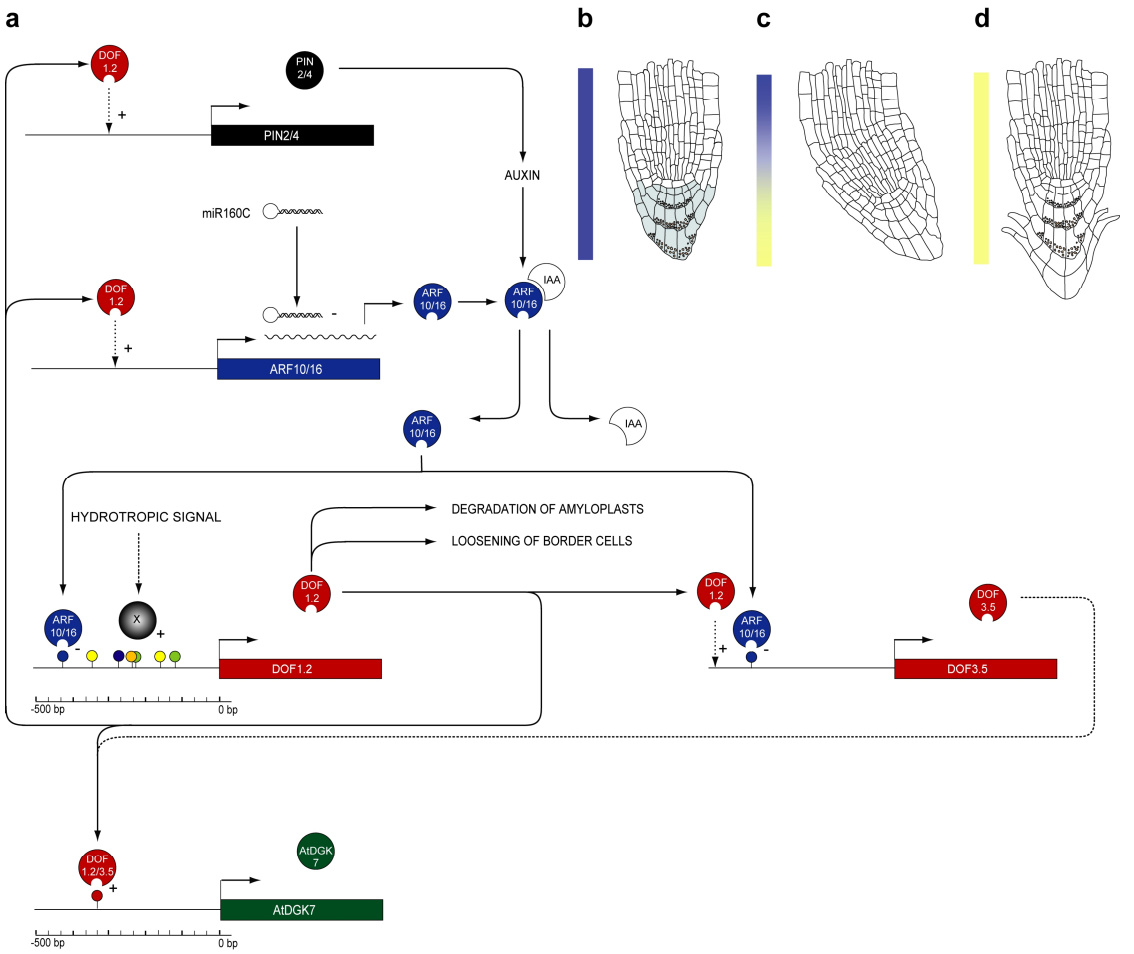

Figure 19. Proposed model of the DOF1.2 regulatory pathway.

(**a, b**) A basic low expression level of *DOF1.2* precisely controlled by the auxin efflux facilitators PIN2 and PIN4 and repressor activity of the auxin response factors ARF10 and ARF16. Under favorable water potential conditions, an unknown hydrotropic signal X induces *DOF1.2* expression. Once transcribed, the DOF1.2 protein mediates the degradation of starch and loosening of cell walls, resulting in a curvature of the root (**c**). Under long-term drought stress, the suppression of *DOF1.2* gene expression leads to the formation of additional boarder cell layers exerting a protective function in the gravitropic growth to reach deeper regions in the soil with a more favorable water potential (**d**). The possible involvement of AtDGK7 and DOF3.5 in this process has to be clarified.

4. DOF3.1 and DOF5.2 define the status of the root stem cell niche

Jonas Krebs[1], Slobodan Ruzicic[2] & Bernd Mueller-Roeber[1,2]

[1]*University of Potsdam, Institute of Biochemistry and Biology, Karl-Liebknecht-Straße 24-25, Haus 20, 14476 Potsdam, Germany*

[2]*Max-Planck Institute of Molecular Plant Physiology, Am Muehlenberg 1, 14476 Potsdam, Germany*

Manuscript in preparation

Authors´ contributions

The experimental work was performed by Jonas Krebs, with the exception of data shown in Fig.20c and Fig.21d, e. The research was designed and planned by Slobodan Ruzicic and Jonas Krebs. Bernd Mueller-Roeber supervised the group as a whole.

4.1 Abstract

Stem cell niches in the root and shoot apical meristems generate appropriate tissues over the lifetime of a plant, by self-renewal while remaining undifferentiated and the maintaining capacity to differentiate into specialized cell types (Dinneny and Benfey, 2008). In *Arabidopsis*, concentration gradients of auxin (Friml et al., 2003; Grieneisen et al., 2007; Muller and Sheen, 2008), routed by auxin influx (Swarup et al., 2001) and efflux carriers (Friml et al., 2003; Blilou et al., 2005), instruct the positioning of the root stem cell niche. Hardly any further regulatory genes are known to contribute to the maintenance of the meristem niche (Dinneny and Benfey, 2008). Here we identified a novel mechanism of root stem cell niche specific gene expression and demonstrate the developmental importance of two *DOF* genes in the process of stem cell niche maintenance. We demonstrate the existence of a novel *cis*-element responsible for the expression in the quiescent centre (QC) and surrounding stem cells and show that it is bound by a subclass of ETHYLENE-RESPONSIVE FACTORS (ERFs). Conserved in promoter position, this element is crucial for expression of *WOX5* (Sarkar et al., 2007) (*WUSCHEL-RELATED HOMEOBOX 5*) and a novel *DOF3.1* gene. We show that DOF3.1 acts redundantly with a further DOF-family member (DOF5.2) and together affect the status of the root meristem niche. These results provide a novel molecular model of specific expression in the root stem-cell niche and indicate a role of two novel *DOF* genes in maintenance of meristem function.

4.2 Introduction

Analogous to animal stem cells, meristems continuously generate the tissues that constitute the plant body (Dinneny and Benfey, 2008). In roots, specific tissues are generated from four different types of stem cells that are under control of the quiescent centre. In *Arabidopsis*, the four rarely dividing cells of the quiescent centre influence the maintenance of the identity of surrounding stem-cells through direct cell-cell interactions (van den Berg et al., 1997). The identity of the quiescent centre and hence the function of the associated stem cells rely on two convergent pathways (Dinneny and Benfey, 2008). The plant signalling molecule auxin acts longitudinally being directionally transported cell-to-cell by PIN transporters (Wisniewska et al., 2006) which establishes a local maximum of auxin in the root stem cell niche (Sabatini et al., 1999). Along the root´s radial axis the transcription factors SCARECROW (SCR) and SHORT ROOT (SHR) direct a signalling pathway and deliver positional information (Levesque et al., 2006). Despite its crucial role in root development (van den Berg et al., 1997), only few genes with preferential expression in the quiescent centre were hitherto functionally characterised (Aida et al., 2004; Sarkar et al., 2007; Welch et al., 2007). One of them is *WOX5*, which acts downstream of the *SCR*/*SHR* genes (Sarkar et al., 2007). Yet, the mechanisms controlling selective transcription in quiescent centre cells remain poorly understood (Nawy et al., 2005). Here we demonstrate that two novel genes encoding members of the plant-specific family of DOF zinc finger proteins, which are specifically expressed in the quiescent centre, contribute to the maintenance of the stem cell domain. In addition, we demonstrate the existence of a

transcription-dependent mechanism for quiescent centre-specific expression, and reveal its importance for root development.

4.3 Material and Methods

4.3.1 Plant work

The T-DNA insertion lines *dof3.1-1* (SALK_136364), *dof3.1-2* (SALK_095816), *dof5.2-1* (GABI_782H09), *wox5-1* (SALK_038262), *arf5-1* (SALK_023812), *at5g11090-1* (SALK_011427) and *at5g11090-2* (SALK_103711) were obtained from the Nottingham Arabidopsis Stock Centre (NASC, UK) as was the GAL4-GFP enhancer-trap line J0571 (N9094). All T-DNA insertion sites were verified by genotyping. The mutant lines *shr-1* and *scr-3* were kindly provided by Ben Scheres (Utrecht University, Netherlands), the DR5rev::GFP plasmid by Gerd Juergens (University of Tuebingen, Germany) and the pER8 plasmid by Nam-Hai Chua (Rockefeller University, New York, USA). Seedlings were grown on vertically orientated plates under long day conditions (16 h light, 22°C and 8 h dark, 18°C).

To confirm T-DNA-insertion sites of *dof3.1-1*, *dof3.1-2*, *wox5-1*, *arf5-1*, *at5g11090-1* and *at5g11090-2* PCR reaction was performed using the T-DNA primer LBa1 and the gene specific primer pairs cdsDOF3.1for/cdsDOF3.1rev, cdsWOX5for/cdsWOX5rev, ARF5for/ARF5rev and At5g11090for/At5g11090rev, respectively and in the case of *dof5.2-1* using the T-DNA primer 8409 and the gene specific primer pair DOF5.2for/DOF5.2rev. In all cases the T-DNA insertion could be confirmed and, if necessary, lines were propagated to homozygosity. T-DNA and gene specific primer sequences are listed in **4.3.16**.

4.3.2 General cloning and transformation procedure

All PCR products were amplified using *Pfu* polymerase and after A-tailing first cloned into the pCR2.1 cloning vector (Invitrogen, Karlsruhe, Germany). For subsequent cloning into binary vectors, pCR2.1 vector was digested as described in the following. The used restriction enzyme sites are part of the listed primer sequences and monitored with bold letters. All endpoint PCR primer sequences are listed in **4.3.16**.

All plasmids were transformed for cloning procedures into *E. coli* DH5α competent cells, for plant transformation into the *Agrobacterium tumefaciens* strain GV3101.
Plant transformation was performed by the floral dip method (Clough and Bent, 1998) and if not mentioned differently the *Arabidopsis thaliana* Col-0 ecotype. All primary transformants were selected on nutrient agar medium supplemented with 50mg/l kanamycin, 20mg/l hygromycin or 2.5mg/l sulfadiazine and propagated to T2 generation.

4.3.3 GUS/GFP reporter gene fusions

The p*DOF3.1-DOF3.1* promoter-CDS region was amplified using the primers pDOF3.1D and cdsDOF3.1rev, digested with SmaI and SalI and cloned into pJFH1-GFP that was digested with *Hin*dIII, blunted and subsequently digested with SalI. A 1527bp *DOF5.2* promoter region was amplified using the primers pDOF5.2for and pDOF5.2rev. The promoter fragment was cloned into the pGPTV-KAN that was previously digested with *Sma*I and *Hin*dIII.

DOF3.1 and *WOX5* promoter-GUS constructs were generated using the Gateway system. The reporter Entry clones were generated by PCR on genomic DNA using in the case of *WOX5* the forward primers pWOX5A and pWOX5B and the reverse primer pWOX5C with attB extensions followed by BP reaction with pDONR201 (Invitrogen, Karlsruhe, Germany) resulting in promoter fragments of 910 and 898bp (with respect to ATG), respectively. In the case of *DOF3.1* the forward primers pDOF3.1A and pDOF3.1B and the reverse primer pDOF3.1C were used resulting in promoter fragments of 1136 and 1124bp (with respect to ATG), respectively. Subsequent LR reaction was performed with the pGWB3i GUS vector that was kindly provided by Dr. Tamara Gigolashvili, University of Cologne, Germany.

4.3.4 Inducible overexpression of *DOF3.1 (35Sind::DOF3.1)*

The *DOF3.1* coding sequence was amplified using the primers cdsDOF3.1for and cdsDOF3.1revB. The resulting fragment was digested with *Sal*I and *Spe*I and subsequently cloned into the β-estradiol inducible pER8 vector (Zuo et al., 2000) that was digested with *Xho*I and *Spe*I. The resulting *35Sind::DOF3.1* construct was transformed into the *dof3.1-1* mutant. For expression analysis seeds were grown on nutrient agar plates and transferred DAG into liquid control medium or medium supplemented with 20µM β-estradiol. After 3h and 6h 20 seedlings were transferred to liquid nitrogen and RNA was extracted as described. Confocal microscopy analyses were performed with four day-old seedlings of the inducible lines #1 and #2 and their DR5rev::GFP and J0571 supertransformants which were grown on medium supplemented with 20µM β-estradiol or on medium supplemented with DMSO as control.

4.3.5 Yeast one-hybrid screen

The Yeast one-hybrid screen was performed with a triple tandem copy of the identified *cis*-element as the bait construct. Forward and reverse oligonucleotides YOHfor and YOHrev were annealed as described in the Clontech Matchmaker™ One-Hybrid Library Construction & Screening Kit protocol (http://www.clontech.com/images/pt/PT3529-1.pdf) and subsequently ligated in the pHIS2.1 vector that was previously digested with *Eco*RI and *Spe*I.

Small scale transformation of Y187 cells with the bait construct was transformed as followed: 25ml of yeast cells were grown in liquid YPD medium to an optical density of 0.9, centrifuged 5min at 4000rpm and resuspended in 25ml of sterile water. 1.5ml of the cell suspension were transferred to an 1.5ml Eppendorf tube and centrifuged 2min at 5000rpm. The pelleted cells

were resuspended in a transformation mix (333µl PEG (50%), 50µl 10xTE, 50µl LiAc (1M), 50µl H_2O, 20µl ssDNA (5mg/ml), 1µg plasmid DNA and after 15min incubation time at room temperature mixed with 50µl DMSO and incubated 12min at 42°C. Cells were afterwards stored on ice for 3min and centrifuged 5min at 5000rpm, washed with 1ml water, centrifuged 2min at 5000rpm and resuspended in 150µl sterile water. To test the target sequence for autoactivation by endogenous yeast transcription factors, 75µl of each tube with transformed yeast cells were plated on SD-W-H medium supplemented with 0, 25 and 50mM 3-AT, the remaining 75µl on SD-W control plates. Since no colony growth could be observed on 50mM plate the screen was performed with this concentration. The cDNA library which is derived from root cell culture and was cloned in pACT2 vector was kindly provided by Csaba Koncz (Max-Planck Institute of Plant Breeding, Cologne).

The large scale yeast transformation was performed as follows: 100ml of transformed Y187 cells carrying the described bait construct were grown in liquid SD-W medium to an optical density of 0.9. Cells were pelleted (5min, 2000rpm), resuspended in 15ml transformation mix1 [1.5ml LiAc (1M), 7.5ml sorbitol (2M), 0.75ml 10xTE, 5,25ml H_2O] and after centrifugation (5min, 2000rpm) resuspended again in 1ml transformation mix1. After 10min incubation time at roomtemperature 150µl ssDNA (10mg/ml) and 50µg cDNA were added and mixed with the cells on ice. Subsequently 7ml of transformation mix2 [1ml LiAc (1M), 6,7ml PEG 3350 (60%), 1ml 10xTE, 1,3ml H_2O] were added to the cell suspension, briefly vortexed and incubated 30min at 30°C. After addition of 300µl DMSO cells were vortexed for 30sec and incubated for 20min at 42°C in a water bath. Cells were pelleted (3min, 4000rpm) and resuspended in 4ml sterile water.

Transformation efficiency of $1{,}77 \times 10^6$ was calculated by counting colonies after plating 1µl of transformed cells on SD-W plates. The remaining transformed cells were plated on SD-W-H Medium and incubated at 30°C for 7 days. Of 122 colonies that were grown after 7 days of incubation time, the inserted cDNA from 60 colonies was determined by sequencing. For this purpose the colony was picked with a pipette tip and transferred to a PCR master mix containing the primers pACT2for and pACT2 rev. The resulting PCR product was purified and sent for sequencing with the primer pACT2seq.

4.3.6 Transactivation assay

The above described promoter fragments pDOF3.1A (1136bp) pDOF3.1B (1124bp), pWOX5A (910bp) and pWOX5B (898bp) were cut with *Sal*I, blunted and subsequently digested with *Sma*I and ligated in the pHIS2.1 vector that was previously digested with *Eco*RI and *Spe*I and blunted. The full length coding sequences of *AtERF1* and *AtERF5* were amplified using the primers ERF1for, ERF1rev and ERF5for, ERF5rev, respectively. The fragments were digested with *Xho*I and *Spe*I and ligated into pAD-Gal4-2.1 vector (Stratagene, Amsterdam, The Netherlands) that was previously digested with *Xho*I and *Xba*I. The promoter-reporter gene bait constructs were

transformed into Y187 cells and autoactivation was tested. No colony growth could be observed by using 30mM 3-AT, which was taken for subsequent supertransformation with AtERF1 or AtERF5 prey constructs.

4.3.7 Yeast two-hybrid screen

The coding sequence of *DOF3.1* was amplified using the primers cds*DOF3.1*for and cds*DOF3.1*rev. The resulting fragment was cut with *Sal*I and cloned into pLEX-PD vector that was previously digested with *Sal*I and dephosphorylated.

The resulting bait construct was transformed into the yeast strain L40ccua by following the small scale transformation protocol and cells were plated on SD-W plates. To test the autoactivation of *DOF3.1* yeast cells carrying the bait construct were supertransformed (small scale protocol) with the empty activation domain vector pACT2 and plated on SD-W-L medium as control and SD-W-L-H-U supplemented with increasing concentrations of 3-AT (0, 10, 15, 20, 30, 40, 50mM). No colony growth could be observed on plates supplemented with 20mM or higher concentrations of 3-AT. For this reason 20mM was chosen as the optimal concentration.

The two-hybrid screen was performed following the large scale transformation protocol described above. 1µl, 5µl and 10µl of the transformed yeast cells were added to 70µl sterile water and plated on SD-W-L plates to determine the transformation efficiency, which was $2{,}4x10^6$. To select the strongest interaction partners, the 225 colonies that were grown on SD-W-L-H-U (20mM 3-AT) plates colonies were resuspended in sterile water and plated again on SD-W-L-H-U medium supplemented with 30mM 3-AT. The inserts of 50 of the remaining grown 100 colonies were amplified and sequenced as desribed above.

For confirmation of the YTH screen results the coding sequence of *At5g11090* was cloned into *Sal*I-digested pLEX-PD vector using the primers Atg5g11090for and At5g11090rev. The coding sequence of *DOF3.1* was cloned into *Xho*I-digested pAD-Gal4-2.1 vector using primers cdsDOF3.1for and cdsDOF3.1rev.

4.3.8 Artificial microRNA

The *DOF5.2* directed amiRNA was generated using the Web MicroRNA Designer tool. (http://wmd.weigelworld.org/cgi-bin/mirnatools.pl). PCR reactions were performed as described in the online protocol using the primers amiRNAI, amiRNAII, amiRNAIII and amiRNAIV. The resulting fragment was purified, digested with *Eco*RVI and *Xba*I subsequently cloned in the pBinAR-Hyg vector containing the cauliflower 35S promoter that was previously digested with *Sma*I and *Xba*I.

4.3.9 Transient protoplast transformation

The coding sequences of *DOF3.1* and *At5g11090* were amplified using the primers cdsDOF3.1for and cdsDOF3.1rev and Atg5g11090for and At5g11090rev respectively. Fragments were cut with *Sal*I (*DOF3.1*) and *Xho*I (*At5g11090*) and cloned into pA7-GFP vector that was previously digested with *Xho*I and *Sal*I and dephosphorylated.

Cells from a 7 days old *Arabidopsis thaliana* suspension culture were digested and transformed as followed: Cells were pelleted (800rpm, 8min) and washed twice in MCP (0.5M sorbitol, 1mM $CaCl_2$, 10mM MES, pH 5.6). After following centrifugation (800rpm, 8min), in attempt to digest the cell walls, the cells were resuspended in enzyme solution (MCP supplemented with 0.25% macerozyme R-10, 0.1% BSA, 1% cellulase (Onozuka R-10)) and shaken for 4h (60rpm, 28°C). Resulting protoplasts were separated using a Percoll gradient and washed in W5 solution (154mM NaCl, 125mM $CaCl_2$, 5mM KCl, 5mM Glucose, 1.5mM MES, pH5.6). Following, the protoplasts were incubated on ice for 30min and counted. Subsequently, the cells were precipitated by centrifugation (800rpm, 8min) and resuspended in MaMg solution (0.4M mannitol, 15mM $MgCl_2$, 5mM MES, pH5.6) to a density of $5x10^6$ cells/ml. Afterwards, 50µg plasmid DNA and 50µg ssDNA were added to 300µl of protoplast suspension. After addition of 325µl of PEG solution (0.4M mannitol, 0.1M $Ca(NO_3)_2$, 40% PEG 4000) and brief shaking, the cells were incubated for 30min at room temperature, centrifuged (800rpm, 5min), washed with 10ml of W5 solution, centrifuged and resuspended in 3ml of W5 solution. Prior to confocal microscopy the protoplasts were incubated for 48h at 22°C in the dark.

4.3.10 Plant crossing

dof3.1-1 was crossed with *amiR-dof5.2-1* lines #2, #4, #5, #9 and #11 and propagated to *DOF3.1* homozygosity again. One selected *DR5rev::GFP* transformant was crossed with the *DOF3.1* inducible overexpression lines #1 and #2 and the *dof3.1-1 amiR-dof5.2-1* lines #9 and #11 which were propagated to *DOF3.1* homozygosity again. The cortex/endodermis GFP markerline J0571 was crossed with the *DOF3.1* inducible overexpression lines #1 and #2.

4.3.11 Brassinolide effects

Seeds were grown on nutrient agar plates and transferred 3 DAG into liquid control medium (1x Murashige and Skooge, 1% sucrose, pH 5.8) or medium supplemented with 0.5; 5 or 50nM epi-brassinolides. After 6h, 12h, 1d, 2d and 3d seedlings were transferred to GUS staining buffer and analysed under microscopy as described.

4.3.12 Quantitative RT-PCR

cDNA was prepared from 3µg of total RNA with Superscript III reverse transcriptase (Invitrogen, Karlsruhe, Germany) and quantified using SYBR green master mix (ABI). PCR was performed in 96 well reaction plates (ABI) by use of the standard Absolute quantification protocol. Realtime PCR primer pairs were designed using the Primer Express software tool (ABI). Expression levels were normalized to EF1α expression levels. All realtime PCR experiments were done in three technical replicates and statistical relevance was estimated using the t-test. All realtime PCR primer sequences are listed in **4.3.17**. The primer efficiency was calculated using LinRegPCR (Ramakers et al., 2003).

4.3.13 *In situ* hybridisation

In situ hybridization on whole-mount tissues was performed manually as previously described (Hejatko et al., 2006). Riboprobes were prepared using the oligonucleotides DOF3.1iRfor and DOF3.1iRrev.

4.3.14 Microscopy

Starch granules (Willemsen et al., 1998) and β-glucuronidase (Schoof et al., 2000) activity were visualized as described and photographed with Nomarski optics on NIKON eclipse E600 microscope and a NIKON DXM1000 camera.

For laser scanning confocal microscopy 4DAG-old seedlings were mounted in 10μM propidium iodide solution. Microscopy was performed using the Helium/Neon laser of a Leica SP2 microscope. GFP and propidium iodide were excited using a single wavelength excitation at 488nm. Emission was characterized from 500 to 520nm (GFP) and 600 to 650nm (propidium iodide). DAPI (4´,6-diamidino-2-phenylindole, dihydrochloride) was excited at 364nm using the UV laser. Emission was observed at 460nm.

4.3.15 Sequences and bioinformatic tools

All *Arabidopsis* gene sequences were derived from TAIR database (www.arabidopsis.org). Promoter comparison analyses were performed using the FootPrinter webserver (http://genome.cs.mcgill.ca/cgi-bin/FootPrinter3.0/FootPrinterInput2.pl). Genome-wide search for promoters containing the QC-SPE was performed using the Patchmatch tool of the TAIR webpage (http://www.arabidopsis.org/cgi-bin/patmatch/nph-patmatch.pl) and the motif "ATTYTCT" as input for pattern search. Overrepresentation of the QC-SPE in 1kb promoter region of published QC genes was analysed with POBO (Kankainen and Holm, 2004) using the motif "ATTYTCT" as in put for the "search consensus pattern" option.

4.3.16 endpoint PCR primer sequences

primer name	Primer sequence (5´→3´)	primer name	Primer sequence (5´→3´)
pDOF3.1A	ACAAGTTTGTACAAAAAAGCAGGCTATTC TCTTATAAGCAAAATATTTTT	DOF3.1iRrev	AAGCTTGCTTCCACCAATCTCCATACCC TT
pDOF3.1B	ACAAGTTTGTACAAAAAAGCAGGCTGCA AAATATTTTTAGCAAAAATTTT	YOHfor	AATTCATTCTCTTATAAATTCTCTTATAAA TTCTCTTATAAA
pDOF3.1C	ACCACTTTGTACAAGAAAGCTGGGTTTTT CTTCAACCTTTATTCAAAAAT	YOHrev	CTAGTTTATAAGAGAATTTATAAGAGAAT TTATAAGAGAATG
pDOF3.1D	CCCGGGGTCTACTTATTCTTGAGCCA	pWOX5A	ACAAGTTTGTACAAAAAAGCAGGCTATTT TCTTATAAAAGAGAATAAAAT
cdsDOF3.1for	GTCGACATGCAGGATCCAGCAGCATA	pWOX5B	ACAAGTTTGTACAAAAAAGCAGGCTAAG AGAATAAAATTTCAAATTTCCT
cdsDOF3.1rev	GTCGACGTTTTTCTCCGCTCTGTTCA	pWOX5C	ACCACTTTGTACAAGAAAGCTGGGTGTT CAGATGTAAAGTCCTCAACTGT
cdsDOF3.1revB	ACTAGTTCAGTTTTTCTCCGCTCTGT	ERF1for	ACAAGTTTGTACAAAAAAGCAGGCTACT CGAGATGTTAGTTTACGGTATCCTCA
pDOF5.2for	AAGCTTGGTCTGAAATAAAGGTACTA	ERF1rev	ACCACTTTGTACAAGAAAGCTGGGTACT AGTTTATAAAACCAATAAACGATCG

pDOF5.2rev	CCCGGGGGTAATGATTCCTTTTCACT	ERF5for	ACAAGTTTGTACAAAAAAGCAGGCTACT CGAGGCGACTCCTAACGAAGTAT
ARF5for	ATGATGGCTTCATTGTCTTG	ERF5rev	ACCACTTTGTACAAGAAAGCTGGGTACT AGTTCAAACAACGGTCAACTGGGA
ARF5rev	TTATGAAACAGAAGTCTTAA	amiRNAI	GATTTATTCTTACGTCTCCCGGCTCTCTC TTTTGTATTCC
At5g11090for	CTCGAGATGGTGACTACATCGTCACG	amiRNAII	GAGCCGGGAGACGTAAGAATAAATCAAA GAGAATCAATGA
At5g11090rev	CTCGAGATTCTCATCAGCTTTCGCCA	amiRNAIII	GAGCAGGGAGACGTATGAATAATTCACA GGTCGTGATATG
DOF5.2for	GAGAAGAAGGTGATGATGTT	amiRNAIV	GAATTATTCATACGTCTCCCTGCTCTACA TATATATTCCT
DOF5.2rev	CTATGAGCTCTCATGGAAGT	pACT2for	CTATCTATTCGATGATGAAG
LBa1	TGGTTCACGTAGTGGGCCATCG	pACT2rev	ACAGTTGAAGTGAACTTGCG
8409	ATATTGACCATCATACTCATTGC	pACT2seq	TACCCATACGATGTTCCAGA
DOF3.1iRfor	GGATCCAACGCAACCAAACGATCCACTT CT		

4.3.17 quantitative RT-PCR primer sequences

Primer name	**Primer sequence 5´→ 3´**	**Primer name**	**Primer sequence 5´→ 3´**
EF1a for	TGAGCACGCTCTTCTTGCTTTCA	PIN4 for	CGGATGCTGAGATAGGAAACGA
EF1a rev	GGTGGTGGCATCCATCTTGTTACA	Pin4 rev	TCTCGATGCGTTTGATTTCCTC
UBQ10 for	CACACTCCACTTGGTCTTGCGT	PIN5 for	TGTACGGACAACAGGCTGTTGA
UBQ10 rev	TGGTCTTTCCGGTGAGAGTCTTCA	PIN5 rev	CCACACGATGGCTTGAAATACC
DOF3.1 for	AGCTCGTTGTTGGCGAATAA	PIN6 for	ATCATTTCAGATGCAGGTCTTGGG
DOF3.1 rev	CTCCTCAAACCCAAACCCAT	PIN6 rev	CAGCGCCATAAACAGGCCTAAAC
DOF5.2 for	CAGAGATATTGGACAGCTGGTGG	PIN7 for	CGTGTGGCCATTGTTCAAGCTG
DOF5.2 rev	TCTTACGTCTCCCAGCACCAAC	PIN7 rev	CCCTGTACTCAAGATTGCGGGATG
WOX5 for	CGTGAAAGGTCGAAGCTTACGTG	PIN8 for	ATGGCCATGTTCAGCTTAGGTC
WOX5 rev	ATTCCATCTCCCGCACTTCGTC	PIN8 rev	CTGATGCAATACGCAGAAGCAATC
PLT1 for	AGTTCGTGGCTGCCATTAGAAGG	AUX1 for	CAGCTGCGCATCTAACCAAGTG
PLT1 rev	ATCTTCCATGTTGGTGATGCCTTG	AUX1 rev	GATGAGATAAGCAGTCCAGCTTCC
PLT2 for	GAAGATGGCAAGCAAGGATCGG	CTR1 for	TCTTGTGGGAGCTTGCTACATTGC
PLT2 rev	GCTTCTTCCTCCGTGCTGAATG	CTR1 rev	AAACCAACCGCAGCTACAACCTG
MP for	TTACGCATCCCACAAACTCTTCC	ETR1 for	TCCGATCAATTCTTCCCAAGTGTG
MP rev	GCTCGGGTTGGAAGCTTGTATATG	ETR1 rev	GCTGGCCATTGCGGTTCAATAC
BDL for	GCTTCTCCTCCTCGTTCAAGTC	EIN2 for	TCATGGCGATTTCGAAGGTCT
BDL rev	TCTCCTTCTTCCGCTCTTGCTG	EIN2 rev	AGGAAGCCCTAACAGAGCAAC
SHR for	AGGGTTTGCTTCGAGTCATGG	EIN3 for	AACTGGCATGTCCACATCGAGAC
SHR rev	TGCACGCTCTAGCATCAACCTC	EIN3 rev	ATGAAACCTGGATGGTGCTGCTC
SCR for	AAGGGAAGCTGTGGCTGTTCAC	ASA1 for	ATGCATATAAGCTCCACGGTGAC
SCR rev	AGTGTGTGCATCAGAGCCAGT	ASA1 rev	GTACGTCCCAGCAAGTCAAACC
PIN1 for	GGCATGGCTATGTTCAGTCTTGGG	ASB1 for	ACGAATCCCACAAGAGTTTCCG
PIN1 rev	ACGGCAGGTCCAACGACAAATC	ASB1 rev	GATTCCGCCATTTCAATCGAAGC
PIN2 for	ATGATCACCGGCAAAGACATGT	IAA1 for	TTGGGATTACCCGGAGCACAAG
PIN2 rev	TAGCAACGTATAGCGGCACCA	IAA1 rev	GCGCTTGTTGTTGCTTCTGACG
PIN3 for	AAGGCGGAAGATCTGACCAAGG	IAA2 for	AGCGTCTATTTGAGGAAACTCGTG
PIN3 rev	TGCTGGATGAGCTACAGCTTTG	IAA2 rev	GGTGGCCAACCAACGATTTGAG

4.4 Results and discussion

4.4.1 *DOF3.1* is expressed in the quiescent centre and its embryonic progenitor

Expression of *DOF3.1::GUS* reporter gene initiates in early globular embryos. It was not detactable prior to the division of the hypophysis (Fig.20a). Upon its horizontal division, GUS signal was observed in the upper hypophyseal derivate (UHD) representing the direct precursor of the quiescent centre (Fig.20b). This expression persists throughout embryogenesis and during post-germinative growth and occurred specifically in the quiescent centre, sometimes accompanied by weaker signals in the surrounding initials (Fig.20c).

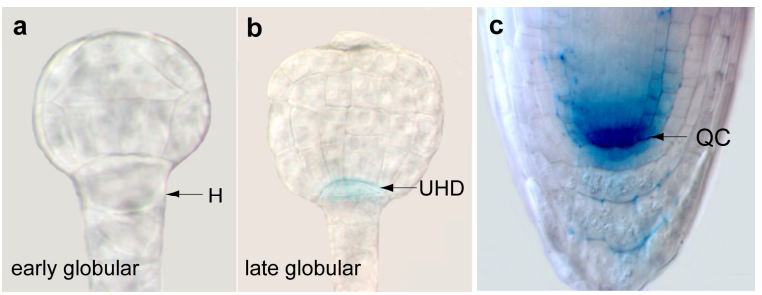

Figure 20. *DOF3.1* expression pattern in the embryo and primary root tip.

DOF3.1::GUS expression in the globular stage of embryogenesis (**a, b**) and in the primary root tip (**c**). H, hypophysis; QC, quiescent centre; UHD, upper hypophysial derivate

4.4.2 *DOF3.1* is expressed during initiation of lateral root formation

Expression was also evident in pericycle cells upon the initiation of lateral roots and coincides with the formation of the QC (Fig.21a-c). Expression of *DOF3.1* messenger RNA (Fig.21d-e) and distribution of GFP protein in *DOF3.1::GFP* reporter lines (data not shown) were congruent with the observed *GUS* reporter expression pattern.

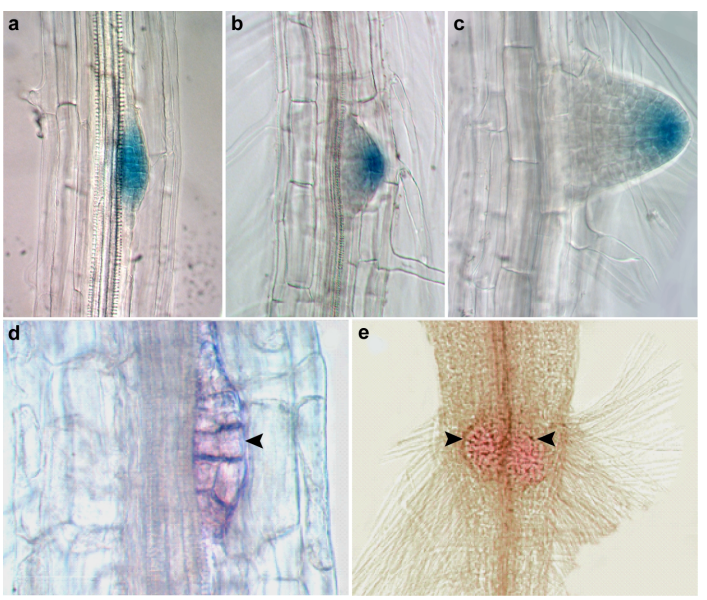

Figure 21. *DOF3.1* expression in lateral roots.

a-c, *DOF3.1::GUS* expression correlates with the development of lateral root. GUS activity could be identified in broader region of the pericycle prior to any signs of periclinal divisions adjacent to the xylem pole (data not shown). (**a**) In early lateral root primordia, the expression was initially observed in both, the inner and outer layer. (**b**) In later developmental stages, reporter gene signals were persistently shifted towards future root tip and finally coincident with the identity of newly formed stem cell niche (**c**). **d-e,** *DOF3.1* mRNA abundance in lateral root primordial long the xylem pole (**d**) and on the hypocotyl-root junction (**e**).

4.4.3 DOF3.1 protein strongly localizes in the QC

Intercellular protein movement was shown to play a crucial role in the downstream regulation pathway of transcription factors (Lee *et al.*, 2006). One prominent example is the *SHR* gene, which is transcribed exclusively in the vascular tissue, but the SHR protein moves on cell layer outwards to the endodermis including the cortex/endodermis initials and the QC cells (Cui *et al.*, 2007). Thus, we asked, whether the DOF3.1 protein localisation recapitulates the expression pattern observed in the *DOF3.1* promoter-reporter gene fusion and *in-situ* hybridisation as an indication for its functional role in the stem cell niche. DOF3.1 protein localizes in nuclei of quiescent centre cells and to some weaker extent in the surrounding stem-cells (Fig.22a, b). Remarkably, the *DOF3.1::DOF3.1:GFP* protein signal disappears in cells that have undergone any differentiation-related divisions. In the cortex/endodermis initials (CEI) it was only detectable prior to the periclinal cell division that results in the formation of the two cell files of cortex and endodermis (Fig.22b).

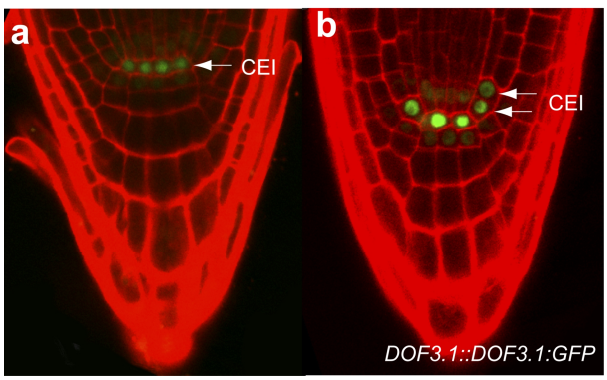

Figure 22. *DOF3.1::DOF3:1:GFP* localization in the root apical meristem.

a, b, Maximum fluorescence was detectable in the quiescent centre cells whereas weaker signals were observed in the surrounding stem cells. In the cortex/endodermis initials GFP was only detectable prior to their periclinal division and the differentiation to cortex and endodermis cell files (**b**). CEI, cortex/endodermis initial

4.4.4 *DOF3.1* and *WOX5* possess similar expression pattern and common promoter architecture

The expression pattern of *DOF3.1* strongly resembles expression of the *WOX5::GUS* reporter gene in embryos and roots of juvenile plants (Sarkar et al., 2007). We investigated, whether the remarkably similar expression pattern of the two genes is due to a common promoter architecture. Indeed, an alignment of 1kb of both promoter sequences revealed that *DOF3.1* and *WOX5* share several common motifs, whereby one motif of 12 nucleotides was located at a position relative to the transcription start site that was closely similar in both genes (Fig.23a, blue box).

4.4.5 Common promoter element is essential for *DOF3.1* and *WOX5* expression

To reveal the relevance of the identified spatially conserved motif on *DOF3.1* and *WOX5* gene expression, promoter-GUS fusion constructs were generated, including and excluding the common motif. We found that the identified element was crucial for the QC-specific expression of both genes, whereby the first three nucleotides on the 5'-end turned out to be essential for functionality of the downstream promoter sequence of *DOF3.1* (Fig.23b).

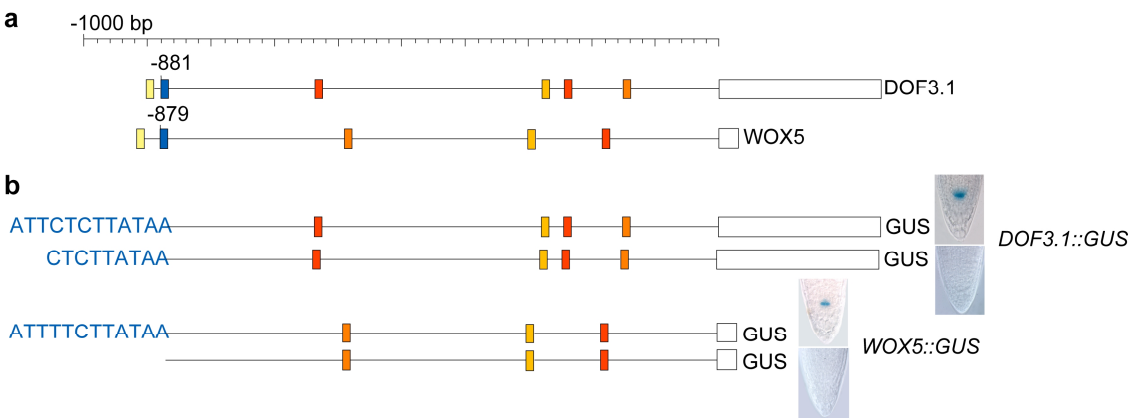

Figure 23. *DOF3.1* and *WOX5* genes share common promoter architectures.

a, Schematic representation of *DOF3.1* and *WOX5* 1kb promoter sequences (with respect to transcription start site). Coloured boxes indicate all common motives of 12 nucleotides length with one allowed mutation, white boxes represent the 5´-UTR. Motif ATTYTCTTATAA (blue box, QC-SPE) is located in both promoters at nearly the same position. **b,** Promoter deletion studies revealed that in *DOF3.1* and *WOX5* promoters a QC-SPE is necessary to drive GUS expression in the QC. In the *DOF3.1* promoter the first three nucleotides on the 5'-end of the QC-SPE are arbitrative.

Table 3. Genes with confirmed expression in root stem cell niche and distribution of QC-SPE in their promoter regions.

Locus ID	Description	QC-specific element			Reference
		Start[A]	End[A]	Sequence	
AT4G3765	*SHR*	-154	-148	ATTCTCT	(Benfey et al., 1993)
		-103	-97	ATTCTCT	
AT3G5422	*SCR*	-951	-945	ATTTTCT	(Di Laurenzio et al., 1996)
AT3G2084	*PLT1*	-461	-455	ATTTTCT	(Aida et al., 2004)
AT1G5119	*PLT2*	-1042	-1036	ATTTTCTT	(Aida et al., 2004)
AT5G1051	*PLT3/AIL6*	-141	-135	ATTCTCT	(Galinha et al., 2007)
		-72	-66	ATTTTCTT	
AT5G1743	*BBM*	-196	-190	ATTCTCT	(Galinha et al., 2007)
AT5G0315	*JKD*	-91	-84	ATTTTCTT	(Welch et al., 2007)
AT1G0384	*MGP*	-737	-730	ATTCTCTT	(Welch et al., 2007)
		-30	-24	ATTTTCT	
AT3G1126	*WOX5*	-879	-872	ATTTTCTT	(Sarkar et al., 2007)
AT3G2127	*DOF3.1*	-881	-874	ATTCTCTT	
		-657	-651	ATTTTCT	
AT5G3966	*DOF5.2*	-924	-918	ATTTTCT	
AT5G0573	*WEI2*	-707	-701	ATTCTCT	(Ivanchenko et al., 2008)
AT1G2522	*WEI7*	-1682	-1675	ATTTTCTT	(Ivanchenko et al., 2008)
AT1G6953	*AtEXPA1*	-957	-951	ATTTTCT	(Wieczorek et al., 2006)
		-593	-586	ATTTTCTT	
		-573	-566	ATTTTCTT	
		-224	-217	ATTTTCTT	
AT4G3288	*AtHB-8*	-938	-931	ATTTTCTT	(Baima et al., 1995)
AT2G3471	*PHB*	-410	-403	ATTTTCTT	(Hawker and Bowman, 2004)
		-368	-361	ATTTTCTT	
AT5G6216	*AGL42*	-907	-901	ATTCTCT	(Nawy et al., 2005)
AT5G5484	*AtSGP1*	-881	-875	ATTCTCT	(Bedhomme et al., 2009)
		-854	-847	ATTTTCTT	
		-56	-50	ATTTTCT	
AT2G0142	*PIN4*	-1798	-1792	ATTTTCT	(Friml et al., 2002)

[A] Position of the element in the promoter region relative to the transcription start site.

4.4.6 QC-SPE is overrepresented in promoters of stem cell niche-expressed genes

To reveal if the identified *cis*-element play a general role in QC-specific gene expression, we investigated, whether other genes with well confirmed expression in the root stem cell niche (Table 3) also harbour this motif (in the follwing assigned as quiescent centre-specific promoter element, QC-SPE). Indeed, considering the first seven or eight nucleotides of the element (counted from its 5'-end), we could confirm a clear overrepresentation in promoters of the tested subset of genes in comparison to random sets of promoter sequences (Fig.24). We therefore reasoned that the motif ATTYTCT could be conserved in different genes with an expression in the root stem cell niche.

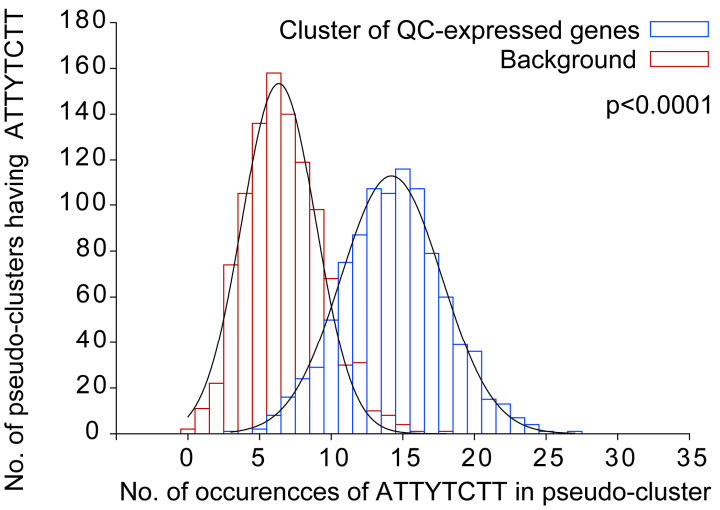

Figure 24. Overrepresentation of the QC-SPE in published QC expressed genes.

The cis-element analysis tool POBO revealed that stretches of the 5´-located seven (data not shown) or eight nucleotides of the QC-SPE are clearly overrepresented ($P < 0.0001$) in the promoter sequences of published QC-expressed genes (Table 3) when compared to background.

4.4.8 Genome-wide screen of the QC-SPE confirm its role in stem cell niche expression

To identify novel genes with a putative expression in the QC or genes with an expression in the QC but lacking a described functional role in the stem cell niche and thus were not part of our previous investigation, we performed a genome-wide screen for genes possessing the first seven nucleotides of the QC-SPE in their promoter regions. To narrow down the amount of genes we concentrated in this analysis on genes with a distance of the QC-SPE relative to the transcription start site similar to that of *DOF3.1* (-881bp) with an allowance of +/- two nucleotides. The search resulted in 59 genes (Table 4), among which an experimentally visualized expression pattern was shown for eight genes, namely cytochrome P450 *CYP86A1* (Hofer *et al.*, 2008), a gene encoding for an adenine nucleotide transporter (Leroch *et al.*, 2008), *THREONINE ALDOLASE 2* (Joshi *et al.*, 2006), a gene encoding for a amevalonate kinase (Lluch *et al.*, 2000), a gene encoding for a monomeric G-protein (Bedhomme *et al.*, 2009), the glucosyltransferase *UGT74B1* (Grubb et al., 2004), *WOX5* (Sarkar *et al.*, 2007) and the sucrose-H^+ symporter *SUC2* (Truernit and Sauer, 1995). Astonishingly, with the exception of *SUC2*, remaining seven displayed an accumulation of reporter gene signal in the stem cell niche, whereby signals of the monomeric G-protein (*AT5G54840*) and *UGT74B1* (*AT2G23260*)

were in root exclusively accumulated in the quiescent centre. These data indicate that identified element is required for some aspects of QC-specific gene expression.

Table 4. Genes with QC-SPE located on the position +/-2 nucleotides relative to position of QC-SPE in the *DOF3.1* promoter.

Locus ID	Description	QC-specific element				Expression in root[C]
		Fr.[A]	Start[B]	End[B]	Sequence	
AT5G58860	CYP86A	2	-881	-875	ATTTTCT	root tip
AT5G42420	transporter-related	3	-882	-876	ATTTTCT	root tip
AT3G04520	THA2 (THREONINE ALDOLASE 2)	2	-880	-874	ATTTTCT	root tip
AT5G27450	MK/MVK; mevalonate kinase	1	-882	-876	ATTCTCT	root tip
AT5G54840	GTP-binding family protein	3	-881	-875	ATTCTCT	QC
AT2G23260	UGT84B1 (UDP-GLUCOSYL TRANSFERASE 84B1)	3	-880	-874	ATTTTCT	QC
AT3G11260	WOX5	1	-879	-873	ATTTTCT	QC
AT3G21270	DOF3.1	2	-881	-875	ATTCTCT	QC
AT1G22710	SUC2 (SUCROSE-PROTON SYMPORTER 2)	2	-882	-876	ATTCTCT	Not
AT1G80950	phospholipid/glycerol acyltransferase family protein	1	-879	-873	ATTTTCT	NDD
AT5G51060	RHD2 (ROOT HAIR DEFECTIVE 2)	2	-879	-873	ATTTTCT	NDD
AT1G68480	JAG (JAGGED)	2	-879	-873	ATTTTCT	NDD
AT5G62020	AT-HSFB2A (heat shock transcription factor B2A)	2	-881	-875	ATTTTCT	NDD
AT5G46570	protein kinase family protein	1	-879	-873	ATTTTCT	NDD
AT4G34220	leucine-rich repeat transmembrane protein kinase	2	-883	-877	ATTCTCT	NDD
AT4G24780	pectate lyase family protein	1	-883	-877	ATTTTCT	NDD
AT5G46740	UBP21 (UBIQUITIN-SPECIFIC PROTEASE 21)	1	-883	-877	ATTTTCT	NDD
AT5G25360	similar to unknown protein	2	-882	-876	ATTTTCT	NDD
AT5G11200	DEAD/DEAH box helicase, putative	1	-881	-875	ATTCTCT	NDD
AT5G53190	nodulin MtN3 family protein	1	-880	-874	ATTTTCT	NDD
AT3G49910	60S ribosomal protein L26 (RPL26A)	2	-882	-876	ATTTTCT	NDD
AT1G24600	similar to unknown protein	1	-883	-877	ATTTTCT	NDD
AT3G45930	histone H4	1	-883	-877	ATTTTCT	NDD
AT4G29840	MTO2 (METHIONINE OVER-ACCUMULATOR)	2	-882	-876	ATTTTCT	NDD
AT5G46190	KH domain-containing protein	1	-883	-877	ATTCTCT	NDD
AT2G34470	UREG (urease accessory protein G)	1	-879	-873	ATTCTCT	NDD
AT5G64750	putative AP2 transcription factor	4	-883	-877	ATTTTCT	NDD
AT3G21070	NADK1 (NAD kinase 1)	2	-883	-877	ATTTTCT	NDD
AT1G75400	protein binding/zinc ion binding	1	-882	-876	ATTCTCT	NDD
AT1G66720	S-adenosyl-L-methionine:carboxyl methyltransferase	1	-879	-873	ATTTTCT	NDD
AT4G19510	disease resistance protein (TIR-NBS-LRR class)	1	-882	-876	ATTTTCT	NDD
AT2G42200	squamosa promoter-binding protein-like 9 (SPL9)	4	-879	-873	ATTTTCT	NDD
AT5G20840	phosphoinositide phosphatase family protein	1	-882	-876	ATTTTCT	NDD
AT1G30600	subtilase family protein	1	-882	-876	ATTTTCT	NDD
AT2G01600	epsin N-terminal homology (ENTH) protein	1	-879	-873	ATTTTCT	NDD
AT4G12480	pEARLI 1; lipid binding	2	-879	-873	ATTCTCT	NDD
AT5G41410	BEL1 (BELL 1)	2	-879	-873	ATTTTCT	NDD
AT4G10330	glycine-rich protein	2	-880	-874	ATTTTCT	NDD
AT3G06670	unknown protein	1	-879	-873	ATTCTCT	NDD
AT1G30972	thionin family protein	2	-883	-877	ATTCTCT	
AT1G48930	ATGH9C1 (GLYCOSYL HYDROLASE 9C1)	3	-882	-876	ATTTTCT	
AT1G10720	BSD domain-containing protein	2	-882	-876	ATTTTCT	
AT2G37770	aldo/keto reductase family protein	1	-882	-876	ATTTTCT	
AT3G24820	BSD domain-containing protein	1	-882	-876	ATTCTCT	
AT4G24800	MA3 domain-containing protein	1	-882	-876	ATTCTCT	
AT5G58900	myb family transcription factor	1	-882	-876	ATTTTCT	
AT2G30930	similar to unknown protein	2	-881	-875	ATTTTCT	
AT3G06170	TMS membrane family protein	2	-881	-875	ATTCTCT	
AT5G26330	plastocyanin-like domain-containing protein	2	-881	-875	ATTTTCT	
AT3G50150	similar to unknown protein	1	-881	-875	ATTTTCT	
AT3G61600	ATPOB1 (POZ/BTB containing-protein 1)	1	-881	-875	ATTTTCT	
AT5G53330	similar to hypothetical protein	1	-881	-875	ATTTTCT	
AT4G10490	Oxidoreductase	1	-880	-874	ATTTTCT	
AT4G25360	similar to YLS7 (yellow-leaf-specific gene 7)	3	-879	-873	ATTTTCT	
AT1G17680	transcription factor-related	2	-879	-873	ATTCTCT	
AT1G70470	similar to unknown protein	2	-879	-873	ATTTTCT	
AT1G50710	unknown protein	1	-879	-873	ATTTTCT	
AT4G29930	basic helix-loop-helix (bHLH) family protein	1	-879	-873	ATTTTCT	
AT5G67390	unknown protein	1	-879	-873	ATTCTCT	

[A] Occurrence of QC-SPE in 1000 bp long promoter region relative to transcription start. [B] Position of QC-SPE in the promoter region relative to transcription start. [C] Expression in root according to references. QC, quiescent centre; NDD, no detailed data.

4.4.9 Identification of QC-SPE-binding proteins

Screening of public available databases revealed that the QC-SPE does not contain any previously described *cis*-element. To isolate QC-SPE binding factors, we performed a yeast one-hybrid screen using a DNA fragment containing three tandem copies of QC-SPE of the *DOF3.1* promoter fused to the *HIS3* minimal promoter upstream of the *HIS3* reportergene (Fig.25b). Among the 15 recovered clones that possessed a cDNA fragment in frame with the activation domain, 11 were assigned as transcription factors, encoding five different ETHYLENE RESPONSIVE FACTORS (ERFs; Table 5).

Table 5. Identified putative QC-SPE binding proteins.

Locus identifier	Description	Occurrence
At4g17500	AtERF#100	5
At5g47230	AtERF#102	3
At4g17490	AtERF#103	1
At5g61600	AtERF#104	1
At5g61590	AtERF#105	1
At1g23140	C2 domain-containing protein	1
At4g13195	AL3	1
At1g06500	unknown protein	1
At2g28430	unknown protein	1

4.4.10 ERFs of subgroup IXa and IXb activate *WOX5* and *DOF3.1* gene expression

The *Arabidopsis* ERF family consists of 122 members belonging to 12 major phylogenetic groups (Nakano et al., 2006). Astonishingly, all ERFs identified in our screen were classified as members of groups IXa and IXb (Fig.25a, highlighted in red), characterized by a conserved N-terminal CMIX-2 motif representing an acid amino acid region that might function as a transcriptional activation domain (Nakano et al., 2006).

To verify the putative interaction of the identified ERFs with the QC-SPE, plasmids expressing the full-length AtERF#100 and AtERF#102 proteins (which were the most represented ERFs among the identified clones) were cotransformed into yeast cells with *DOF3.1* and *WOX5* promoter-reporter gene constructs that included and excluded the QC-SPE. The ERF-mediated transcriptional activation of the *HIS3* reporter gene was only observed, when the *DOF3.1* and *WOX5* promoter sequences were not truncated for the QC-SPE element (Fig.25b). Taken together, these data strongly suggest that members of the CMIX-2 subgroup of ERFs activate transcription of *DOF3.1* and *WOX5* and probably other QC-SPE-containing genes.

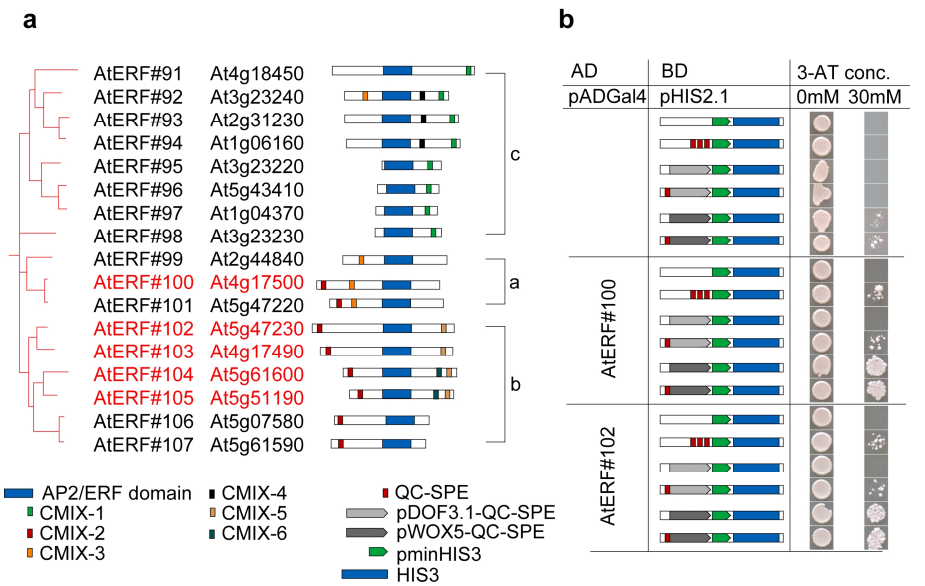

Figure 25. Identification and verification of putative QC-SPE binding proteins.

a, All identified ERFs (marked in red) belong phylogenetically to subgroups IXa and b of the *Arabidopsis* ERF family (displayed). Subgroup IXa and b uniquely possess a conserved CMIX-2 motif (red box). **b,** Transactivation assay. The capability to drive expression from native promoter of *DOF3.1* and *WOX5* was tested with full-length coding sequences of *AtERF#100* and *AtERF#102.* Positive transactivation was dependent on the presence of QC-SPE. Autoactivation was suppressed with 30mM 3-AT. 3-AT, 3-amino-1,2,4-triazole; AD, activation domain; BD, DNA binding domain; CMIX-2, conserved motif 2 of subgroup IX; ERF, ethylene response factor; HIS3, imidazoleglycerol-phosphate dehydratase; pminHIS3, HIS3 minimal promoter; QC-SPE, QC-specific promoter element

4.4.11 Identified *dof3.1* mutants do not show phenotypcal alterations

Next we assessed the importance of DOF3.1 in the developmental maintenance of quiescent centre identity. Two T-DNA insertion lines, assigened as *dof3.1-1* (SALK_136364) and *dof3.1-2* (SALK_095816), could be identified (Fig.26a) for the *DOF3.1* gene and were propagated to homozygosity (Supplementary Fig.1). By quantitative RT-PCR deacreased levels of transcript abundance could be measured in both mutant alleles. In the case of *dof3.1-1* the *DOF3.1* expression level was 4-fold reduced, in the case of *dof3.1-2* 16-fold, when compared to wild-type (data not shown). However, a full length *DOF3.1* fragment could not be amplified from cDNA of both mutants (data not shown).

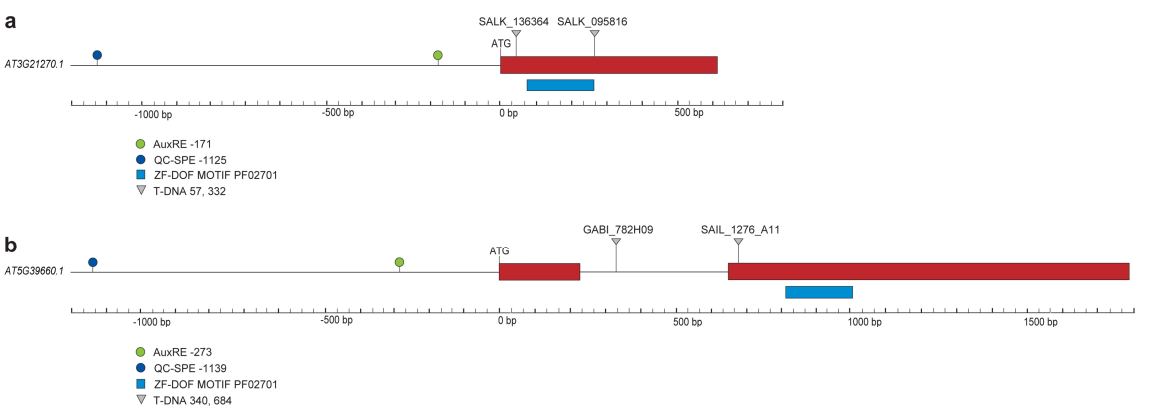

Figure 26. Schematic representation of the *DOF3.1* and *DOF5.2* gene structures.

a, b, Predicted gene structure of (**a**) *DOF3.1* and (**b**) *DOF5.2*, based on sequence information obtained form TAIR v9 (http://www.arabidopsis.org/). Red boxes represent exons, the thin black line (between the two boxes) depicts an intron. Blue boxes under the transcript model represent ZF DOF motif PF02701 according to the Pfam Database (http://pfam.sanger.ac.uk/). Translation initiation codon is indicated by ATG. The positions of available T-DNA insertion lines are shown above the genes. In the case of *DOF3.1* insertions are located at position 57 (SALK_136364) and 332 (SALK_095816), in the case of *DOF5.2* in the intron at position 340 (GABI_782H09). The T-DNA insertion line SAIL_1276_A11 with a predicted insertion at position 684 could not be confirmed. In both genes, an auxin response element (AuxRE) is found (green circle) upstream of the predicted translation site (ATG). The *cis*-elements are located at position -171 (*DOF3.1*) and -273 (*DOF5.2*). The identified QC-specific promoter element (QC-SPE, blue circle) is present at position -1125 (*DOF3.1*) and -1139 (*DOF5.2*).

In neither *dof3.1* mutant significant abnormalities in the quiescent centre or surrounding initials were detected, indicating a functional redundancy with other DOF proteins.

4.4.12 Identification of *DOF5.2* with expression pattern in the QC

To identify other *DOF* genes expressed in the root stem cell niche, we screened a collection of promoter-reporter gene constructs for the *Arabidopsis DOF* genes that was generated in our group. Among the 36 members of the DOF-family in *Arabidopsis* (Yanagisawa, 2002), *DOF5.2* (At5g39660) turned out to be the only gene besides *DOF3.1* highly expressed in the quiescent centre, with a somewhat weaker expression in the surrounding stem cells (Fig.27a). As expression of *DOF5.2::GUS* reporter gene could not be observed prior to 4 days after germination, we propose that *DOF5.2* is regulated by a mechanism, different from that of *DOF3.1* and *WOX5*. At later stages of plant development, *DOF5.2* is additionally expressed in the vascular tissue of the root elongation zone and leaves.

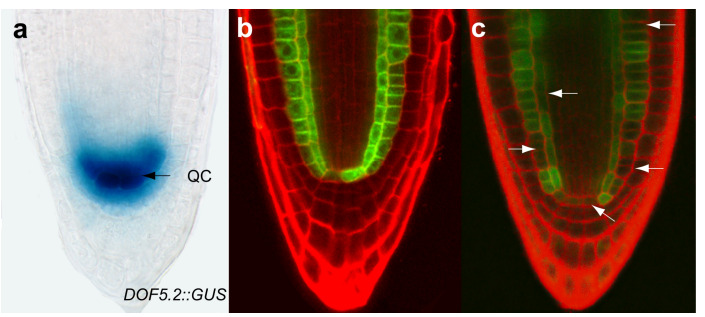

Figure 27. Expression pattern of *DOF5.2* and GFP marker J0571.

a, *DOF5.2::GUS* expression in the QC and surrounding initials. **b,c,** J0571 GFP enhancer trap line (**b**) marks the QC and cortex/endodermis cell files, including their initials. In roots of induced *35Sind::DOF3.1* plants (**c**) GFP signal is hardly detectable in QC and discontinuous in cortex and endodermis cell files (arrows).

4.4.13 Identification and generation of *dof5.2* mutant lines

With the aim to identify *DOF5.2* T-DNA insertion lines and to generate *dof3.1/dof5.2* double mutants to verify the putative redundant function of both *DOF* genes in the QC, we screened public *Arabidopsis* seed collection databases. Two T-DNA insertion lines, assigned as *dof5.2-1* and *dof5.2-2*, were reported for the *DOF5.2* gene (Fig.26b). The *dof5.2-1* mutant (GABI_782H09) possesses an insertion in the intron, which could be confirmed by PCR-based genotypisation (Supplementary Fig.1). However, most probably due to properly spliced mRNA, no reduction in transcript level could be measured when compared to wild-type (data not

shown). In the case of *dof5.2-2* (SAIL_1276_A11) the reported T-DNA insertion in the second exon could not be confirmed. We therefore generated transgenic plants expressing an artificial micro-RNA (Schwab et al., 2006) of *DOF5.2* (assigned as *amiR-dof5.2.-1*). In two out of eight investigated *amiR-dof5.2.-1* lines (*amiR-dof5.2.*-1 #9 and #11) decreased levels of *DOF5.2* transcript abundance could be measured, which were 32-fold and 64-fold reduced in comparison to wild-type, respectively (data not shown). The expression level of *DOF3.1* was unaffected in all investigated lines (data not shown). None of the identified mutants and transgenic lines of *DOF5.2* displayed any phenotypical aberration at any developmental stage.

4.4.14 Generation and characterisation of *dof3.1-1amiR-dof5.2-1* double mutants

Next we generated *dof3.1-1 amiR-dof5.2-1* double mutants by crossing the *amiR-dof5.2.-1* lines #2, #4, #5, #9 and #11 with the *dof3.1-1* mutant followed by propagation to *DOF3.1* homozygosity. In all five lines expression levels of the *DOF3.1* and *DOF5.2* genes were measured by qRT-PCR. All lines displayed a similar reduction of *DOF3.1* transcript abundance that was measured in the *dof3.1-1* single knock-out mutant (Fig.28a). Also in the case of *DOF5.2,* the measurements recapitulated the significant reduction of the *DOF5.2* gene expression level in line #9 and #11, which was previously measured in the *amiR-dof5.2-1* lines, whereas #2, #4 and #5 did not display any significant reductions.

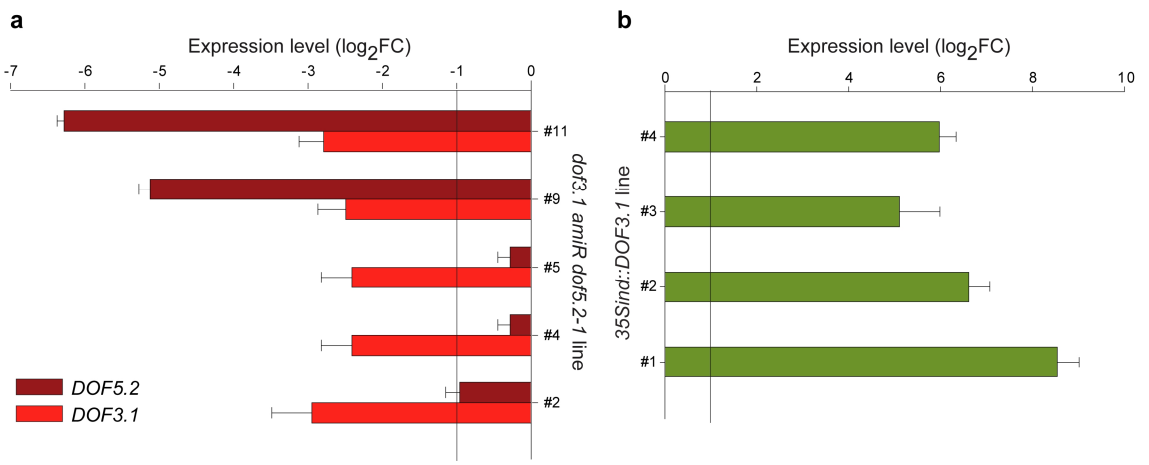

Figure 28. Expression levels of *DOF3.1 and DOF5.2* in *dof3.1 amiR-dof5.2* (A) and of *DOF3.1* in induced *35Sind::DOF3.1* (B) transgenic plants.

(**a**) *DOF3.1* and *DOF5.2* expression levels in 4DAG-old *dof3.1-1 amiR-dof5.2-1* mutants. While the *DOF3.1* expression level is consistingly reduced in all lines, *DOF5.2* transcript abundance is only significantly decreased in #9 and #11. (**b**) *DOF3.1* expression level in 6DAG-old induced *35Sind::DOF3.1* lines. Seedlings of *35Sind::DOF3.*1 and *dof3.1-1* as control were grown on nutrient agar medium and transferred to liquid medium supplemented with 20µM β-estradiol. RNA was extracted 6h after the induction. Gene expression levels were measured by quantitative RT-PCR. All induced *35Sind::DOF3.*1 lines possess an increased expression of *DOF3.1*, varying from 32-to 256-fold change when compared to the *dof3.1-1* control.

We observed that roots of the *dof3.1-1 amiR-dof5.2-1* double mutant lines #9 and #11 displayed an altered differentiation of cells in the proximal meristem (Fig.29a, d) which start to elongate at a shorter distance to the quiescent centre in comparison to wild-type (Fig.29b, e, g).

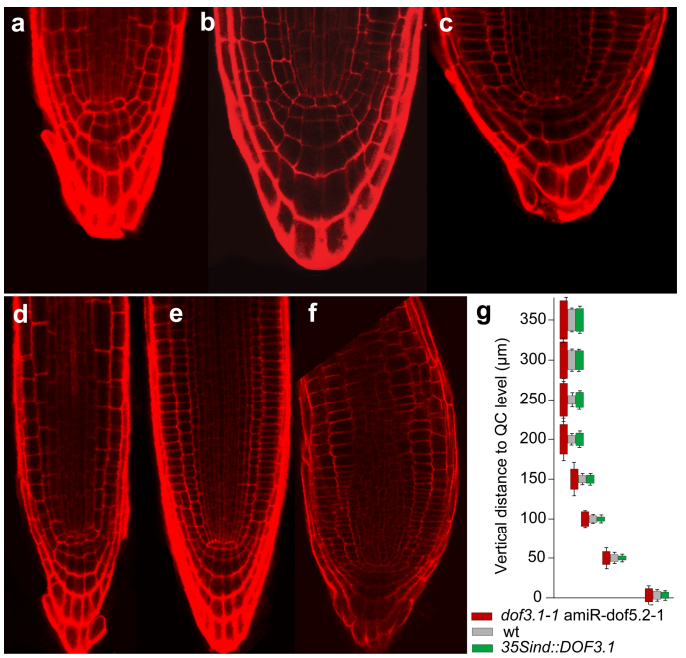

Figure 29. Phenotypic analyses of transgenic *DOF3.1* gain-of function and *DOF3.1/DOF5.2* loss-of function mutants.
(**a**, **d**) *dof3.1-1 amiR-dof5.2-1* #11 displays defects in QC cell division pattern and increased cell elongation of cells in the proximal meristem in comparison to the wild-type (**b, e**). Inversely, in induced *35Sind::DOF3.1* (**c, f**) cells of the proximal and distal meristem are broader and less elongated. **g**, Cortex cell lengths in the proximal meristem at defined distances to the QC.

Furthermore, an altered cell division pattern was observed in the root stem cell niche of *dof3.1-1 amiR-dof5.2-1* double mutants (Fig.29d; Table 6). Root growth was strongly reduced in the double mutant seedlings when compared to wild-type or single-gene mutants (Fig.30a, b). Interestingly, the length of ground tissue and cortex cells in *dof3.1-1* amiR-dof5.2-1 mutants was increased up to three times when compared to that of wild-type so that shorter roots resulted from a strongly reduced number of cells (Fig.29g). These results show that DOF3.1 and DOF5.2 are redundantly crucial for the maintenance of root stem cell niche properties: maintaining cells in the proximal meristem in an undifferentiated (non-elongated) status and promoting division.

Table 6. Frequency of root defects in *DOF3.1* and *DOF5.2* loss-of and gain-of lines.

dof3.1-1 amiR-dof5.2 #9		*dof3.1-1 amiR-dof5.2 #11*		*35Sind::DOF3.1*	
n	%	n	%	n	%
75	31	72	38	60	100

n, number of analysed roots; %, percentage of observed root defects

4.4.15 Generation and characterization of *DOF3.1* overexpression lines

To further analyse the function of *DOF3.1*, we investigated the consequences of its overexpression using a β-estradiol inducible system (Zuo et al., 2000). In four selected positive *35Sind::DOF3.1* transformants strongly increased levels of *DOF3.1* gene expression were measured six hours after the induction by β-estradiol when compared to the control (Fig.28b). *35Sind::DOF3.1* plants growing on nutrient agar medium supplemented with the inducer β-estradiol and thus continuously overexpressing *DOF3.1* showed dwarfism and arrested in

development after rudimentary formation of roots that displayed thickened, curly phenotypes (Fig.30c, e, Table 6). The same phenotype was also evident when plants were first grown under non-inducing conditions and β-estradiol was applied directly on roots of 7DAG-old seedlings expressing *35Sind::DOF3.1* (data not shown). No phenotypical alteration could be observed neither after application of the solvent DMSO on *35Sind::DOF3.1* plants nor after the application of β-estradiol on roots of plants carrying the empty vector (data not shown).

Figure 30. Macroscopic phenotypes of *DOF3.1* and *DOF5.2* transgenic lines.

(**a**) Roots of four day-old *dof3.1-1 amiR-dof5.2-1* and (**c**) estradiol-induced *35Sind::DOF* seedlings are significantly reduced in length compared to wild-type (**b**). While *dof3.1-1 amiR-dof5.2-1* roots develop further, induced *35Sind::DOF* mutants arrest in growth and develop rudimentary thickened and curly roots (**e**), a phenotype which is not present when seedlings grow on non-inducing medium (**d**). scale bars 3mm.

On the cellular level, gain-of *DOF3.1* function retards longitudinal and provokes transverse elongation of the meristem, as well as of the ground tissue and epidermis, and columella cells (Fig.29c, f, g). To test whether ground tissue or quiescent centre have undergone a change in their cell fates in *DOF3.1* gain-of lines, the expression pattern of the J0571 GFP-marker (http://www.plantsci.cam.ac.uk/Haseloff/IndexCatalogue.html) was analysed. In J0571 seedlings, GFP is expressed in the quiescent centre, the cortex/endodermis and their initials (Fig.27b). In the majority of J0571 plants crossed with the *35Sind::DOF3.1* line, induced expression of *DOF3.1* resulted in an absence of GFP signal in the quiescent centre and discontinuous signals along the longitudinal axis (Fig.27c, arrows). This indicates that ectopic expression of *DOF3.1* leads to a partial loss of ground tissue and quiescent centre identity and alters the differentiation status of the root stem cell niche.

4.4.16 Brassinolide induce expression of *DOF3.1*

The hormonal status plays a critical role in root stem cells specification. Beside the transient and antagonistic interaction between auxin and cytokinin (Muller and Sheen, 2008), ethylene (Ortega-Martinez et al., 2007) and brassinolide (Mouchel et al., 2006) are further factors

controlling proper gene expression necessary for specifying the root stem-cell niche. No changes in the intensity or pattern of *DOF3.1* expression was observed after the application of auxin and its transport inhibitors, cytokinin, nor precursors or inhibitors of ethylene synthesis. Also a mutation of an ARF binding site (Ulmasov et al., 1997) located in the 5´UTR of the *DOF3.1* gene (Fig.26a) did not show any quantitative or qualitative changes in the expression of *DOF3.1::GFP* reporter gene (data not shown). Application of brassinolide in a wide concentration range leads to an increase of *DOF3.1* expression and a spread of GUS signal to the proximal vascular region (Fig.31a, arrow).

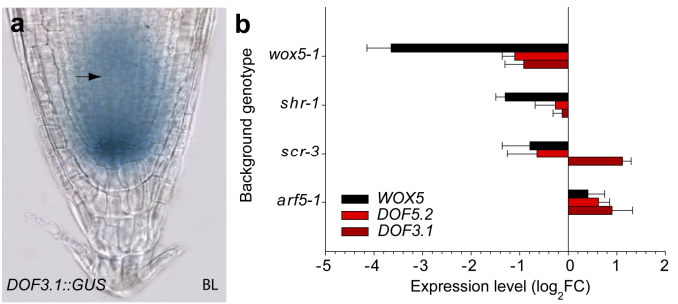

Figure 31. *DOF3.1* upstream regulating factors.

a, *DOF3.1::GUS* expression extends to vascular tissue (black arrow) after 1d of 0,5nM BL application. **b,** Relative *DOF3.1*, *DOF5.2* and *WOX5* expression levels in *wox5-1*, *shr-1*, *scr-3* and *arf5-1* mutant background.

4.4.17 *DOF3.1* expression level is increased in the *scarecrow* mutant *scr-3*

Despite the fact that *DOF3.1* did not react to the application of auxin or auxin transport inhibitors, we asked whether *SHORT ROOT*, *SCARECROW* and *MONOPTEROS*, genes whose transcription is auxin dependent and play an essential role in the maintenance of the root meristem, affect the expression of *DOF3.1* or *DOF5.2*. Only in scr-3 mutants we observed a significant increase of *DOF3.1* expression. Whereas in *shr-1* or *arf5-1* (*MONOPTEROS*) mutants the expression of both *DOF* genes remained unaffected. Recent studies indicated the importance of *WOX5* in stem cell signalling (Sarkar et al., 2007). In *wox5-1* mutants, both, *DOF3.1* and *DOF5.2* showed a slight reduction in expression level (Fig.31b). However, expression of *WOX5* appeared to be significantly reduced in *dof3.1-1 amiR-dof5.2-1* transgenics (Fig.32d).

4.4.18 Altered *DOF3.1* and *DOF5.2* expression levels change auxin distribution

Next we asked to which extent *DOF3.1* affects auxin distribution in the stem-cell niche. In the *dof3.1-1* amiR-dof5.2 double mutants, the auxin response marker *DR5::GFP* (Sabatini et al., 1999) displayed a distal shift of its maximal expression to the outer columella layer and an almost complete loss of signal in the quiescent centre and proximal columella (Fig.32b). The induced overexpression of the *DOF3.1* gene (*35Sind::DOF3.1* plants growing on medium supplemented with the inducer β-estradiol) led to an accumulation of GFP signal in the vascular initials, and strong reduction of the signal in the quiescent centre and central columella (Fig.32c). Collectively, these data suggest that *DOF3.1* and *DOF5.2* affect auxin flux through stem cell niche, stimulating its acropetal transport upon a reduction in their expression level.

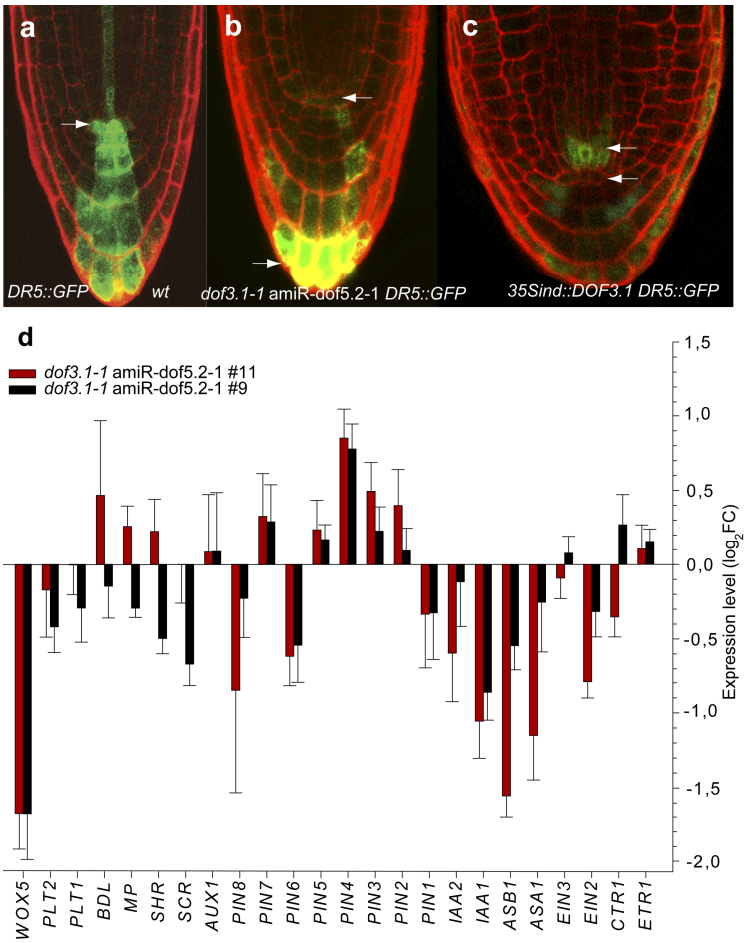

Figure 32. *DOF3.1* downstream genes.

(**a**) *DR5::GFP* expression in wt with maximum in the quiescent centre (arrow), (**b**) in *dof3.1-1 amiR-dof5.2-1* with low abundance in the QC and an increasing gradient towards the distal root tip (arrows) and (**c**) in roots of induced *35Sind::DOF3.1* plants with an accumulation in provascular cells and absence of signal in the quiescent centre (arrows). (**d**) Relative expression of selected genes involved in SHR/SCR signalling pathway, auxin transport and auxin/ethylene interaction in root tissue in *dof3.1-1* amiR-dof5.2-1 transgenics (two lines with strongest reduction of *DOF5.2* expression, #9 and #11, were independently tested). *WOX5* transcript levels are consistently reduced in both lines whereas *PIN4* levels are slightly increased. Expression was tested by qRT-PCR. FC, FoldChange;

4.4.19 *WOX5* and *PIN4* are differentially expressed in the *dof3.1-1* amiR-dof5.2-1 mutant

Previous data indicated the existence of two mechanisms necessary for the establishment of quiescent centre identity: On the longitudinal plane auxin distribution and on the radial plane the SHORT ROOT/SCARECROW signalling pathway. We asked whether any of the genes contributing to these mechanisms could be located downstream of DOF3.1/DOF5.2. Quantitative RT-PCR measurements revealed that only the expression of *WOX5* appeared significantly reduced in *dof3.1-1* amiR-dof5.2-1 transgenic lines (Fig.32d). In addition we tested several genes contributing to auxin-ethylene pathway interaction. Intriguingly, among all tested genes, solely the transcript level of *PIN4* was consistently increased in both transgenic lines (Fig.32d). Out of eight PIN proteins, PIN4 is the only one which distribution coincides with the root stem-cell niche (Feraru and Friml, 2008). We therefore concluded that DOF3.1 and DOF5.2 redundantly exert a repressor effect on expression of *PIN4*, which could explain an increase in the acropetal transport of auxin through the root stem cell niche observed in *dof3.1-1 amiR-dof5.2-1* mutants.

4.4.20 Two serine-rich proteins and AtEXP1 posssess capacity to bind DOF3.1 protein

To assess the capacity of DOF3.1 for interaction with further proteins and identify putative novel components of its way of action, we performed a yeast two-hybrid screen. Among the 16 recovered clones, which possessed a cDNA fragment in-frame with the activation domain, two serine-rich related proteins (At5g11090 and its phylogenetically closely related member At5g25280) were found to be overrepresented (Fig.33).

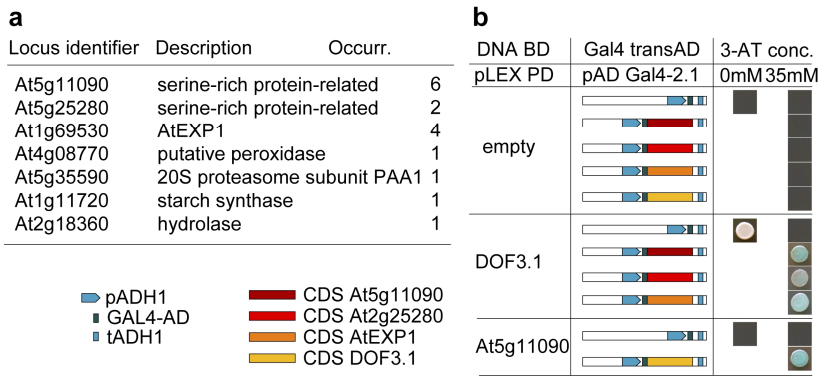

Figure 33. DOF3.1 putative protein interaction partners.

(**a**) Recovered clones identified in the yeast two-hybrid screen. The serine-rich proteins AT5G11090 and AT5G25280 as well as AtEXP1 occur with highest frequency. (**b**) Combination of constructs used for the screen and their ability to drive reporter gene expression. The interaction of DOF3.1 and AT5G11090 was also detectable after the exchange of AD and BD vectors. 3-AT, 3-amino-1,2,4-triazole; AD, activation domain; ADH1, alcohol dehydrogenase 1; BD, DNA binding domain.

Intriguingly, the screen revealed also the capacity of DOF3.1 to bind to EXPANSIN A1 (AtEXP1, At1g69530), the promoter of which drives clear expression of a reporter gene in the root stem cell niche (Wieczorek et al., 2006). Next, we showed that a fusion of the serine-rich related protein AT5G11090 to GFP results in nuclear localization (Fig.34c). However, in protoplast cells the signals were concentrated in nuclear speckles, which are supposed to function as splicing factor compartments. Interestingly, last studies on the organization of these nuclear bodies over the developmental zones of the root revealed that in meristematic cells, a rather homogenous than focal distribution of splicing factor proteins is observed (Docquier et al., 2004). Therefore, the observed localisation of AT5G11090 in nuclear speckles of *Arabidopsis* protoplasts has not to reflect the *in vivo* localisation in the root stem cell niche. For this reason we still speculate possibilities of putative interaction between DOF3.1 and these proteins on the level of root stem cell niche.

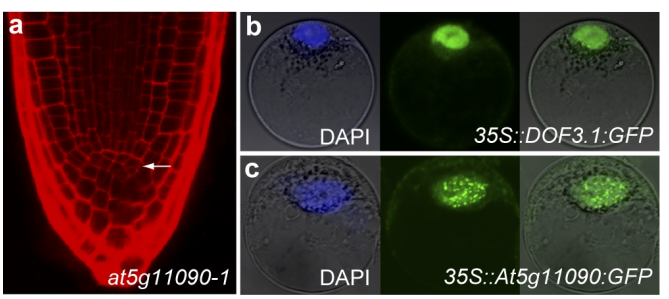

Figure 34. DOF3.1 putative protein interaction partners.

a, Altered cell division pattern occurs (arrow) in the stem cell niche of the *at5g11090-1* mutant. (**b**) Subcellular localisation of DOF3.1 in the nucleus and (**c**) AT5G11090 in nuclear speckles of *Arabidopsis* protoplasts. DAPI staining, blue.

Furthermore, we asked to which extent the loss of function of *AT5G11090* would affect the root stem cell niche. Notably, upon investigation of *at5g11090-1* and *at5g11090-2* mutant plants we could observe massive aberrant divisions in the region of quiescent centre and columella (Fig.34a, Table 7). We concluded that this putative protein interaction partner of DOF3.1 possesses the strong capacity to affect the structure of the root stem cell niche.

Table 7. Frequency of root defects in *at5g11090* mutants.

at5g11090-1		*at5g11090-2*	
n	%	n	%
78	25	80	28

n, number of analysed roots; %, percentage of observed root defects

4.4.21 Conclusions and proposed model of the DOF3.1 and DOF5.2 regulatory pathway

Our results support pathway of transcriptional control in the boundaries of the root stem cell niche, which involves ERF transcription factors of the subgroup IX and the novel *cis*-element QC-SPE. An analysis of expression patterns of further genes containing the QC-SPE will be required to explore whether a position of the element distal to the transcription start site is needed for a root stem cell niche specific expression. Although previous studies identified the GCC-box as the target element of ERFs, there is evidence for the existence of further non-GCC box binding sites (Chakravarthy et al., 2003). Spatial analysis of ERF IX gene expression in the root tip will give more insights into the mechanism of this transcription factor-*cis*-element interaction.

We could demonstrate that DOF3.1 and DOF5.2 redundantly contribute to the maintenance of the root stem cell niche status in a dosage-dependent manner (Fig. 35). A redundant way of gene function was proposed to be a general phenomenen in the root meristem tissue, since many characterized single loss-of function mutants of genes with an expression pattern in the root stem cell niche lacked phenotypes (Nawy et al., 2005). Despite the facts that most prominent phenotypical effects of the *dof3.1-1* amiR-dof5.2 double mutant resembles to mutants of the auxin transporter *pin4* (Friml et al., 2002) or plants with increased endogenous auxin levels (Swarup et al., 2007), we suppose that the observed effects of the changes in auxin distribution (Fig.35) are further downstream of the direct transcriptional regulation of the two DOF transcription factors. The identification of direct target genes will therefore be required to understand the fundamental role of these genes. However, DOF3.1 and DOF5.2 represent important factors that contribute to our knowledge of understanding the maintenance of the root stem cell niche status, offering a redundant way of action, which one could also expect in other plant species.

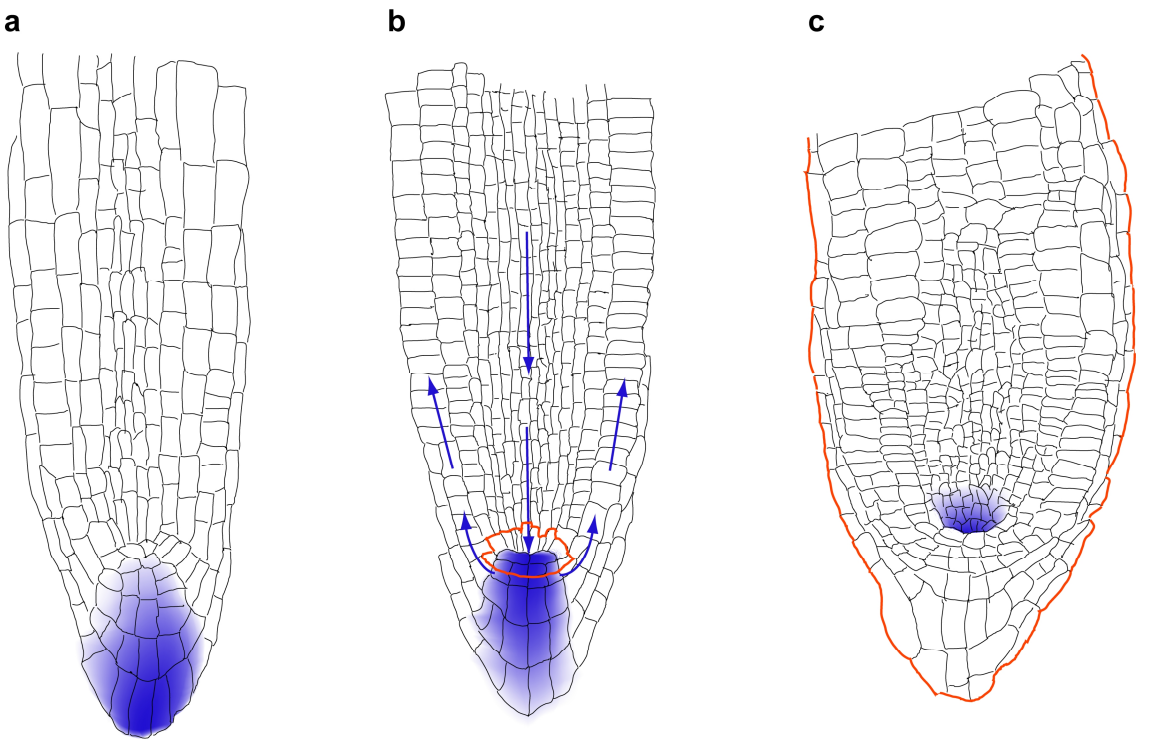

Figure 35. Proposed model of the DOF3.1 and DOF5.2 regulatory pathway.

Expression domains of *DOF3.1* and *DOF5.2* (orange frame) overlap in wild-type plants (**b**) strictly with the root stem cell niche and culminate in the centrally located four cells of the quiescent centre (QC). The identity of the QC and surrounding stem cells relays on continuous auxin flux (blue arrows) and distribution (blue stained cells). In roots of *dof3.1-1 amiR-dof5.2-1* plants (**a**) highly reduced transcript levels of the redundant *DOF3.1* and *DOF5.2* genes are detectable. Consequently, a shift of auxin maximum and provoked differentiation (elongation) of the proximal meristem cells was evoked. (**c**) The expansion of the *DOF3.1* expression domain (orange frame) results in an accumulation of auxin in the cells immediately above the QC. This was followed with a delay in cell elongation relative to the distance of cells from the QC in comparison to the wild-type.

Acknowledgements

We thank T. Guilfoyle, B. Scheres, G. Jürgens NH Chua, T. Gigolashvili, and C. Koncz for kind providing of published material. We acknowledge GABI-Kat, SALK and NASC *Arabidopsis* stock centres for providing mutant lines. We appreciate funding from the German Research Foundation and Ministry of Education and Research. We thank J. Bergstein for photographic work and E. Maksimova for assistance with microscopy. We thank G. Plesch, K. Czempinski, N. Gaedeke, C. Voelker and S. Brandt for experiments performed in the early phase of this study. We also thank J. Friml, MI. Zanor, I. Witt and D. Kupper for kind sharing of unpublished results. We thank C. Voelker, K. Schulz and A. Schneider for the assistance in the lab, M. Kwasniewski for discussion on promoter conserved elements, H. Dortay for establishing the yeast work and A. Rachfalowska for assistance on bioinformatic analysis.

5. A novel bipartite nuclear localization signal with an atypical long linker in DOF transcription factors

Jonas Krebs[1], Bernd Mueller-Roeber[1,2,§], Slobodan Ruzicic[2]

[1]University of Potsdam, Institute of Biochemistry and Biology, Karl-Liebknecht-Strasse 24-25, Haus 20, 14476 Potsdam-Golm, Germany; [2]Max-Planck Institute of Molecular Plant Physiology, Am Muehlenberg 1, 14476 Potsdam-Golm, Germany

[§] Corresponding author

Manuscript submitted (Journal of Plant Physiology, October 2009)

Authors´ contributions

The experimental work was entirely performed by Jonas Krebs. The research was designed and planned by Jonas Krebs and Slobodan Ruzicic. Bernd Mueller-Roeber supervised the group as a whole.

5.1 Summary

Large molecules require a nuclear localization signal (NLS) for translocation into the nucleus. Classical NLSs are rich in basic amino acids and based on their structural features they represent three groups: SV40 T-antigen-type, yeast mating factor Matα-2-type and bipartite NLSs. DNA-binding-with-one-finger (DOF) transcription factors play important roles in plants and although their nuclear localization has been demonstrated in several cases, public protein localization prediction tools fail to detect NLS motifs in these proteins. Here we demonstrate that an atypical bipartite NLS with a 17 amino acid long linker between its flanking basic regions directs *Arabidopsis thaliana* DOF proteins to the cell nucleus. The novel bipartite NLS is highly conserved in plant DOF transcription factors including the single DOF protein in the green alga *Chlamydomonas reinhardtii*.

Keywords

Arabidopsis; transcription regulation; bipartite NLS; nucleus

Abbreviations

aa, amino acid(s); CT, C-terminus; DAPI, 4´,6-diamidino-2-phenylindole; GFP, green fluorescent protein; NLS, nuclear localisation signal; NT, N-terminus

5.2 Introduction

While proteins of a molecular mass of 40–60 kDa can enter the cell nucleus in a diffusion-based process, larger proteins depend on the presence of a translocation signal, called the nuclear localization signal (NLS), for transport through the nuclear pore (Faustino et al., 2007). One common feature of NLSs is an abundant occurrence of the basic amino acids arginine and lysine in their primary structures. NLSs have been subdivided into three groups, according to their structural features (Dingwall and Laskey, 1991): i) those resembling the SV40 T-antigen NLS (P**KKKRK**V) that consists of a short stretch of 4-8 basic aa (Kalderon et al., 1984; Lanford and Butel, 1984); ii) those with similarity to the NLS of the yeast mating factor Matα-2 (**K**IPI**K**) that has been shown to be also functional in plants (Raikhel, 1992), and iii) bipartite NLSs, which are composed of two basic regions separated by a short stretch of up to ten aa (e.g. nucleoplasmin **K**AV**KR**PAATKKAGQA**KKKK**LD**K**EDES; (Smith et al., 1997)).

DNA-binding-with-one-finger (DOF) transcription factors constitute a plant-specific family of transcriptional regulators, which in *Arabidopsis thaliana* is encoded by 36 functional genes. In maize, it has been demonstrated that transcription factor DOF1 contains a basis region in the centre of the protein between aa 120 and 129 (**KKK**PAS**KKRR**) that resembles the SV40 and classical bipartite NLSs. Its fusion to GFP led to protein accumulation in the nucleus, indicating that it can function as an NLS (Yanagisawa, 2001). Maize DOF1 is so far the only member of the transcription factor family characterized for its nuclear localization signal. Furthermore, the identified region is absent from other known DOF proteins with respect to its primary structure and position, indicating that other motifs for nuclear targeting exist in DOF transcription factors. Here we demonstrate that a highly conserved bipartite NLS with an unusually long spacer segment of 17 aa controls nuclear targeting of DOF factors.

5.3 Material and Methods

5.3.1 Protein alignment

All protein sequences were derived from the Arabidopsis Information Resource (TAIR) database (http://www.arabidopsis.org). The sequences were aligned using the MUltiple Sequence Comparison by Log-Expectation (MUSCLE) tool (http://www.ebi.ac.uk/Tools/muscle/index.html) of the European Bioinformatics Institute (EBI) with default parameter settings and the MSF output format. The alignment was edited with Jalview software tool (http://www.jalview.org). The DOF domain was stained in grey using the color parameter “by conservation” and a conservation color increment threshold value of 31. For better illustration of basic region 2, the alignment was corrected manually. The basic aa residues R and K were highlighted in red.

5.3.2 Vector construction

The pA7-GFP vector containing the coding sequence of eGFP under control of the CaMV 35S promoter was kindly provided by Dr. Katrin Czempinski, University of Potsdam. To introduce a second copy of eGFP, the vector was digested with *Sal*I, followed by a blunting reaction and subsequent digestion with *Sma*I. The obtained fragment encoding for eGFP was ligated into the original pA7-GFP vector that was previously digested with *Sma*I. All PCR products were amplified using *Pfu* polymerase and after A-tailing subcloned into the pCR2.1 cloning vector (Invitrogen, Karlsruhe, Germany). For subsequent cloning into the destination vector pA7-2xGFP, the pCR2.1 vector containing the deletion fragments was digested with *Xho*I and *Sal*I. The used restriction enzyme sites are part of the listed primer sequences and tagged with bold letters.

The full-length coding sequences of *DOF1.7* and *DOF4.7* were amplified using the primers DOF1.7CDSfor, DOF1.7CDSrev and DOF4.7CDSfor, DOF4.7CDSrev, respectively. To amplify the sequences encoding for the N-terminal parts of proteins excluding the bipartite NLS, primer pairs DOF4.7CDSfor, DOF4.7NTrev and DOF1.7CDSfor, DOF1.7NTrev were used. For the N-terminus including the putative bipartite NLS the primer combinations DOF4.7CDSfor, DOF4.7NLSrev and DOF1.7CDSfor, DOF1.7NLSrev were employed. The putative bipartite NLS sequence of DOF4.7 and DOF1.7 was amplified using the primer pairs DOF4.7NLSfor, DOF4.7NLSrev and DOF1.7NLSfor, DOF1.7NLSrev, respectively. In the case of the C-terminus including the full putative bipartite NLS, the primer pairs DOF4.7NLSfor, DOF4.7CDSrev and DOF1.7NLSfor, DOF1.7CDSrev were used. To amplify the C-terminus including only basic region 2, the primer pairs DOF4.7B2for, DOF4.7CDSrev and DOF1.7B2for, DOF1.7CDSrev, respectively were used.

5.3.3 Protoplast transformation

Cells from a 7 days old *Arabidopsis thaliana* suspension culture were digested and transformed as followed: Cells were pelleted (800rpm, 8min) and washed twice in MCP (0.5M sorbitol, 1mM $CaCl_2$, 10mM MES, pH 5.6). After following centrifugation (800rpm, 8min), in attempt to digest the cell walls, the cells were resuspended in enzyme solution (MCP supplemented with 0.25% macerozyme R-10, 0.1% BSA, 1% cellulase (Onozuka R-10)) and shaken for 4h (60rpm, 28°C). Resulting protoplasts were separated using a Percoll gradient and washed in W5 solution (154mM NaCl, 125mM $CaCl_2$, 5mM KCl, 5mM Glucose, 1.5mM MES, pH5.6). Following, the protoplasts were incubated on ice for 30min and counted. Subsequently, the cells were precipitated by centrifugation (800rpm, 8min) and resuspended in MaMg solution (0.4M mannitol, 15mM $MgCl_2$, 5mM MES, pH5.6) to a density of $5x10^6$ cells/ml. Afterwards, 50µg plasmid DNA and 50µg ssDNA were added to 300µl of protoplast suspension. After addition of 325µl of PEG solution (0.4M mannitol, 0.1M $Ca(NO_3)_2$, 40% PEG 4000) and brief shaking, the cells were incubated for 30min at room temperature, centrifuged (800rpm, 5min), washed with

10ml of W5 solution, centrifuged and resuspended in 3ml of W5 solution. Prior to confocal microscopy the protoplasts were incubated for 48h at 22°C in the dark.

5.3.4 Microscopy

Fluorescence signals were analyzed using a Leica SP2 laser scanning microscope. Nuclei were stained with DAPI (1 mg/ml in H_2O). Excitation and observed emission wavelengths were 488 nm and 509 nm for GFP, and 364 nm and 460 nm for DAPI, respectively.

5.3.5 Primer sequences

Primer name	Primer sequence
DOF4.7CDSfor	**CTCGAG**ATGATGACGTCATCCCATCA
DOF4.7CDSrev	**GTCGAC**GAGCAGAGCATTATTATTAG
DOF4.7NLSfor	**CTCGAG**ATGAAGAACTGTCGTCGTTACTG
DOF4.7NLSrev	**GTCGAC**CTTGTTCTTGTTTCGAGTGG
DOF4.7CTfor	**CTCGAG**ATGCCTTGCAGCCTCCAAGTCAT
DOF4.7NTrev	**GTCGAC**GCAGTAGTGACGTGGCTGAG
DOF4.7B2for	**CTCGAG**ATGCGAAACAAGAACAAGCCTTG
DOF1.7CDSfor	**CTCGAG**ATGCAGGATCTGACGTCAGC
DOF1.7CDSrev	**GTCGAC**ATTCTTCTCCATTCTGTTCA
DOF1.7NLSfor	**CTCGAG**ATGAAAAACTGTCGTCGTTACTG
DOF1.7NLSrev	**GTCGAC**TCGTTTGTTGCTTTTCCGAG
DOF1.7CTfor	**CTCGAG**ATGTCCGGTTCTTCTCCGTCTAG
DOF1.7NTrev	**GTCGAC**GCAAAAGTGACGGGGCTGTG
DOF1.7B2for	**CTCGAG**ATGCGGAAAAGCAACAAACGATC

5.4 Results and discussion

5.4.1 No classical NLS can be found in majority of DOF proteins

Using publicly available protein localization prediction tools like PSORT (http://psort.nibb.ac.jp/form.html) none of the 36 *Arabidopsis* DOF transcription factors was predicted to be transported into the nucleus and thus lacked a “positive” status for nuclear localization. For five proteins (AT1G47655, AT3G45610, AT3G52440, AT4G21050 and AT4G38000) the prediction for nuclear localization was „not clear“. For the remaining 31 members the prediction analysis delivered a “negative” nuclear localization status. These results suggested that DOF proteins contain a yet uncharacterized NLS different from the three known basic types of NLSs, thus precluding its recognition by the available localization prediction tools.

5.4.2 DOF protein alignment reveals two basic stretches separated by a 17 aa linker

The absence of the NLS previously identified in the maize DOF1 transcription factor in other members of the DOF family prompted us to search for other common motifs with putative NLS properties in the *Arabidopsis* DOF proteins. To this end an alignment of all 36 *Arabidopsis* DOF protein sequences was generated and analyzed for the presence of conserved basic motives

(Fig.36a). We excluded DOF1.9 (AT1G65935) from our analyses, as it possesses a stop codon in the DOF domain and is therefore considered to be a pseudogene. Notably, the 52 aa long DOF domain of these transcription factors (Fig.36b) includes two stretches of basic aa at conserved positions (Fig.36a). One stretch (basic region 1; designated B1 in the following; Fig.36a) is located in the centre of the DOF domain, while the second stretch (basic region 2; B2) is located at its C-terminal end. As this region strongly resembles the structure of a classical bipartite NLS, but contains an atypically long spacer of 17 aa, we proposed it to be a putative novel NLS of DOF transcription factors.

5.4.3 Bipartite basic region is conserved in DOF protein among the plant species

Next we analyzed DOF proteins from other sequenced plant species by referring to plant transcription factor databases including PlnTFDB (Pérez-Rodríguez, 2009). We found that CGL19, the only putative DOF transcription factor of the green alga *Chlamydomonas reinhardtii*, as well as DOF proteins from *Zea mays*, *Nicotiana tabacum* and *Oryza sativa* all possess the novel bipartite motif in the same region and with the same conserved structure (data not shown).

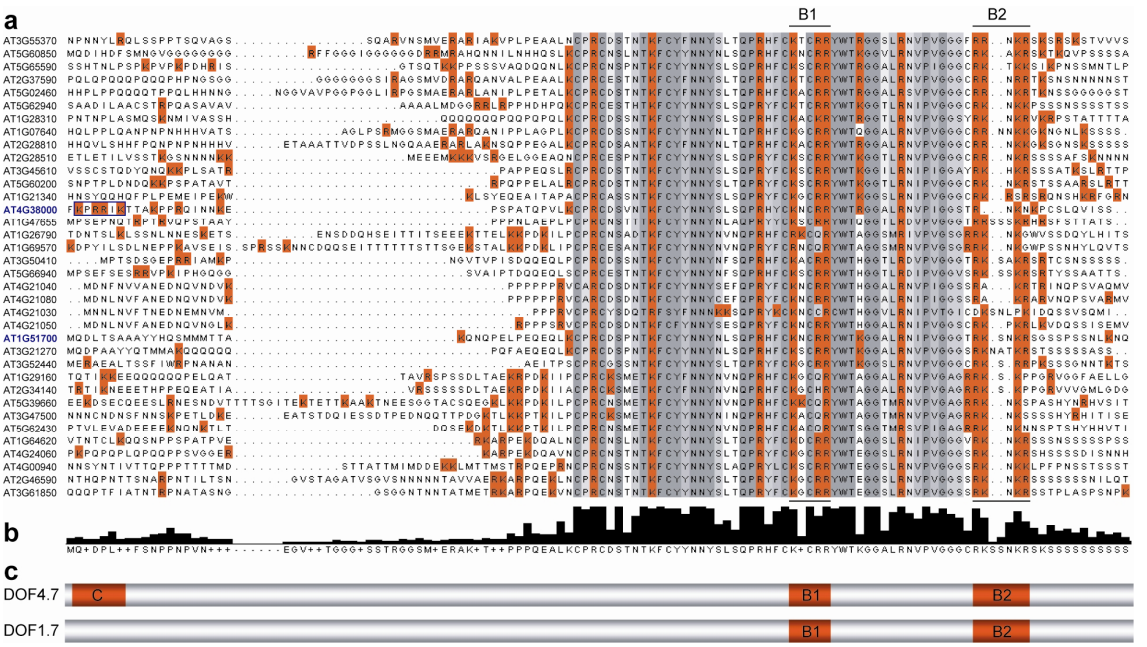

Figure 36. Alignment of *Arabidopsis* DOF proteins and localization of the proposed novel NLS.

a. Alignment of the N-terminal parts of DOF proteins. The DOF domain is highlighted in grey, R and K residues are shown in red. The putative bipartite NLS is indicated by B1 and B2. DOF4.7 and DOF1.7 are marked in blue. The region resembling a classic monopartite NLS (C) in the N-terminal region of DOF4.7 is highlighted by a blue frame. **b.** Consensus sequence derived from the alignment. The highness of the columns indicates the degree of conservation. c. Schematic representation of the DOF4.7 and DOF1.7 N-terminal parts. Basic clusters are marked in red.

Basic region B1 is composed of five aa represented by consensus sequence KXCRR (Fig.36b), where X represents any aa. Within this stretch, K, C and the latter R residue are highly conserved, whereas the penultimate R is replaced by other aa in eight of the *Arabidopsis* sequences. Basic region B2 with the consensus sequence RKXKR exhibits a higher degree of

variation. It starts with a highly conserved R residue present in 35 of the 36 DOF members. The second position is occupied by a basic aa (R, seven members; K, 26 members) in a total of 33 proteins. The third position is not basic. At the fourth (K in 32 members, R in two members) and fifth (R, 22 members; K, 6 members) position, again, basic residues are overrepresented. Notably, B2 possesses three basic out of five aa residues and thus fulfills the criterion for the second basic stretch of bipartite NLS proposed by (Robbins et al., 1991). The protein encoded by AT4G21030 is the only member of the *Arabidopsis* DOF family that does not follow the above described structure; it possesses only two basic aa residues in B2.

5.4.4 Five Arabidopis DOF proteins posssess an additional classical monopartite NLS

Beside the putative novel bipartite NLS present in the majority of the DOF proteins, the five proteins with a “not clear” nuclear localization status harbored an additional putative classic monopartite NLS at non-conserved positions. In the case of DOF4.7 (AT4G38000) this monopartite NLS with the sequence KPRRIK is located at the N-terminus near the DOF domain (Fig.36a, blue frame).

5.4.5 Generation of GFP fusion proteins to reveal the relevance of the putative NLS

To analyze the function of the putative novel bipartite NLS, we selected two members of the DOF transcription factor family: DOF1.7 (AT1G51700) as a candidate with only the bipartite basic region, and DOF4.7 (AT4G3800) that additionally contains a classic monopartite NLS, whose possible independency of the bipartite region was also investigated. To investigate the functional importance of the proposed novel NLS, we subdivided both proteins into three parts: i) the NT which ends directly upstream of B1, ii) the putative bipartite NLS consisting of B1, the 17 aa spacer and B2, and finally iii) the CT, which starts directly after B2. To analyze the relevance of the putative NLS for the transport of DOF proteins into the nucleus, six different deletion constructs were prepared and fused to GFP: 1) The full-length protein, comprising the NT, the bipartite NLS and the CT; 2) the isolated NT; 3) the isolated putative bipartite NLS; 4) the NT including the putative bipartite NLS; 5) the CT including the putative bipartite NLS; and 6) the isolated CT including only B2 (Fig.37).

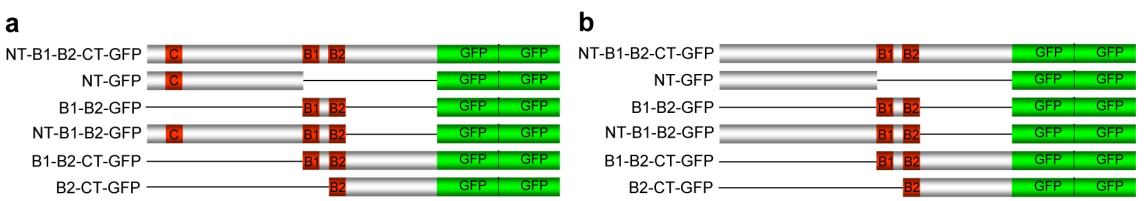

Figure 37. Schematic representation of (a) DOF4.7-GFP and (b) DOF1.7-GFP fusion proteins.

Various combinations of the N-terminus, the putative bipartite NLS and the C-terminus were translationally fused to two copies of GFP. NT, N-terminus; B1, basic region 1; B2, basic region 2; C, classical monopartite NLS; CT, C-terminus; GFP, green fluorescent protein.

The DOF1.7 and DOF4.7 deletion constructs were fused to two copies of GFP and introduced *via* transient transformation into *Arabidopsis thaliana* protoplasts, where the genes were

expressed under control of the Cauliflower Mosaic Virus 35S promoter. Two copies of GFP were used to increase the overall size of the fusion protein and thus abolish a possible simple diffusion through the nuclear pore complex (Groover, 2007).

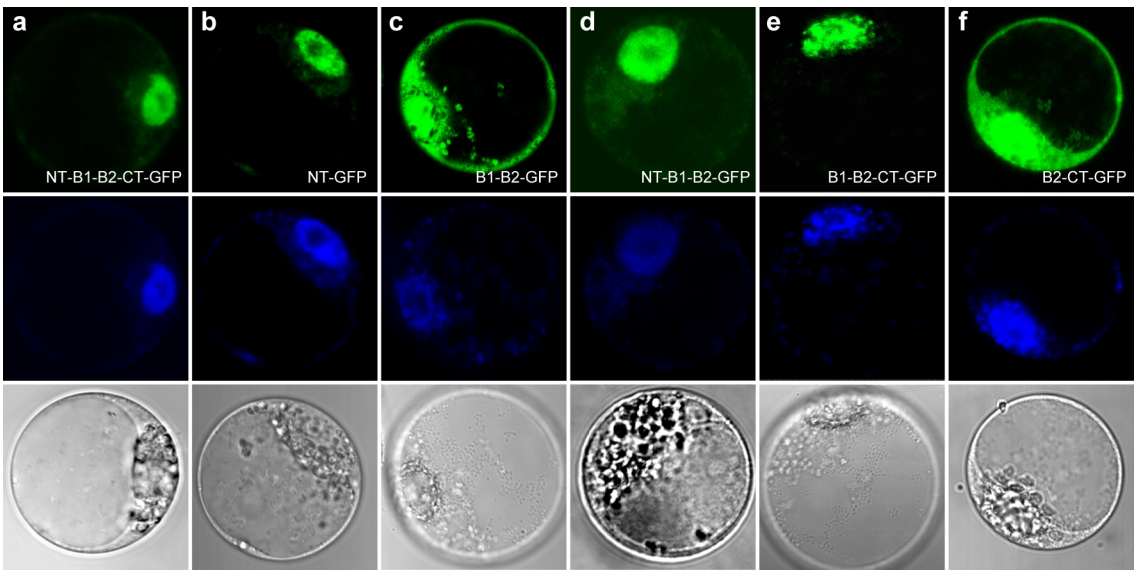

Figure 38. Subcellular localization of DOF4.7-GFP fusion proteins in *Arabidopsis* protoplasts.

The construct names correspond to the nomenclature described in Fig.37. **a.** Fusion of the DOF4.7 full length protein with GFP. **b.** Fusion of the N-terminal part of DOF4.7 (without putative bipartite NLS) and GFP. **c.** Putative DOF4.7 bipartite NLS alone fused with GFP. **d.** Fusion of the N-terminal part of DOF4.7 including the putative bipartite NLS and GFP. **e.** Fusion of the C-terminal part of DOF4.7 including the putative bipartite NLS with GFP. **f.** Fusion of the C-terminal part of DOF4.7 including B2 of the putative bipartite NLS with GFP. First row: detection of GFP signal. Second row: control staining of nuclei with DAPI. Third row: protoplasts under transmission light.

5.4.6 Putative novel NLS is necessary but not sufficient for the nuclear import

When the full-length coding sequences of transcription factors DOF4.7 and DOF1.7 were fused to GFP, the fluorescent signal was detected with high specificity in the nucleus (Fig.38a and 39a, respectively), confirming the capability of both proteins to spatially evolve their role as transcriptional regulators.

The fusion of the isolated NT to GFP resulted in different localization patterns depending on the protein: in the case of DOF4.7 the fluorescence signal was only observed in the nucleus, similar to the results obtained with the full-length protein fusion (Fig.38b), while in the case of DOF1.7 the GFP signal was equally distributed in the cytoplasm and the nucleus (Fig.39b).

A further extension of the NT beyond the postulated bipartite NLS did not change the distribution of the signal compared to the fusion proteins that solely contained the NT (Fig.38d and 39d). Only in the case of DOF4.7 this construct led to an accumulation of GFP in the nucleus.

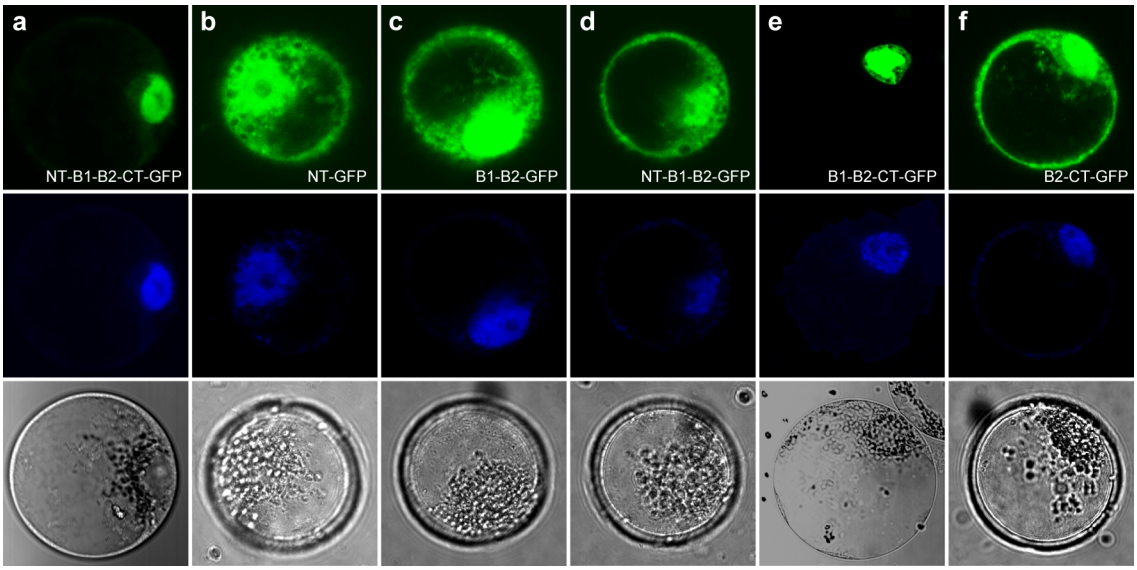

Figure 39. Subcellular localization of DOF1.7-GFP fusion proteins in *Arabidopsis* protoplasts.

The construct names correspond to the nomenclature described in Fig.37. **a.** Fusion of the DOF1.7 full length protein with GFP. **b.** Fusion of the N-terminal part of DOF1.7 (without putative bipartite NLS) and GFP. **c.** Putative DOF1.7 bipartite NLS alone fused with GFP. **d.** Fusion of the N-terminal part of DOF1.7 including the putative bipartite NLS and GFP. **e.** Fusion of the C-terminal part of DOF1.7 including the putative bipartite NLS with GFP. **f.** Fusion of the C-terminal part of DOF1.7 including B2 of the putative bipartite NLS with GFP. First row: detection of GFP signal. Second row: control staining of nuclei with DAPI. Third row: protoplasts under transmission light.

A fusion protein consisting of the putative bipartite NLS alone and GFP did not lead to an accumulated fluorescence signal in the nucleus, neither in DOF4.7 nor DOF1.7 (Fig.38c and 39c). Surprisingly however, in both cases the additional presence of the CT led to a specific accumulation of GFP signal in nuclei (Fig.38e and 39e). However, a further deletion of B1 and the 17 aa long spacer was sufficient to diminish nuclear accumulation of the proteins. In this case, the fusion proteins appeared equally distributed in the cytoplasm and nucleus (Fig.38f and 39f).

5.4.7 Conclusion

We reasoned that the long 17 aa spacer precludes the bipartite motif from being recognized as an NLS by the available subcellular localization prediction tools. Indeed, by using virtually truncated spacer regions of ten or less aa residues, the subcellular prediction changed its status from “negative” to “unclear”. In the case of the five DOF members with additional monopartite NLS motifs the status even changed from “not clear” to “positive”. Since no additional basic region can be found in the CT of the DOF proteins and since the fusion of B2 in combination with the CT is not sufficient for an accumulation in the nucleus it can be concluded that the identified bipartite region plays a crucial role in the nuclear transport of DOF proteins. A possible explanation for the results can be found in the three dimensional structure of the DOF proteins. Region B1 is located in the middle of the DOF domain, B2 follows it. Since the DOF domain, by virtue of its high similarity to Zn-fingers of steroid hormone receptors, is expected to form a loop

structure through the involvement of four cysteine residues (Shimofurutani et al., 1998), it might be possible that the two identified basic stretches need a distinct spatial organization that only forms in combination with the proteins´ CT part. The three-dimensional structure of a DOF protein has not been elucidated by X-ray crystallography so far. However, it was demonstrated that in C2H2 zinc finger proteins the NLS is only formed upon appropriate folding of the protein (Hatayama et al., 2008).

Moreover, our investigations revealed the presence of an additional classic monopartite NLS in the protein sequence of five members of the *Arabidospsis* DOF family. DOF4.7 was chosen as one of these candidates to elucidate the putative function of these monopartite stretches independent from the bipartite structure. Indeed, it could be demonstrated that the monopartite NLS of DOF4.7 is sufficient for the translocation to the nucleus even in the absence of the conserved bipartite NLS.

Acknowledgements

We thank K. Czempinski for providing the pA7-GFP plasmid. We appreciate funding from the German Research Foundation (MU1199/4-1 and MU1199/8-1) and the Ministry of Education and Research (BMBF 0312854). We further acknowledge Eugenia Maximova for assistance with microscopy. We thank C. Voelker, K. Schulz and A. Schneider for assistance in the lab.

6. General discussion and outlook

6.1 Overview

This thesis concentrated on the molecular and physiological characterization of four members of the *Arabidopsis thaliana* DOF TF family DOF1.2, DOF3.1, DOF3.5 and DOF5.2 which play a role in diverse aspects of root development. DOF1.2, DOF3.1 and DOF3.5 have not been characterized yet, while DOF5.2 (cycling DOF factor 2, CDF2) was shown to regulate redundantly with other CFDs the leaf phototrophic flowering response (Fornara et al., 2009). The genes were selected through different approaches: While DOF1.2 and DOF3.5 were identified by promoter deletion studies of the root cap specific expressed gene *diacylglycerolkinase 7* (*AtDGK7*), DOF3.1 and DOF5.2 were chosen as candidates because of their expression in the quiescent centre (QC) of the roots stem cell niche which was approachable through the GUS reporter gene collection of the DOF family available in our group.

DOF1.2 and *DOF3.5* are specifically and exclusively expressed in the root cap, including the central root cap (columella) and the lateral root cap, an expression pattern which is in the case of *DOF1.2* consistent with publically available expression data provided by databases like Genevestigator (http://www.genevestigator.com). In the case of *DOF3.5* available data are much more limited due o its absence from the ATH1 microarray, contributing to the circumstance that molecular and physiological characterization in this project mainly concentrated on *DOF1.2*.

To reveal the biological processes which are controlled by *DOF1.2*, transgenic gain- and loss-of-function lines were analysed comprising T-DNA insertion lines, the artificial microRNA (amiRNA) system as well as constitutive and inducible overexpression. It could be demonstrated that *DOF1.2* overexpression lines grow agravitropically and possess reduced root lengths in comparison with the wild-type. The phenotype is much more severe in the inducible than in the constitutive overexpression situation. Root cap cells possess a highly reduced number of starch-containing amyloplasts (statoliths) and altered auxin distribution which could cause the observed agravitropic growth. Furthermore it could be demonstrated that *DOF1.2* overexpression lines possess abnormal cell division patterns in the columella and degraded root cap boarder cells which might be caused by an impaired releasing process. Altered starch content could not be observed in the amiRNA lines. However, reduced levels of *DOF1.2* lead to an increase of boarder cell root layers and abnormal cell divisions in the columella.

DOF3.1 was chosen for detailed characterization because of its very specific and exclusive GUS expression in the QC, and T-DNA as well as inducible overexpression line were analysed to reveal its biological function. Inducible overexpression lines displayed roots which are thickened and highly reduced in length. Confocal microscopy analysis furthermore revealed that

root cells are broader and longitudinally less expanded than in the wild-type situation. The plant hormone auxin which is acropetally transported to the root tip and possesses a concentration maximum in the QC cells in the wild-type is absent from QC in the inducible overexpression lines but instead accumulates one cell layer above in the vascular initials. No phenotype could be observed in two independent DOF3.1 T-DNA insertion lines, leading to the question whether other DOF TFs redundantly control similar biological processes. This hypothesis was supported by the identification of DOF5.2 which is also expressed in the QC. Since no T-DNA insertion line was available for *DOF5.2,* a *DOF3.1/DOF5.2* double knock-out situation was prepared by crossing *DOF5.2* amiRNA lines with the *DOF3.1-1* T-DNA insertion line. The resulting *dof3.1-1*/*dof5.2* lines displayed thinner roots with cells which strongly elongate already in the promeristem prior to reaching the elongation zone. Furthermore auxin accumulated not in the QC like in wild-type but in the basal (close to the root tip) columella cells.
Various molecular biological approaches were used to identify genes which work upstream and downstream of DOF3.1 as well to find protein interaction partners. In this context it was possible to identify the *cis*-element which is related to gene expression in the QC.

Beside the physiological characterization of the described four DOF TFs it was tried to identify the nuclear localization signal (NLS) of DOF proteins since no publically available subcellular prediction tool indicated their nuclear status. By protein-deletion GFP-fusion studies it could be demonstrated that DOF proteins possess a novel bipartite NLS which is necessary but not sufficient to translocate DOF TFs to the nucleus.

6.2 DOF1.2, DOF3.1, DOF3.5 and DOF5.2 in the context of the DOF family

As a plant specific TF family DOF proteins have been proposed to play a key role in divergent plant including seed development and germination (Vicente-Carbajosa et al., 1997; Washio, 2001; Gualberti et al., 2002; Mena et al., 2002; Papi et al., 2002; Isabel-LaMoneda et al., 2003; Diaz et al., 2005; Moreno-Risueno et al., 2007), primary and secondary metabolism (Yanagisawa and Sheen, 1998; Yanagisawa, 2000; Skirycz et al., 2006; Skirycz et al., 2007), flowering (Imaizumi et al., 2005) and light signaling (Park et al., 2003; Ward et al., 2005). However, except for OBP3 (DOF3.6), which leads to reduced root lengths and less root hairs when overexpressed (Kang and Singh, 2000), the role of DOF proteins in root specific processes has not been described so far in *Arabidopsis thaliana*. In the sweetpotatoe it was recently shown that overexpression of *SRF1*, which encodes a DOF TF, results in higher storage root dry matter content and higher starch content per fresh weight in comparison to the wild-type (Tanaka et al., 2009).
An interesting finding is that three of the characterized *DOF* genes *DOF1.2*, *DOF3.1* and *DOF3.5*) are exclusively expressed in the root tip. In the case of *DOF3.1* this expression is already observed in its embryonic progenitor cells, suggesting their very specialized roles in root development and signaling. DOF5.2 possesses a broader expression pattern in the leaf veins, hydathodes and the root vascular tissue beside its expression in the QC.

6.3 Evolution of the DOF TF family

From an evolutionary point of view, the divergent functions of DOF TFs discussed above are related to the duplication-led expansion of the DOF family (Yang et al., 2006; Moreno-Risueno et al., 2007). Different hypothesis have been proposed about the fate of duplicated genes. According to the DRNNF (duplication, retention, non-/neofunctionalization) theory (Ohno, 1970), after a duplication event, one daughter gene retains the preduplication function (retention), while the other one, in the majority of cases, accumulates deleterious mutations and is eliminated (nonfunctionalization), or, in the minority of cases, survives by gaining a new function (neofunctionalization). Due to observations on genome-wide duplication events that are contradictory to DRNN, another model, called duplication-degeneration-complementation (DDC), was proposed to also include regulatory element functions (Force et al., 1999). Under this model, the majority of duplicated genes accumulates degenerative mutations for a period of time and then undergoes functional specialization by complementary partition of ancestral functions. Moreover, it was suggested that epigenetic changes might play important roles in the evolution of duplicated genes (Rodin and Riggs, 2003; Rapp and Wendel, 2005; Rodin et al., 2005). In the phylogenetic tree built from all *DOF* genes of poplar (*Populus trichocarpa*), Arabidopsis (*Arabidopsis thaliana*), and rice (*Oryza sativa*), 27 pairs of paralogous *DOF* genes in the terminal nodes were identified and grouped into six different gene fates which provided evidence that the proposed DRNNF and DDC hypotheses are complementary with, not alternative to each other (Yang et al., 2006).

In another approach, to investigate the origin of the DOF TFs, the complete or nearly complete genome sequences of the moss *Physcomitrella patens*, the green alga *Chlamydomonas reinhardtii*, the red alga *Cyanidioschyzon merolae* and the diatom *Thalassiosira pseudonana* were surveyed. Interestingly, 19 non-redundant sequences encoding the DOF domain in the moss and only one such sequence in *Chlamydomonas* were identified, but no DOF domain sequence in the red alga and the diatom. Based on the phylogenetic tree of DOF domains from these species and *Arabidopsis* and rice, DOF TFs were separated into three groups (Shigayo et al., 2006). Group A contains six moss DOF domains, some of the angiosperm domains and the single *Chlamydomonas* DOF domain. Group B comprises moss DOF domains exclusively, whereas the majority of the DOF domains from the angiosperms and two of these domains from moss were assigned to group C. Based upon suggested evolutionary events, it was speculated that the group A-type DOF domain proteins, the group B-type DOF domain proteins and the group C-type DOF domain proteins might be associated with the biological processes common among all green organisms, specific to the moss and linked to the development of organs in vascular plants, respectively. Consistent with this assumption four (CDF1-3 and COG1) among seven *Arabidopsis* genes belonging to this group were previously described to be involved in light signaling (Park et al., 2003; Imaizumi et al., 2005). Group C contains indeed a number of TFs related to seed development and germination, including HvPBF, HvSAD, AtDAG1/2 and

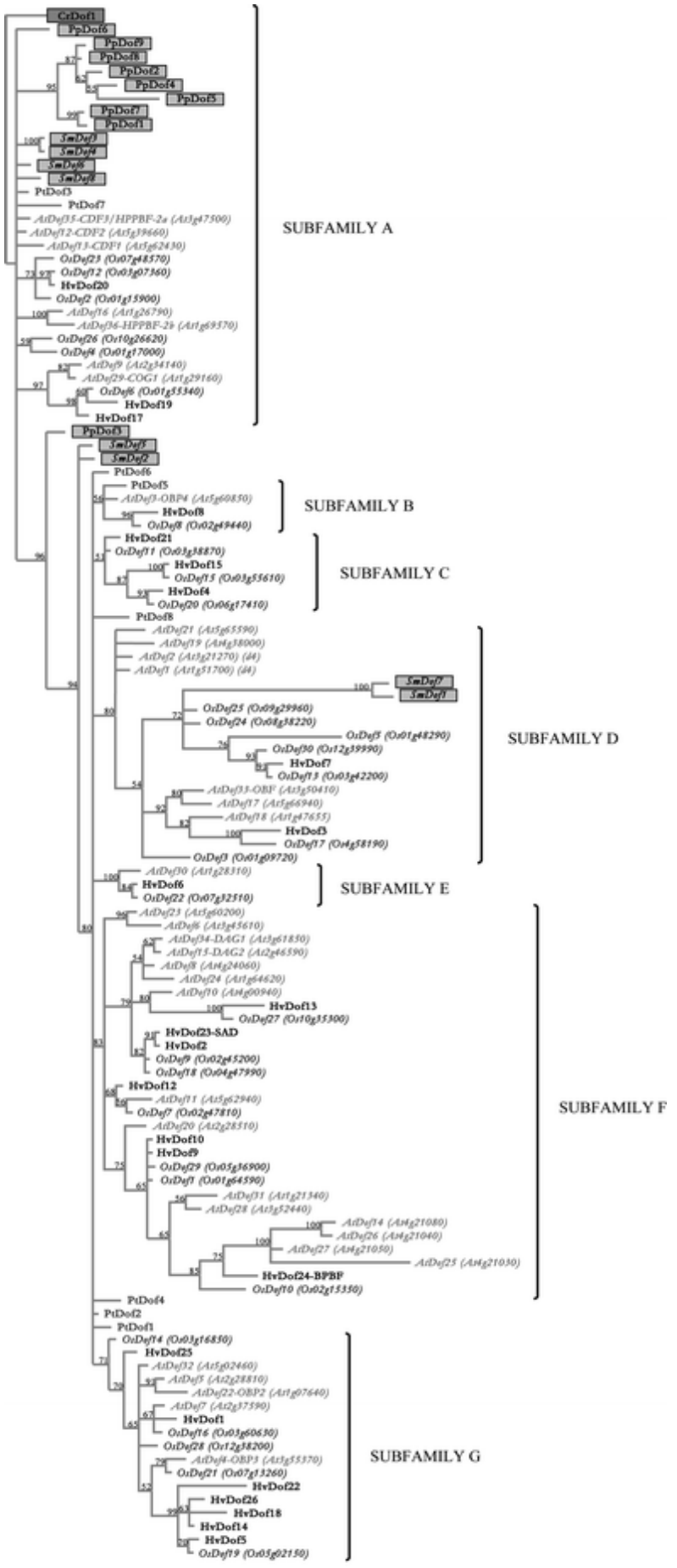
CrDof1
PpDof6
PpDof9
PpDof8
PpDof2
PpDof4
PpDof5
PpDof7
PpDof1
SmDof3
SmDof4
SmDof6
SmDof8
PtDof3
PtDof7
AtDof35-CDF3/HPPBF-2a (At3g47500)
AtDof32-CDF2 (At5g39660)
AtDof33-CDF1 (At5g62430)
OsDof23 (Os07g48570)
OsDof12 (Os03g07360)
HvDof20
OsDof2 (Os01g15900)
AtDof16 (At1g26790)
AtDof36-HPPBF-2b (At1g69570)
OsDof26 (Os10g26620)
OsDof4 (Os01g17000)
AtDof9 (At2g34140)
AtDof29-COG1 (At1g29160)
OsDof6 (Os01g55340)
HvDof19
HvDof17
SUBFAMILY A
PpDof3
SmDof5
SmDof2
PtDof6
PtDof5
AtDof3-OBP4 (At5g60850)
HvDof8
OsDof8 (Os02g49440)
SUBFAMILY B
HvDof21
OsDof11 (Os03g38870)
HvDof15
OsDof15 (Os03g55610)
HvDof4
OsDof20 (Os06g17410)
SUBFAMILY C
PtDof8
AtDof21 (At5g65590)
AtDof19 (AtMg38000)
AtDof2 (At3g21270) (44)
AtDof1 (At1g51700) (44)
SmDof7
SmDof1
OsDof25 (Os09g29960)
OsDof24 (Os08g38220)
OsDof5 (Os01g48290)
OsDof30 (Os12g39990)
HvDof7
OsDof13 (Os03g42200)
AtDof33-OBF (At3g50410)
AtDof17 (At5g66940)
AtDof18 (At1g47655)
HvDof3
OsDof17 (Os04g58190)
OsDof3 (Os01g09720)
SUBFAMILY D
AtDof30 (At1g28310)
HvDof6
OsDof22 (Os07g32510)
SUBFAMILY E
AtDof23 (At5g60200)
AtDof6 (At1g45610)
AtDof34-DAG1 (At3g61850)
AtDof15-DAG2 (At2g46590)
AtDof8 (AtMg24060)
AtDof24 (At1g64620)
AtDof10 (AtMg00940)
HvDof13
OsDof27 (Os10g35300)
HvDof23-SAD
HvDof2
OsDof9 (Os02g45200)
OsDof18 (Os04g47990)
HvDof12
AtDof11 (At5g62940)
OsDof7 (Os02g47810)
AtDof20 (At2g28510)
HvDof10
HvDof9
OsDof29 (Os05g36900)
OsDof1 (Os01g64590)
AtDof31 (At1g21340)
AtDof28 (At3g52440)
AtDof14 (AtMg21080)
AtDof26 (AtMg21040)
AtDof27 (AtMg21050)
AtDof25 (AtMg21030)
HvDof24-BPBF
OsDof10 (Os02g15350)
SUBFAMILY F
PtDof4
PtDof2
PtDof1
OsDof14 (Os03g16850)
HvDof25
AtDof32 (At5g02460)
AtDof5 (At2g28810)
AtDof22-OBP2 (At1g07640)
AtDof7 (At2g37590)
HvDof1
OsDof16 (Os03g60630)
OsDof28 (Os12g38200)
AtDof4-OBP3 (At3g55370)
OsDof21 (Os07g13260)
HvDof22
HvDof26
HvDof18
HvDof14
HvDof5
OsDof19 (Os05g02150)
SUBFAMILY G
0.1 substitutions/site

Figure 40. Phylogenetic tree of the DOF family in seven representative species of some of the main viridiplantae lineages.

DOFs from the green algae *C. reinhardtii* are boxed in dark gray, from the moss *P. patens* are boxed in pale gray, from the fern ally S. moellendorffii are in *italics* and boxed in pale gray, from *P. tadea* are in gray, from *H. vulgare* are in black, from *O. sativa* in dark gray and *italics*, and from *A. thaliana* in pale gray and *italics*. The rooted tree was inferred in MrBayes v3.1 by the Dayhoff model over the alignment of a common homologous region spanning 55 amino acids that included the 52 amino acids of the DOF domain of the 116 DOFs from the previously mentioned organisms. The resulting major clusters of orthologous genes (MCOGs) or subfamilies are shown on the right. The scale bar corresponds to 0.1 estimated amino acid substitutions per site. Bayesian posterior probabilities are indicated (Moreno-Risueno et al., 2007).

OsDOF3 (Vicente-Carbajosa et al., 1997; Washio, 2001; Gualberti et al., 2002; Mena et al., 2002; Papi et al., 2002; Isabel-LaMoneda et al., 2003; Diaz et al., 2005).

However, despite several examples to support such evolutionary functional grouping, limitations and ambiguity are also evident. OBP3, for example, belonging to group C, is involved in the regulation of light signalling (Ward et al., 2005).

6.4 DOF1.2, DOF3.1, DOF3.5 and DOF5.2 in the context of evolution

The classification of the four DOF TFs characterized in this work support the suggested grouping: DOF5.2 (CDF2) belongs to the above mentioned group of light signalling related cycling DOF factors and is found in group A. Its role in the QC might represent an evolutionary novelty obtained through the process of neofunctionalization. DOF1.2 and DOF3.1 with their very specialized function in the root cap and DOF3.1 which plays a role in the maintenance of the QC are all found in evolutionary younger group C.

It is further notable that in the DOF phylogenetic tree of the higher plants *Arabidopsis*, rice and barley none of the four DOF TFs in this work characterized *Arabidopsis* seems to possess an orthologue in the other species like it is evident, for example, in the case of OBP3 (At3g55370) and DOF5.6 (At5g62940) and their orthologues in rice Os07g13260 and Os02g47810, respectively (Fig.40). DOF1.2 and DOF3.5 stand alone as a couple in subfamily F. DOF3.1 is closely related to DOF1.7 (AT1g51700), DOF4.7 (At4g3800) and DOF5.7 (At5g65590) of which, however, none is expressed in the QC and plays a role in different physiological processes (data not shown). These four DOFs are members of subfamily D. DOF5.2 together with the two other cycling DOF factors CDF1 and CDF3 is present in subfamily A (Fig.40).

In the phylogenetic tree including DOF proteins of *Populus trichocarpa* it is evident that the *Arabidopsis* protein couple DOF1.2 and DOF3.5 is closely related to the poplar couple PtDOF31 and PtDOF34 which are orthologues of DOF3.5 (Yang et al., 2006). Sequence analyses revealed that the promoters of *PtDOF31* and *PtDOF34* possess significant similarity (Fig.41). Since no expression data are available for the poplar *DOF* genes, their promoter sequences

were compared with those of *AtDOF1.2* and *AtDOF3.5* to reveal if the high similarity they share is also conserved between the species. Neither the *AtDOF3.5* nor the *AtDOF1.2* promoter shows high similarity with the *PtDOF31* and *PtDOF34* promoters. However, several motives of the poplar promoter sequences can be found in AtDOF3.5 but not in AtDOF1.2, supporting the closer relationship of *AtDOF3.5* on the protein level. Among the motives common in *AtDOF3.5* and *PtDOF31* and *PtDOF34* are the sequences CAAGACTTCCACTCCCTTAAC (olive green) and CTGCGTTCTGAATTGCTTCCAAACTCAACAGGAGAGAGAACCAG (grey) and AGCGACACTGAGTATTAGCCTCCGGGGCTGTTACACACC (blue, which all contain MYB TF binding sites. Since expression data are lacking for the poplar DOF TFs it can not be concluded that these motives play a role for the root tip specific expression. Further notable, however, is the finding that the auxin response element TGTCTC in the *AtDOF3.5* promoter (182bp upstream of ATG) can be found at nearly same positions in the *PtDOF31* and *PtDOF34* promoter sequences (240 and 216bp, respectively).

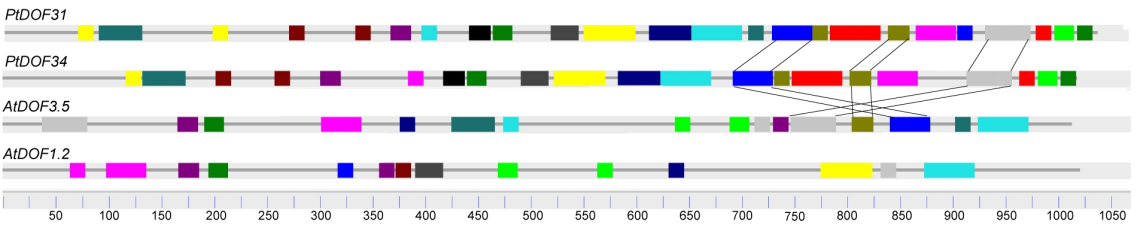

Figure 41. Comparison of the promoter regions of *AtDOF1.2* and *AtDOF3.5* with the corresponding *Populus trichocarpa* orthologues *PtDOF31* and *PtDOF34*.

To identify relevant motives in the DOF1.2 and DOF3.5 promoter regions, putative poplar orthologues were identified. A phylogentic approach was used to compare the upstream intergenic region of *AtDOF1.2* and *AtDOF3.5* (1000bp) with the corresponding segments of the putative orthologues in *Populus trichocarpa* and among each other. *AtDOF3.5* but not *AtDOF1.2* share common motives in the promoter region in comparison with PtDOF31 and PtDOF34 (indicated by connecting lines).

6.5 Outlook

The characterization of the four DOF TFs and their distinct roles in the root tip revealed the complex signaling pathways they are regulating and in the case of DOF3.1 and DOF5.2 their redundant function. In the case of the closely related proteins DOF1.2 and DOF3.5 this putative redundancy was not further analysed beside their identical expression pattern and the involvement in auxin signaling pathway. Because no T-DNA insertion lines are available for *DOF3.5*, knock-down mutants were already prepared in the course of this PhD work by expression of a *DOF3.5* gene specific amiRNA under control of the *DOF1.2* promoter which is active in the same tissue. However, positive transformants did not show any obvious phenotype and also did not show reduced DOF3.5 expression levels which were determined by qRT-PCR (data not shown). For this reason either more transformants have to be screened. Positive knockdown mutants could be subsequently crossed with the DOF1.2 knock-down and knock-out mutants to obtain a double knock-out situation which could be then screened for more severe phenotypes than the single knock-out mutants. Furthermore, constitutive and inducible

overexpression lines of DOF3.5 would reveal if starch content and auxin distribution are affected similarly to the DOF1.2 overexpression situation. To identify beside *AtDGK7* further direct target genes of both TFs, the estradiol mediated inducible overexpression system in combination with microarray based expression profiling could be used whereas at different time points after the induction of the TF whole genome expression profiles are measured. One disadvantage of this system, however, is that ectopic overexpression of TF genes does not reflect a natural situation and the question arises if target genes identified in this approach are real downstream targets. Alternatively, microarray based expression profiling of the single and double knock-out mutants would give indications for target genes.

In the case of DOF3.1, for which a protein-GFP fusion under control of its native promoter (*pDOF3.1::DOF3.1-GFP*) was stably transformed into plants, the ChIP-Chip system (Chromatin immunoprecipitation in combination with microarray chips) could be used for the identification of direct targets. To this end formaldehyd treatment is used to covalently bind DOF3.1-GFP fusion protein to the endogenous DOF3.1 target promoters. After fragmentation of the DNA by sonification and immonprecipotation using an anti-GFP antibody, the bound promoter fragments can be either directly sequenced (ChIP-Seq) or hybridizised with a promoter array (ChIP-Chip). Both systems have been shown to work in animal and plant research fields and could confirm data that were obtained from different approaches (Aparicio et al., 2004; Cui et al., 2007; Lin et al., 2009).

Microarray-based expression profiling using the *dof3.1-1* single T-DNA knock-out mutant and wild-type revealed that genes which respond to oxidative stress or are related to antioxidant, oxidoreductase and peroxidase activity are significantly enriched within the group of differentially expressed genes (data not shown). To reveal if *DOF3.1* mutant lines possess an altered oxidative status in the QC surrounding cells wild-type plants as well as *dof3.1* single and *dof3.1*/*dof5.2* double knock-out lines were transformed with a variant of GFP which is sensitive for the environmental redox status (roGFP) (Jiang et al., 2006). Fluorescence intensity measurements using laser scanning confocal microscopy will reveal if changes in the redox status are detectable.

For a more precise indication of the involvement of distinct genes in the regulation pathways which are controlled by the candidate DOF TFs, crossings with known mutants could be performed. The *no hydrotropic response mutant* (*nhr1*), for example, was shown to play a role in the perception of hydrotropic signals and the resulting curvature of the root. The gene has not been fully mapped so far but can be assigned to the upper arm of chromosome three, and therefore is different from *DOF1.2* and *DOF3.5* (Eapen et al., 2003). To determine if DOF1.2 and DOF3.5 act downstream of *nhr1* promoter-GUS constructs of both *DOF* genes could be introduced into the *nhr* mutant and analysed for GUS expression. Additionally, both *DOF1.2* and

DOF3.5 knock-out mutants could be crossed with the *nhr* mutant line and phenotypically characterized.

Furthermore, crossings with GUS- or GFP-marker lines can give insights into loss or changed cell identities. In the case of DOF3.1/DOF5.2 it would be interesting to find out if QC enhancer trap marker lines like QC25 are still expressed in the double knock-out background with its obvious loss in QC properties, since absence of QC25 GUS signal was demonstrated in the *wox5-1* mutant (Sarkar et al., 2007). In that context it would be also interesting to analyse the expression of the cortex/endodermis GFP markerline J0571, which was shown in this work to be differentially expressed in the *DOF3.1* overexpression lines.

7. References

Aida M, Beis D, Heidstra R, Willemsen V, Blilou I, Galinha C, Nussaume L, Noh YS, Amasino R, Scheres B (2004) The PLETHORA genes mediate patterning of the Arabidopsis root stem cell niche. Cell **119:** 109-120

Alonso JM, Hirayama T, Roman G, Nourizadeh S, Ecker JR (1999) EIN2, a bifunctional transducer of ethylene and stress responses in Arabidopsis. Science **284:** 2148-2152

Aparicio O, Geisberg JV, Struhl K (2004) Chromatin immunoprecipitation for determining the association of proteins with specific genomic sequences in vivo. Curr Protoc Cell Biol **Chapter 17:** Unit 17 17

Baima S, Nobili F, Sessa G, Lucchetti S, Ruberti I, Morelli G (1995) The expression of the Athb-8 homeobox gene is restricted to provascular cells in Arabidopsis thaliana. Development **121:** 4171-4182

Barlow PW (1975) The Root Cap. In The Development and Functions of Roots. Academic Press, London

Baum SFD, J.G.; Rost, T.L. (2002) Apical organization and maturation of the cortex and vascular cylinder in *Arabidopsis thaliana* (*Brassicaceae*) roots. *Am. J. Bot.* **89:** 908-920

Bedhomme M, Mathieu C, Pulido A, Henry Y, Bergounioux C (2009) Arabidopsis monomeric G-proteins, markers of early and late events in cell differentiation. Int J Dev Biol **53:** 177-185

Beemster GT, Baskin TI (1998) Analysis of cell division and elongation underlying the developmental acceleration of root growth in Arabidopsis thaliana. Plant Physiol **116:** 1515-1526

Benfey PN, Linstead PJ, Roberts K, Schiefelbein JW, Hauser MT, Aeschbacher RA (1993) Root development in Arabidopsis: four mutants with dramatically altered root morphogenesis. Development **119:** 57-70

Benfey PN, Scheres B (2000) Root development. Curr Biol **10:** R813-815

Benjamins R, Scheres B (2008) Auxin: the looping star in plant development. Annu Rev Plant Biol **59:** 443-465

Berleth T, Jürgens, G. (1993) The role of monopteros gene in organising the basal body region of the Arabidopsis embryo. Development **118:** 575-587

Birnbaum K, Shasha DE, Wang JY, Jung JW, Lambert GM, Galbraith DW, Benfey PN (2003) A gene expression map of the Arabidopsis root. Science **302:** 1956-1960

Blakeslee JJ, Bandyopadhyay A, Lee OR, Mravec J, Titapiwatanakun B, Sauer M, Makam SN, Cheng Y, Bouchard R, Adamec J, Geisler M, Nagashima A, Sakai T, Martinoia E, Friml J, Peer WA, Murphy AS (2007) Interactions among PIN-FORMED and P-glycoprotein auxin transporters in Arabidopsis. Plant Cell **19:** 131-147

Bleecker AB, Estelle MA, Somerville C, Kende H (1988) Insensitivity to Ethylene Conferred by a Dominant Mutation in Arabidopsis thaliana. Science **241:** 1086-1089

Blilou I, Frugier F, Folmer S, Serralbo O, Willemsen V, Wolkenfelt H, Eloy NB, Ferreira PC, Weisbeek P, Scheres B (2002) The Arabidopsis HOBBIT gene encodes a CDC27 homolog that links the plant cell cycle to progression of cell differentiation. Genes Dev **16:** 2566-2575

Blilou I, Xu J, Wildwater M, Willemsen V, Paponov I, Friml J, Heidstra R, Aida M, Palme K, Scheres B (2005) The PIN auxin efflux facilitator network controls growth and patterning in Arabidopsis roots. Nature **433:** 39-44

Boerjan W, Cervera MT, Delarue M, Beeckman T, Dewitte W, Bellini C, Caboche M, Van Onckelen H, Van Montagu M, Inze D (1995) Superroot, a recessive mutation in Arabidopsis, confers auxin overproduction. Plant Cell **7:** 1405-1419

Casson SA, Topping JF, Lindsey K (2009) MERISTEM-DEFECTIVE, an RS domain protein, is required for the correct meristem patterning and function in Arabidopsis. Plant J **57:** 857-869

Celenza JL, Jr., Grisafi PL, Fink GR (1995) A pathway for lateral root formation in Arabidopsis thaliana. Genes Dev **9:** 2131-2142

Chakravarthy S, Tuori RP, D'Ascenzo MD, Fobert PR, Despres C, Martin GB (2003) The tomato transcription factor Pti4 regulates defense-related gene expression via GCC box and non-GCC box cis elements. Plant Cell **15:** 3033-3050

Chaves ALS, de Mello-Farias, P.C. (2006) Ethylene and fruit ripening: From illumination gas to the control of gene expression, more than a century of discoveries. Genet. Mol. Biol. **29:** 508-515

Clough SJ, Bent AF (1998) Floral dip: a simplified method for Agrobacterium-mediated transformation of Arabidopsis thaliana. Plant J **16:** 735-743

Cole M, Chandler J, Weijers D, Jacobs B, Comelli P, Werr W (2009) DORNROSCHEN is a direct target of the auxin response factor MONOPTEROS in the Arabidopsis embryo. Development **136:** 1643-1651

Cui H, Levesque MP, Vernoux T, Jung JW, Paquette AJ, Gallagher KL, Wang JY, Blilou I, Scheres B, Benfey PN (2007) An evolutionarily conserved mechanism delimiting SHR movement defines a single layer of endodermis in plants. Science **316:** 421-425

del Campillo E, Abdel-Aziz A, Crawford D, Patterson SE (2004) Root cap specific expression of an endo-beta-1,4-D-glucanase (cellulase): a new marker to study root development in Arabidopsis. Plant Mol Biol **56:** 309-323

Dharmasiri N, Dharmasiri S, Weijers D, Lechner E, Yamada M, Hobbie L, Ehrismann JS, Jurgens G, Estelle M (2005) Plant development is regulated by a family of auxin receptor F box proteins. Dev Cell **9:** 109-119

Dharmasiri S, Estelle M (2002) The role of regulated protein degradation in auxin response. Plant Mol Biol **49:** 401-409

Di Laurenzio L, Wysocka-Diller J, Malamy JE, Pysh L, Helariutta Y, Freshour G, Hahn MG, Feldmann KA, Benfey PN (1996) The SCARECROW gene regulates an asymmetric cell division that is essential for generating the radial organization of the Arabidopsis root. Cell **86:** 423-433

Diaz I, Martinez M, Isabel-LaMoneda I, Rubio-Somoza I, Carbonero P (2005) The DOF protein, SAD, interacts with GAMYB in plant nuclei and activates transcription of endosperm-specific genes during barley seed development. Plant J **42:** 652-662

Dingwall C, Laskey RA (1991) Nuclear targeting sequences--a consensus? Trends Biochem Sci **16:** 478-481

Dinneny JR, Benfey PN (2008) Plant stem cell niches: standing the test of time. Cell **132:** 553-557

Dinneny JR, Long TA, Wang JY, Jung JW, Mace D, Pointer S, Barron C, Brady SM, Schiefelbein J, Benfey PN (2008) Cell identity mediates the response of Arabidopsis roots to abiotic stress. Science **320:** 942-945

Docquier S, Tillemans V, Deltour R, Motte P (2004) Nuclear bodies and compartmentalization of pre-mRNA splicing factors in higher plants. Chromosoma **112:** 255-266

Dolan L, Janmaat K, Willemsen V, Linstead P, Poethig S, Roberts K, Scheres B (1993) Cellular organisation of the Arabidopsis thaliana root. Development **119:** 71-84

Driouich A, Durand C, Vicre-Gibouin M (2007) Formation and separation of root border cells. Trends Plant Sci **12:** 14-19

Eapen D, Barroso ML, Campos ME, Ponce G, Corkidi G, Dubrovsky JG, Cassab GI (2003) A no hydrotropic response root mutant that responds positively to gravitropism in Arabidopsis. Plant Physiol **131:** 536-546

Esau K (1965) Plant anatomy. John Wiley & Sons, New York

Faustino RS, Nelson TJ, Terzic A, Perez-Terzic C (2007) Nuclear transport: target for therapy. Clin Pharmacol Ther **81:** 880-886

Feraru E, Friml J (2008) PIN polar targeting. Plant Physiol **147:** 1553-1559

Force A, Lynch M, Pickett FB, Amores A, Yan YL, Postlethwait J (1999) Preservation of duplicate genes by complementary, degenerative mutations. Genetics **151:** 1531-1545

Fornara F, Panigrahi KC, Gissot L, Sauerbrunn N, Ruhl M, Jarillo JA, Coupland G (2009) Arabidopsis DOF transcription factors act redundantly to reduce CONSTANS expression and are essential for a photoperiodic flowering response. Dev Cell **17:** 75-86

Fortin MC, Poff KL (1991) Characterization of thermotropism in primary roots of maize: dependence on temperature and temperature gradient, and interaction with gravitropism. Planta **184:** 410-414

Friml J, Benkova E, Blilou I, Wisniewska J, Hamann T, Ljung K, Woody S, Sandberg G, Scheres B, Jurgens G, Palme K (2002) AtPIN4 mediates sink-driven auxin gradients and root patterning in Arabidopsis. Cell **108:** 661-673

Friml J, Vieten A, Sauer M, Weijers D, Schwarz H, Hamann T, Offringa R, Jurgens G (2003) Efflux-dependent auxin gradients establish the apical-basal axis of Arabidopsis. Nature **426:** 147-153

Friml J, Wisniewska J, Benkova E, Mendgen K, Palme K (2002) Lateral relocation of auxin efflux regulator PIN3 mediates tropism in Arabidopsis. Nature **415:** 806-809

Fujie MK, H.; Suzuki, T.; Kawano, S. and Kuroiwa, T. (1993) Organelle DNA Synthesis in the Quiescent centre of *Arabidopsis thaliana* (Col.). J Exp Botany **44:** 689-693

Fukaki H, Tameda S, Masuda H, Tasaka M (2002) Lateral root formation is blocked by a gain-of-function mutation in the SOLITARY-ROOT/IAA14 gene of Arabidopsis. Plant J **29:** 153-168

Galinha C, Hofhuis H, Luijten M, Willemsen V, Blilou I, Heidstra R, Scheres B (2007) PLETHORA proteins as dose-dependent master regulators of Arabidopsis root development. Nature **449:** 1053-1057

Gazzarrini S, McCourt P (2003) Cross-talk in plant hormone signalling: what Arabidopsis mutants are telling us. Ann Bot (Lond) **91:** 605-612

Gillissen B, Burkle L, Andre B, Kuhn C, Rentsch D, Brandl B, Frommer WB (2000) A new family of high-affinity transporters for adenine, cytosine, and purine derivatives in Arabidopsis. Plant Cell **12:** 291-300

Grieneisen VA, Xu J, Maree AF, Hogeweg P, Scheres B (2007) Auxin transport is sufficient to generate a maximum and gradient guiding root growth. Nature **449:** 1008-1013

Groover A, Jackson, D (2007) Live-Cell Imaging of GFP in Plants. Cold Spring Harbor Protocols **2**

Grubb CD, Zipp BJ, Ludwig-Muller J, Masuno MN, Molinski TF, Abel S (2004) Arabidopsis glucosyltransferase UGT74B1 functions in glucosinolate biosynthesis and auxin homeostasis. Plant J **40:** 893-908

Gualberti G, Papi M, Bellucci L, Ricci I, Bouchez D, Camilleri C, Costantino P, Vittorioso P (2002) Mutations in the Dof zinc finger genes DAG2 and DAG1 influence with opposite effects the germination of Arabidopsis seeds. Plant Cell **14:** 1253-1263

Guilfoyle TJ, Hagen G (2007) Auxin response factors. Curr Opin Plant Biol **10:** 453-460

Guzman P, Ecker JR (1990) Exploiting the triple response of Arabidopsis to identify ethylene-related mutants. Plant Cell **2:** 513-523

Haecker A, Groß-Hardt, R., Geiges, B., Sarkar, A., Breuninger, H., Herrmann, M., Laux, T. (2003) Expression dynamics of *WOX* genes mark cell fate decisions during early embryonic patterning in *Arabidopsis thaliana.* . Development **131:** 657-666

Hagen G, Guilfoyle T (2002) Auxin-responsive gene expression: genes, promoters and regulatory factors. Plant Mol Biol **49:** 373-385

Hamann T, Benkova E, Baurle I, Kientz M, Jurgens G (2002) The Arabidopsis BODENLOS gene encodes an auxin response protein inhibiting MONOPTEROS-mediated embryo patterning. Genes Dev **16:** 1610-1615

Hamann T, Mayer U, Jurgens G (1999) The auxin-insensitive bodenlos mutation affects primary root formation and apical-basal patterning in the Arabidopsis embryo. Development **126:** 1387-1395

Hardtke CS, Ckurshumova W, Vidaurre DP, Singh SA, Stamatiou G, Tiwari SB, Hagen G, Guilfoyle TJ, Berleth T (2004) Overlapping and non-redundant functions of the Arabidopsis auxin response factors MONOPTEROS and NONPHOTOTROPIC HYPOCOTYL 4. Development **131:** 1089-1100

Hasenstein KH, Evans ML (1988) Effects of cations on hormone transport in primary roots of Zea mays. Plant Physiol **86:** 890-894

Hatayama M, Tomizawa T, Sakai-Kato K, Bouvagnet P, Kose S, Imamoto N, Yokoyama S, Utsunomiya-Tate N, Mikoshiba K, Kigawa T, Aruga J (2008) Functional and structural basis of the nuclear localization signal in the ZIC3 zinc finger domain. Hum Mol Genet **17:** 3459-3473

Hawes MC, Gunawardena U, Miyasaka S, Zhao X (2000) The role of root border cells in plant defense. Trends Plant Sci **5:** 128-133

Hawker NP, Bowman JL (2004) Roles for Class III HD-Zip and KANADI genes in Arabidopsis root development. Plant Physiol **135:** 2261-2270

Hejatko J, Blilou I, Brewer PB, Friml J, Scheres B, Benkova E (2006) In situ hybridization technique for mRNA detection in whole mount Arabidopsis samples. Nat Protoc **1:** 1939-1946

Helariutta Y, Fukaki H, Wysocka-Diller J, Nakajima K, Jung J, Sena G, Hauser MT, Benfey PN (2000) The SHORT-ROOT gene controls radial patterning of the Arabidopsis root through radial signaling. Cell **101:** 555-567

Himanen K, Boucheron E, Vanneste S, de Almeida Engler J, Inze D, Beeckman T (2002) Auxin-mediated cell cycle activation during early lateral root initiation. Plant Cell **14:** 2339-2351

Hofer R, Briesen I, Beck M, Pinot F, Schreiber L, Franke R (2008) The Arabidopsis cytochrome P450 CYP86A1 encodes a fatty acid omega-hydroxylase involved in suberin monomer biosynthesis. J Exp Bot **59:** 2347-2360

Imaizumi T, Schultz TF, Harmon FG, Ho LA, Kay SA (2005) FKF1 F-box protein mediates cyclic degradation of a repressor of CONSTANS in Arabidopsis. Science **309:** 293-297

Isabel-LaMoneda I, Diaz I, Martinez M, Mena M, Carbonero P (2003) SAD: a new DOF protein from barley that activates transcription of a cathepsin B-like thiol protease gene in the aleurone of germinating seeds. Plant J **33:** 329-340

Ishikawa H, Evans ML (1990) Electrotropism of maize roots. Role of the root cap and relationship to gravitropism. Plant Physiol **94:** 913-918

Ivanchenko MG, Muday GK, Dubrovsky JG (2008) Ethylene-auxin interactions regulate lateral root initiation and emergence in Arabidopsis thaliana. Plant J **55:** 335-347

Jiang K, Schwarzer C, Lally E, Zhang S, Ruzin S, Machen T, Remington SJ, Feldman L (2006) Expression and characterization of a redox-sensing green fluorescent protein (reduction-oxidation-sensitive green fluorescent protein) in Arabidopsis. Plant Physiol **141:** 397-403

Joshi V, Laubengayer KM, Schauer N, Fernie AR, Jander G (2006) Two Arabidopsis threonine aldolases are nonredundant and compete with threonine deaminase for a common substrate pool. Plant Cell **18:** 3564-3575

Kalderon D, Roberts BL, Richardson WD, Smith AE (1984) A short amino acid sequence able to specify nuclear location. Cell **39:** 499-509

Kang HG, Singh KB (2000) Characterization of salicylic acid-responsive, arabidopsis Dof domain proteins: overexpression of OBP3 leads to growth defects. Plant J **21:** 329-339

Kankainen M, Holm L (2004) POBO, transcription factor binding site verification with bootstrapping. Nucleic Acids Res **32:** W222-229

Kieber JJ, Rothenberg M, Roman G, Feldmann KA, Ecker JR (1993) CTR1, a negative regulator of the ethylene response pathway in Arabidopsis, encodes a member of the raf family of protein kinases. Cell **72:** 427-441

Kim J, Jung JH, Reyes JL, Kim YS, Kim SY, Chung KS, Kim JA, Lee M, Lee Y, Narry Kim V, Chua NH, Park CM (2005) microRNA-directed cleavage of ATHB15 mRNA regulates vascular development in Arabidopsis inflorescence stems. Plant J **42:** 84-94

Kisu Y, Ono T, Shimofurutani N, Suzuki M, Esaka M (1998) Characterization and expression of a new class of zinc finger protein that binds to silencer region of ascorbate oxidase gene. Plant Cell Physiol **39:** 1054-1064

Knight LI, Rose, R.C., Crocker, W. (1910) Effects of various gases and vapors upon etiolated seedlings of the sweet pea. Science **10:** 635-636

Lanford RE, Butel JS (1984) Construction and characterization of an SV40 mutant defective in nuclear transport of T antigen. Cell **37:** 801-813

Laskowski MJ, Williams ME, Nusbaum HC, Sussex IM (1995) Formation of lateral root meristems is a two-stage process. Development **121:** 3303-3310

Le J, Vandenbussche F, Van Der Straeten D, Verbelen JP (2001) In the early response of Arabidopsis roots to ethylene, cell elongation is up- and down-regulated and uncoupled from differentiation. Plant Physiol **125:** 519-522

Lee JY, Colinas J, Wang JY, Mace D, Ohler U, Benfey PN (2006) Transcriptional and posttranscriptional regulation of transcription factor expression in Arabidopsis roots. Proc Natl Acad Sci U S A **103:** 6055-6060

Leroch M, Neuhaus HE, Kirchberger S, Zimmermann S, Melzer M, Gerhold J, Tjaden J (2008) Identification of a novel adenine nucleotide transporter in the endoplasmic reticulum of Arabidopsis. Plant Cell **20:** 438-451

Levesque MP, Vernoux T, Busch W, Cui H, Wang JY, Blilou I, Hassan H, Nakajima K, Matsumoto N, Lohmann JU, Scheres B, Benfey PN (2006) Whole-genome analysis of the SHORT-ROOT developmental pathway in Arabidopsis. PLoS Biol **4:** e143

Lijavetzky D, Carbonero P, Vicente-Carbajosa J (2003) Genome-wide comparative phylogenetic analysis of the rice and Arabidopsis Dof gene families. BMC Evol Biol **3:** 17

Lin B, Wang J, Hong X, Yan X, Hwang D, Cho JH, Yi D, Utleg AG, Fang X, Schones DE, Zhao K, Omenn GS, Hood L (2009) Integrated expression profiling and ChIP-seq analyses of the growth inhibition response program of the androgen receptor. PLoS One **4:** e6589

Liu C, Xu Z, Chua NH (1993) Auxin Polar Transport Is Essential for the Establishment of Bilateral Symmetry during Early Plant Embryogenesis. Plant Cell **5:** 621-630

Liu PP, Montgomery TA, Fahlgren N, Kasschau KD, Nonogaki H, Carrington JC (2007) Repression of AUXIN RESPONSE FACTOR10 by microRNA160 is critical for seed germination and post-germination stages. Plant J **52:** 133-146

Lluch MA, Masferrer A, Arro M, Boronat A, Ferrer A (2000) Molecular cloning and expression analysis of the mevalonate kinase gene from Arabidopsis thaliana. Plant Mol Biol **42:** 365-376

Malamy JE, Benfey PN (1997) Organization and cell differentiation in lateral roots of Arabidopsis thaliana. Development **124:** 33-44

Mattsson J, Ckurshumova W, Berleth T (2003) Auxin signaling in Arabidopsis leaf vascular development. Plant Physiol **131:** 1327-1339

Mayer KF, Schoof H, Haecker A, Lenhard M, Jurgens G, Laux T (1998) Role of WUSCHEL in regulating stem cell fate in the Arabidopsis shoot meristem. Cell **95:** 805-815

Mena M, Cejudo FJ, Isabel-Lamoneda I, Carbonero P (2002) A role for the DOF transcription factor BPBF in the regulation of gibberellin-responsive genes in barley aleurone. Plant Physiol **130:** 111-119

Mikkelsen MD, Hansen CH, Wittstock U, Halkier BA (2000) Cytochrome P450 CYP79B2 from Arabidopsis catalyzes the conversion of tryptophan to indole-3-acetaldoxime, a precursor of indole glucosinolates and indole-3-acetic acid. J Biol Chem **275:** 33712-33717

Mok DW, Mok MC (2001) Cytokinin Metabolism and Action. Annu Rev Plant Physiol Plant Mol Biol **52:** 89-118

Moreno-Risueno MA, Diaz I, Carrillo L, Fuentes R, Carbonero P (2007) The HvDOF19 transcription factor mediates the abscisic acid-dependent repression of hydrolase genes in germinating barley aleurone. Plant J **51:** 352-365

Moreno-Risueno MA, Martinez M, Vicente-Carbajosa J, Carbonero P (2007) The family of DOF transcription factors: from green unicellular algae to vascular plants. Mol Genet Genomics **277:** 379-390

Mouchel CF, Osmont KS, Hardtke CS (2006) BRX mediates feedback between brassinosteroid levels and auxin signalling in root growth. Nature **443:** 458-461

Muller A, Guan C, Galweiler L, Tanzler P, Huijser P, Marchant A, Parry G, Bennett M, Wisman E, Palme K (1998) AtPIN2 defines a locus of Arabidopsis for root gravitropism control. EMBO J **17:** 6903-6911

Muller B, Sheen J (2008) Cytokinin and auxin interaction in root stem-cell specification during early embryogenesis. Nature **453:** 1094-1097

Nakajima K, Sena G, Nawy T, Benfey PN (2001) Intercellular movement of the putative transcription factor SHR in root patterning. Nature **413:** 307-311

Nakano T, Suzuki K, Fujimura T, Shinshi H (2006) Genome-wide analysis of the ERF gene family in Arabidopsis and rice. Plant Physiol **140:** 411-432

Nawy T, Lee JY, Colinas J, Wang JY, Thongrod SC, Malamy JE, Birnbaum K, Benfey PN (2005) Transcriptional profile of the Arabidopsis root quiescent center. Plant Cell **17:** 1908-1925

Noh B, Murphy AS, Spalding EP (2001) Multidrug resistance-like genes of Arabidopsis required for auxin transport and auxin-mediated development. Plant Cell **13:** 2441-2454

Ohno S (1970) Evolution by gene duplication. Springer-Verlag, Heidelberg

Okada K, Shimura Y (1990) Reversible Root Tip Rotation in Arabidopsis Seedlings Induced by Obstacle-Touching Stimulus. Science **250:** 274-276

Ortega-Martinez O, Pernas M, Carol RJ, Dolan L (2007) Ethylene modulates stem cell division in the Arabidopsis thaliana root. Science **317:** 507-510

Ouyang J, Shao X, Li J (2000) Indole-3-glycerol phosphate, a branchpoint of indole-3-acetic acid biosynthesis from the tryptophan biosynthetic pathway in Arabidopsis thaliana. Plant J **24:** 327-333

Pan JW, Ye D, Wang LL, Hua J, Zhao GF, Pan WH, Han N, Zhu MY (2004) Root border cell development is a temperature-insensitive and Al-sensitive process in barley. Plant Cell Physiol **45:** 751-760

Papi M, Sabatini S, Altamura MM, Hennig L, Schafer E, Costantino P, Vittorioso P (2002) Inactivation of the phloem-specific Dof zinc finger gene DAG1 affects response to light and integrity of the testa of Arabidopsis seeds. Plant Physiol **128:** 411-417

Paponov IA, Teale WD, Trebar M, Blilou I, Palme K (2005) The PIN auxin efflux facilitators: evolutionary and functional perspectives. Trends Plant Sci **10:** 170-177

Park DH, Lim PO, Kim JS, Cho DS, Hong SH, Nam HG (2003) The Arabidopsis COG1 gene encodes a Dof domain transcription factor and negatively regulates phytochrome signaling. Plant J **34:** 161-171

Park WJ, Schafer A, Prinsen E, van Onckelen H, Kang BG, Hertel R (2001) Auxin-induced elongation of short maize coleoptile segments is supported by 2,4-dihydroxy-7-methoxy-1,4-benzoxazin-3-one. Planta **213:** 92-100

Pérez-Rodríguez P, Riaño-Pachón, D.M., Corrêa, L.G.G., Rensing, S.A., Kersten, B. and Mueller-Roeber, B. (2009) PlnTFDB: Updated content and new features of the Plant Transcription Factor Database. Nucl. Acids Res. **in press**

Plesch G, Ehrhardt T, Mueller-Roeber B (2001) Involvement of TAAAG elements suggests a role for Dof transcription factors in guard cell-specific gene expression. Plant J **28:** 455-464

Pollmann S, Muller A, Piotrowski M, Weiler EW (2002) Occurrence and formation of indole-3-acetamide in Arabidopsis thaliana. Planta **216:** 155-161

Ponce G, Barlow PW, Feldman LJ, Cassab GI (2005) Auxin and ethylene interactions control mitotic activity of the quiescent centre, root cap size, and pattern of cap cell differentiation in maize. Plant Cell Environ **28:** 719-732

Qu LJ, Zhu YX (2006) Transcription factor families in Arabidopsis: major progress and outstanding issues for future research. Curr Opin Plant Biol **9:** 544-549

Raikhel N (1992) Nuclear Targeting in Plants. Plant Physiol **100:** 1627-1632

Ramakers C, Ruijter JM, Deprez RH, Moorman AF (2003) Assumption-free analysis of quantitative real-time polymerase chain reaction (PCR) data. Neurosci Lett **339:** 62-66

Rapp RA, Wendel JF (2005) Epigenetics and plant evolution. New Phytol **168:** 81-91

Riechmann JL, Heard J, Martin G, Reuber L, Jiang C, Keddie J, Adam L, Pineda O, Ratcliffe OJ, Samaha RR, Creelman R, Pilgrim M, Broun P, Zhang JZ, Ghandehari D, Sherman BK, Yu G (2000) Arabidopsis transcription factors: genome-wide comparative analysis among eukaryotes. Science **290:** 2105-2110

Robbins J, Dilworth SM, Laskey RA, Dingwall C (1991) Two interdependent basic domains in nucleoplasmin nuclear targeting sequence: identification of a class of bipartite nuclear targeting sequence. Cell **64:** 615-623

Rodin SN, Parkhomchuk DV, Riggs AD (2005) Epigenetic changes and repositioning determine the evolutionary fate of duplicated genes. Biochemistry (Mosc) **70:** 559-567

Rodin SN, Riggs AD (2003) Epigenetic silencing may aid evolution by gene duplication. J Mol Evol **56:** 718-729

Rubery PH, Sheldrake, A.H. (1974) Carrier mediated auxin transport. Planta **5:** 101-121

Sabatini S, Beis D, Wolkenfelt H, Murfett J, Guilfoyle T, Malamy J, Benfey P, Leyser O, Bechtold N, Weisbeek P, Scheres B (1999) An auxin-dependent distal organizer of pattern and polarity in the Arabidopsis root. Cell **99:** 463-472

Sabatini S, Heidstra R, Wildwater M, Scheres B (2003) SCARECROW is involved in positioning the stem cell niche in the Arabidopsis root meristem. Genes Dev **17:** 354-358

Sack FD (1997) Plastids and gravitropic sensing. Planta **203:** S63-68

Sarkar AK, Luijten M, Miyashima S, Lenhard M, Hashimoto T, Nakajima K, Scheres B, Heidstra R, Laux T (2007) Conserved factors regulate signalling in Arabidopsis thaliana shoot and root stem cell organizers. Nature **446:** 811-814

Scheres B, Benfey, P., Dolan, L. (2002) Root Development. *In* The Arabidopsis Book. American Society of Plant Biologists, Rockville, MD

Scheres B, DiLaurenzio, L., Willemsen, V., Hauser, M.T., Janmaat, K., Weisbeek, P., and Benfey, P. (1995) Mutations affecting the radial organisation of the Arabidopsis root display specific defects throughout the embryo axis. Development **121:** 53-62

Scheres BW, H.; Willemsen, V.; Terlouw, M.; Lawson, E.; Dean, C.; and Weisbeek, P. (1994) Embryonic origin of the *Arabidopsis* primary root and root meristem initials. Development **120:** 2475-2487

Schoof H, Lenhard M, Haecker A, Mayer KF, Jurgens G, Laux T (2000) The stem cell population of Arabidopsis shoot meristems in maintained by a regulatory loop between the CLAVATA and WUSCHEL genes. Cell **100:** 635-644

Schwab R, Ossowski S, Riester M, Warthmann N, Weigel D (2006) Highly specific gene silencing by artificial microRNAs in Arabidopsis. Plant Cell **18:** 1121-1133

Shimofurutani N, Kisu Y, Suzuki M, Esaka M (1998) Functional analyses of the Dof domain, a zinc finger DNA-binding domain, in a pumpkin DNA-binding protein AOBP. FEBS Lett **430:** 251-256

Skirycz A, Jozefczuk S, Stobiecki M, Muth D, Zanor MI, Witt I, Mueller-Roeber B (2007) Transcription factor AtDOF4;2 affects phenylpropanoid metabolism in Arabidopsis thaliana. New Phytol **175:** 425-438

Skirycz A, Reichelt M, Burow M, Birkemeyer C, Rolcik J, Kopka J, Zanor MI, Gershenzon J, Strnad M, Szopa J, Mueller-Roeber B, Witt I (2006) DOF transcription factor AtDof1.1 (OBP2) is part of a regulatory network controlling glucosinolate biosynthesis in Arabidopsis. Plant J **47:** 10-24

Skoog F, Miller CO (1957) Chemical regulation of growth and organ formation in plant tissues cultured in vitro. Symp Soc Exp Biol **54:** 118-130

Smalle J, Haegman M, Kurepa J, Van Montagu M, Straeten DV (1997) Ethylene can stimulate Arabidopsis hypocotyl elongation in the light. Proc Natl Acad Sci U S A **94:** 2756-2761

Smith HM, Hicks GR, Raikhel NV (1997) Importin alpha from Arabidopsis thaliana is a nuclear import receptor that recognizes three classes of import signals. Plant Physiol **114:** 411-417

Steinmann T, Geldner N, Grebe M, Mangold S, Jackson CL, Paris S, Galweiler L, Palme K, Jurgens G (1999) Coordinated polar localization of auxin efflux carrier PIN1 by GNOM ARF GEF. Science **286:** 316-318

Stepanova AN, Alonso JM (2005) Arabidopsis ethylene signaling pathway. Sci STKE **2005:** cm4

Stepanova AN, Hoyt JM, Hamilton AA, Alonso JM (2005) A Link between ethylene and auxin uncovered by the characterization of two root-specific ethylene-insensitive mutants in Arabidopsis. Plant Cell **17:** 2230-2242

Swarup R, Friml J, Marchant A, Ljung K, Sandberg G, Palme K, Bennett M (2001) Localization of the auxin permease AUX1 suggests two functionally distinct hormone transport pathways operate in the Arabidopsis root apex. Genes Dev **15:** 2648-2653

Swarup R, Kramer EM, Perry P, Knox K, Leyser HM, Haseloff J, Beemster GT, Bhalerao R, Bennett MJ (2005) Root gravitropism requires lateral root cap and epidermal cells for transport and response to a mobile auxin signal. Nat Cell Biol **7:** 1057-1065

Swarup R, Perry P, Hagenbeek D, Van Der Straeten D, Beemster GT, Sandberg G, Bhalerao R, Ljung K, Bennett MJ (2007) Ethylene upregulates auxin biosynthesis in Arabidopsis seedlings to enhance inhibition of root cell elongation. Plant Cell **19:** 2186-2196

Szemenyei H, Hannon M, Long JA (2008) TOPLESS mediates auxin-dependent transcriptional repression during Arabidopsis embryogenesis. Science **319:** 1384-1386

Taatjes DJ, Marr, M.T., Tjian, R. (2004) Regulatory diversity among metazoan co-activator complexes. Nature Reviews Molecular Cell Biology **5:** 403-410

Takahashi H (1997) Hydrotropism: the current state of our knowledge. J Plant Res **110:** 163-169

Takahashi N, Yamazaki Y, Kobayashi A, Higashitani A, Takahashi H (2003) Hydrotropism interacts with gravitropism by degrading amyloplasts in seedling roots of Arabidopsis and radish. Plant Physiol **132:** 805-810

Tanaka M, Takahata Y, Nakayama H, Nakatani M, Tahara M (2009) Altered carbohydrate metabolism in the storage roots of sweetpotato plants overexpressing the SRF1 gene, which encodes a Dof zinc finger transcription factor. Planta **230:** 737-746

Tanimoto M, Roberts K, Dolan L (1995) Ethylene is a positive regulator of root hair development in Arabidopsis thaliana. Plant J **8:** 943-948

Teal WD, Ditengou, F.A., Dovzhenko, A.D., Li, X., Molendijk, A.M., Ruperti, B., Paponov, I., Palme, K. (2008) Auxin as a Model for the Integration of Hormonal Signal Processing and Transduction. Molecular Plant **22:** 229-237

Thomann A, Lechner E, Hansen M, Dumbliauskas E, Parmentier Y, Kieber J, Scheres B, Genschik P (2009) Arabidopsis CULLIN3 genes regulate primary root growth and patterning by ethylene-dependent and -independent mechanisms. PLoS Genet **5:** e1000328

Truernit E, Sauer N (1995) The promoter of the Arabidopsis thaliana SUC2 sucrose-H+ symporter gene directs expression of beta-glucuronidase to the phloem: evidence for phloem loading and unloading by SUC2. Planta **196:** 564-570

Tsugeki R, Fedoroff NV (1999) Genetic ablation of root cap cells in Arabidopsis. Proc Natl Acad Sci U S A **96:** 12941-12946

Ulmasov T, Hagen G, Guilfoyle TJ (1997) ARF1, a transcription factor that binds to auxin response elements. Science **276:** 1865-1868

v. Guttenberg H (1960) Die Entwicklung der Wurzel. *In* Grundzüge der Histogenese höherer Pflanzen, Vol VIII. Gebr. Borntraeger Stuttgart

van den Berg C, Willemsen V, Hendriks G, Weisbeek P, Scheres B (1997) Short-range control of cell differentiation in the Arabidopsis root meristem. Nature **390:** 287-289

Vicente-Carbajosa J, Moose SP, Parsons RL, Schmidt RJ (1997) A maize zinc-finger protein binds the prolamin box in zein gene promoters and interacts with the basic leucine zipper transcriptional activator Opaque2. Proc Natl Acad Sci U S A **94:** 7685-7690

Vicente-Carbajosa J, Onate L, Lara P, Diaz I, Carbonero P (1998) Barley BLZ1: a bZIP transcriptional activator that interacts with endosperm-specific gene promoters. Plant J **13:** 629-640

Vidaurre DP, Ploense S, Krogan NT, Berleth T (2007) AMP1 and MP antagonistically regulate embryo and meristem development in Arabidopsis. Development **134:** 2561-2567

Wang JW, Wang LJ, Mao YB, Cai WJ, Xue HW, Chen XY (2005) Control of root cap formation by MicroRNA-targeted auxin response factors in Arabidopsis. Plant Cell **17:** 2204-2216

Ward JM, Cufr CA, Denzel MA, Neff MM (2005) The Dof transcription factor OBP3 modulates phytochrome and cryptochrome signaling in Arabidopsis. Plant Cell **17:** 475-485

Washio K (2001) Identification of Dof proteins with implication in the gibberellin-regulated expression of a peptidase gene following the germination of rice grains. Biochim Biophys Acta **1520:** 54-62

Welch D, Hassan H, Blilou I, Immink R, Heidstra R, Scheres B (2007) Arabidopsis JACKDAW and MAGPIE zinc finger proteins delimit asymmetric cell division and stabilize tissue boundaries by restricting SHORT-ROOT action. Genes Dev **21:** 2196-2204

Wieczorek K, Golecki B, Gerdes L, Heinen P, Szakasits D, Durachko DM, Cosgrove DJ, Kreil DP, Puzio PS, Bohlmann H, Grundler FM (2006) Expansins are involved in the formation of nematode-induced syncytia in roots of Arabidopsis thaliana. Plant J **48:** 98-112

Willemsen V, Bauch M, Bennett T, Campilho A, Wolkenfelt H, Xu J, Haseloff J, Scheres B (2008) The NAC domain transcription factors FEZ and SOMBRERO control the orientation of cell division plane in Arabidopsis root stem cells. Dev Cell **15:** 913-922

Willemsen V, Wolkenfelt H, de Vrieze G, Weisbeek P, Scheres B (1998) The HOBBIT gene is required for formation of the root meristem in the Arabidopsis embryo. Development **125:** 521-531

Wisniewska J, Xu J, Seifertova D, Brewer PB, Ruzicka K, Blilou I, Rouquie D, Benkova E, Scheres B, Friml J (2006) Polar PIN localization directs auxin flow in plants. Science **312:** 883

Yanagisawa S (2000) Dof1 and Dof2 transcription factors are associated with expression of multiple genes involved in carbon metabolism in maize. Plant J **21:** 281-288

Yanagisawa S (2001) The transcriptional activation domain of the plant-specific Dof1 factor functions in plant, animal, and yeast cells. Plant Cell Physiol **42:** 813-822

Yanagisawa S (2002) The Dof family of plant transcription factors. Trends Plant Sci **7:** 555-560

Yanagisawa S, Schmidt RJ (1999) Diversity and similarity among recognition sequences of Dof transcription factors. Plant J **17:** 209-214

Yanagisawa S, Sheen J (1998) Involvement of maize Dof zinc finger proteins in tissue-specific and light-regulated gene expression. Plant Cell **10:** 75-89

Yang X, Tuskan GA, Cheng MZ (2006) Divergence of the Dof gene families in poplar, Arabidopsis, and rice suggests multiple modes of gene evolution after duplication. Plant Physiol **142:** 820-830

Zimmermann P, Hirsch-Hoffmann M, Hennig L, Gruissem W (2004) GENEVESTIGATOR. Arabidopsis microarray database and analysis toolbox. Plant Physiol **136:** 2621-2632

Zuo J, Niu QW, Chua NH (2000) Technical advance: An estrogen receptor-based transactivator XVE mediates highly inducible gene expression in transgenic plants. Plant J **24:** 265-273

8. Supplementary information

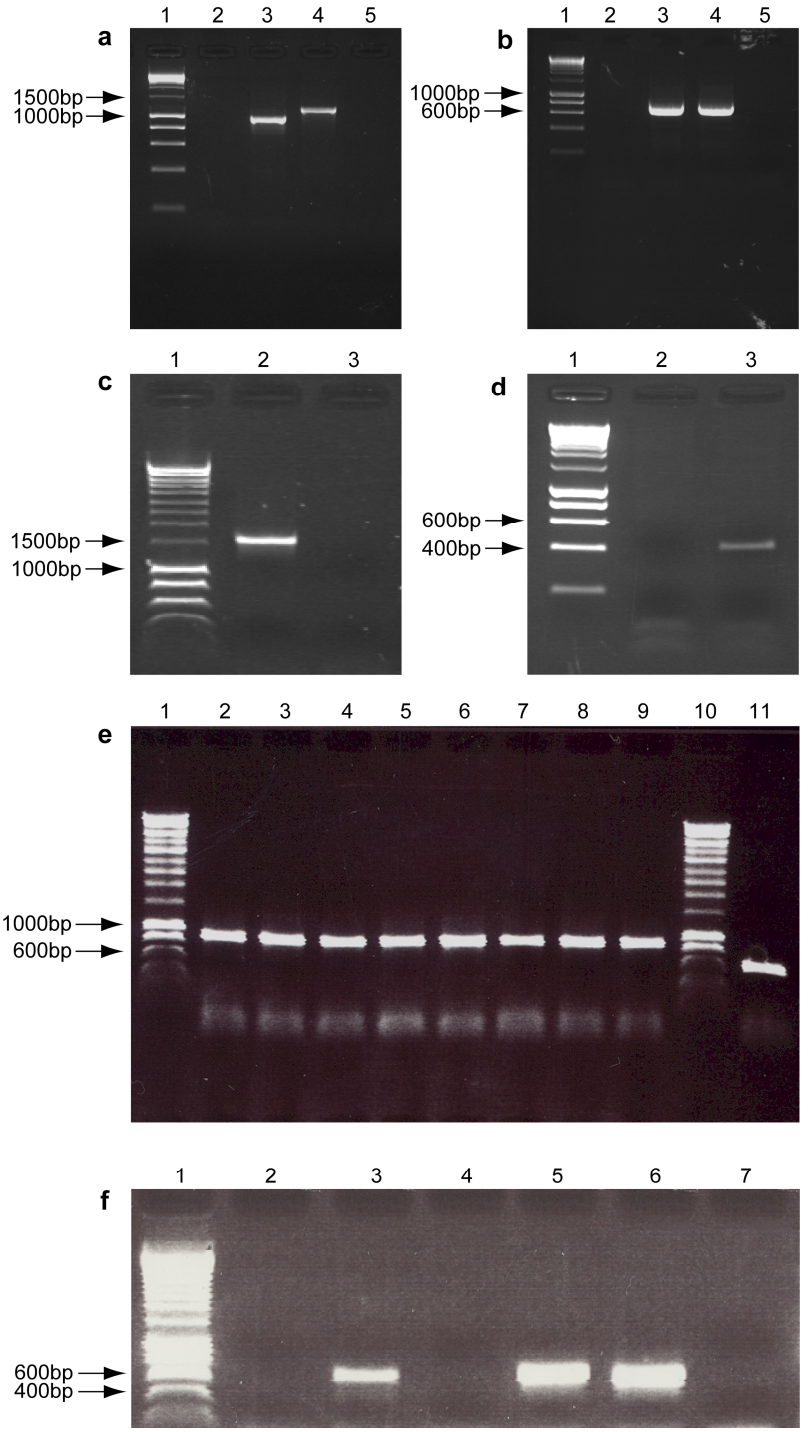

Supplementary Figure 1. PCR-based genotypisation of the characterized T-DNA insertion lines.

(**a**) Confirmation of the homozygosity of *dof1.2-1* (GABI_921E09). Primer sequences are listed in **3.3.1**. Using gene-specific forward and reverse primers, a fragment in length of 1176bp could be amplified from genomic DNA of wildtpye (lane 4) but not of *dof1.2-1* (lane 2). Using the T-DNA primer 8409 and the gene specific reverse primer resulted in a fragment of 997bp in *dof1.2-1* (lane 3) but in no amplicon in wild-type (lane 5). (**b**) Confirmation of the homozygosity of *dof1.2-2* (SAIL_99_C09). Primer sequences are listed in

3.3.1. Using gene-specific forward and reverse primers, a fragment in length of 783bp could be amplified from genomic DNA of wildtpye (lane 4) but not of *dof1.2-2* (lane 2). Using the T-DNA primer LB3 and the gene specific forward primer resulted in a fragment of 712bp in *dof1.2-2* (lane 3) but in no amplicon in wild-type (lane 5). (**c, d**) Confirmation of the homozygosity of *dof5.2-1* (GABI_782H09). Primer sequences are listed in **4.3.16**. Using the gene-specific primers DOF5.2for and DOF5.2rev, a fragment in length of 1616bp could be amplified from genomic DNA of wildtpye (**c,** lane 2) but not of *dof5.2-1* (**c,** lane 3). Using the T-DNA primer 8409 and the gene specific primer DOF5.2for resulted in a fragment of 441bp in *dof5.2-1* (**d,** lane 3) but in no amplicon in wild-type (**d,** lane 2). (**e**) Confirmation of the homozygosity of *dof3.1-1* (SALK_136364). Primer sequences are listed in **4.3.16**. Using gene-specific primers cdsDOF3.1for and cdsDOF3.1rev and the T-DNA primer LBa1, a fragment in length of 615bp corresponding to the wild-type *DOF3.1* coding sequence could be amplified from genomic DNA of wildtpye (lane 11) but not in the testet plants of *dof1.2-1* (lane 2-9), where PCR lead only to the amplification of the T-DNA fragment with a fragment size of 802bp (**f**) Confirmation of the homozygosity of *dof3.1-2* (SALK_095816). Primer sequences are listed in **4.3.16**. Using the gene-specific primers cdsDOF3.1for and cdsDOF3.1rev, a fragment in length of 615bp could be amplified from genomic DNA of wildtpye (lane 6) but not from the tested plants of *dof3.1-2* (lane 2 and 4). Using the T-DNA primer LBa1 and the gene specific reverse primer resulted in a fragment of 567bp in the tested *dof3.1-2* plants (lane 3 and 5) but in no amplicon in wild-type (lane 7)

Deutsche Zusammenfassung

Mehr noch als Tiere, die ihren Lebensraum unter widrigen Umständen verlassen können, sind Pflanzen mit einem festen Standort auf ihre Anpassungsfähigkeit angewiesen. Einen entscheidenden Beitrag dazu leistet die Genregulation, d.h. das gezielte An- und Ausschalten von Erbanlagen, den Genen. Vermittelt wird dieser Regulationsprozess unter anderem durch Transkriptionsfaktoren: Proteine, die die Fähigkeit besitzen, an bestimmte Regionen der Gene zu binden und damit deren Aktivität zu beeinflussen. In der Ackerschmalwand (*Arabidopsis thaliana*), die als Modellpflanze in der Genetik verwendet wird, existieren etwa 2000 solcher Transkriptionsfaktoren, eingeteilt in Familien, von denen einige auch in tierischen Organismen auftreten, andere pflanzenspezifisch sind. Auf Grund ihrer Funktion als wichtige Kontrollelemente sind sie von großem wissenschaftlichem und biotechnologischem Interesse.

Im Rahmen dieser Doktorarbeit sollte die Funktion von vier pflanzenspezifischen Transkriptionsfaktoren, genannt DOF1.2, DOF3.1, DOF3.5 und DOF5.2, untersucht werden, welche durch ihre spezifische Aktivität in der Wurzelspitze der Ackerschmalwand identifiziert wurden. Um die Funktion dieser vier Regulatoren aufzuklären, wurden an der Modellpflanze gentechnische Veränderungen durchgeführt und die so veränderten, auch als transgen bezeichneten Pflanzen mit molekularbiologischen und physiologischen Methoden untersucht. Es konnte gezeigt werden, dass DOF1.2 und DOF3.5 eine wesentliche Funktion beim gerichteten Wurzelwachstum spielen und ein seitliches Wachsen der Wurzel aufgrund veränderter Umwelteinflüsse verhindern, bzw. hervorrufen können. Die beiden anderen Proteine DOF3.1 und DOF5.2 erfüllen ihre Funktion in der Stammzellnische der Wurzel. Vergleichbar mit tierischen Stammzellen sind auch pflanzliche Stammzellen nicht zu einem bestimmten Zelltyp herangereift, sondern verbleiben in einem sogenannten undifferenzierten Zustand. Es konnte gezeigt werden, dass DOF3.1 und DOF5.2 zum Erhalt dieses Zustands benötigt werden, da nach Inaktivierung beider Proteine Zellspezialisierungen auftreten, die bei gentechnisch unveränderten Pflanzen nicht auftreten.

Desweiteren konnte in dieser Arbeit geklärt werden, welcher Proteinabschnitt der DOF-Proteine für ihren Transport in den Zellkern notwendig ist. Denn da die pflanzlichen Erbanlagen im Zellkern vorliegen, muss für eine Einflussnahme auf deren Aktivität zunächst ein Transport der Regulationsproteine in den Zellkern stattfinden.

Zusammengenommen konnte mit dieser Doktorarbeit das Wissen über Transkriptionsfaktoren und Entwicklungsprozesse der Wurzel erheblich erweitert werden. Zudem ist die Grundlage für interessante zukünftige Arbeiten gelegt worden. Dabei wird es von zentraler Bedeutung sein, komplexe Regulationsnetzwerke verstehen zu lernen und durch gezielte Manipulationen biotechnologisch nutzen zu können.